

Rank-two 5d SCFTs from M-theory at isolated toric singularities: a systematic study

Vivek Saxena[‡]

[‡]*C.N. Yang Institute for Theoretical Physics, Stony Brook University
Stony Brook, NY 11794-3840, USA*

E-mail: vivek.saxena@stonybrook.edu

ABSTRACT: We carry out a detailed exploration of the deformations of rank-two five-dimensional superconformal field theories (SCFTs) $\mathcal{T}_{\mathbf{X}}$, which are geometrically engineered by M-theory on the space transverse to isolated toric Calabi-Yau (CY) threefold singularities \mathbf{X} . Deformations of 5d $\mathcal{N} = 1$ SCFTs can lead to “gauge-theory phases,” but also to “non-gauge-theoretic phases,” which have no known Lagrangian interpretation. In previous work, a technique relying on fiberwise M-theory/type IIA duality was developed to associate a type IIA background to any resolution of \mathbf{X} which admits a suitable projection of its toric diagram. The type IIA background consists of an A-type ALE space fibered over the real line, with stacks of coincident D6-branes wrapping 2-cycles in the ALE resolution. In this work, we combine that technique with some elementary ideas from graph theory, to analyze mass deformations of $\mathcal{T}_{\mathbf{X}}$ when \mathbf{X} is an isolated toric CY_3 singularity of rank-two (that is, it has two compact divisors). We explicitly derive type IIA descriptions of all isolated rank-two CY_3 toric singularities. We also comment on the renormalization group flows in the extended parameter spaces of these theories, which frequently relate distinct geometries by flowing to theories with lower flavor symmetries, including those that describe non-gauge-theoretic phases.

KEYWORDS: Superconformal theories in higher dimensions, geometric engineering.

Contents

1	Introduction	1
2	5d $\mathcal{N} = 1$ theories and M-theory on a CY_3 singularity	6
2.1	Review of 5d $\mathcal{N} = 1$ gauge theories	6
2.2	The prepotential on the Coulomb branch	8
2.3	BPS objects on the Coulomb branch	10
2.4	M-theory on a CY_3 singularity	11
2.5	Graph-theoretic perspective	17
3	Rank-two isolated toric CY_3 singularities	19
3.1	The $E_1^{2,2}$ singularity and $SU(3)_2$ gauge theory	22
3.2	The $E_1^{2,1}$ singularity and $SU(3)_1$ gauge theory	27
3.3	The $E_1^{2,0}$ singularity and $SU(3)_0$ gauge theory	30
3.4	The $E_2^{2,\frac{3}{2}}$ singularity and $SU(3)_{\frac{3}{2}}$ $N_f = 1$ gauge theory	33
3.5	The $E_2^{2,\frac{1}{2}}$ singularity and $SU(3)_{\frac{1}{2}}$ $N_f = 1$ gauge theory	48
3.6	The $E_3^{2,1}$ singularity and $SU(3)_1$ $N_f = 2$ gauge theory	60
3.7	The $E_3^{2,0}$ singularity and $SU(3)_0$ $N_f = 2$ gauge theory	70
A	Field theory prepotentials and instanton masses	71
B	Triple-intersection numbers of the $E_3^{2,1}$ geometry	75
C	M-theory prepotentials of the $E_3^{2,1}$ geometry	79

1 Introduction

Five-dimensional $\mathcal{N} = 1$ supersymmetric gauge theories are curious entities in the landscape of string/M-theory compactifications, interpolating between their more extensively-studied four- and six- dimensional cousins. Being non-renormalizable, they are intrinsically ill-defined as quantum field theories, and yet, are interesting systems to study for they have a well-defined ultraviolet (UV) completion in string/M-theory [1–3]. The basic tool for studying them in the context of this paper is geometric engineering in

M-theory [4–7]. (For reviews of geometric engineering, see [8, 9].) Specifically, five-dimensional gauge theories with $\mathcal{N} = 1$ supersymmetry can be geometrically engineered via the decoupling limit of M-theory on a local Calabi-Yau (CY) threefold \mathbf{X} . In the limit where all the Kähler moduli of the threefold shrink to zero size, one gets a five-dimensional superconformal field theory (SCFT) in the ultraviolet (UV) along the spacetime transverse to \mathbf{X} :

$$\text{M-theory on } \mathbb{R}^{1,4} \times \mathbf{X} \quad \longleftrightarrow \quad \mathcal{T}_{\mathbf{X}} \equiv \text{SCFT}(\mathbf{X}) . \quad (1.1)$$

The geometric engineering analysis in this paper is largely based on [10], where a program to study the mass deformations of these SCFTs was initiated, focusing on the properties *away* from the conformal point. See also [11–23] for recent developments. Alternative constructions of 5d SCFTs rely on (p, q) -web diagrams in type IIB [2, 3, 24–28], which are dual to the M-theory geometry when \mathbf{X} is toric. The existence of 5d UV fixed points is also motivated by the AdS/CFT correspondence [29–39].

Five-dimensional SCFTs are strongly coupled [40], and do not admit any marginal deformations [41, 42], but do admit (relevant) flavor current deformations (with mass dimension one). Therefore a deformation of the UV SCFT can lead to an infrared (IR)-free gauge theory. In the geometric engineering approach, a relevant deformation of the 5d $\mathcal{N} = 1$ SCFT $\mathcal{T}_{\mathbf{X}}$ of (1.1) is equivalent to a crepant resolution of the singularity:

$$\pi_{\ell} : \widehat{\mathbf{X}}_{\ell} \longrightarrow \mathbf{X} , \quad (1.2)$$

which yields a smooth (or at the very least, less singular) local CY_3 -fold $\widehat{\mathbf{X}}_{\ell}$. Different crepant resolutions are related by flop transitions. Under suitable conditions satisfied by $\widehat{\mathbf{X}}_{\ell}$ that were spelled out in [10] for the toric case, the resulting geometry gives rise to a five-dimensional $\mathcal{N} = 1$ supersymmetric gauge theory.

In this paper, we apply the methods developed in [10] to analyze deformations of $\mathcal{T}_{\mathbf{X}}$ when \mathbf{X} is a “rank-two” isolated toric singularity. The latter refers to the fact that \mathbf{X} is described by a two-dimensional toric diagram with two interior points (that is, two compact divisors). There is a well-known classification of two-dimensional convex toric diagrams with one interior point [43, 44] (“rank-one” in this terminology). A classification of lattice polygons with two-interior points was given by [13, 45], a subset of which describe *isolated* canonical singularities of toric CY_3 -folds. The advantage of working with isolated singularities is that there is a one-to-one correspondence between crepant resolutions of these singularities and chambers of the corresponding gauge theories that they engineer. This feature is unfortunately lost in the non-isolated case. Nevertheless, we remark that the non-isolated case is extremely important, for instance, for engineering five-dimensional T_N theories [27].¹ In Figure 1, we show a map

¹A discussion of non-isolated singularities and 5d T_N theories has also appeared in [10].

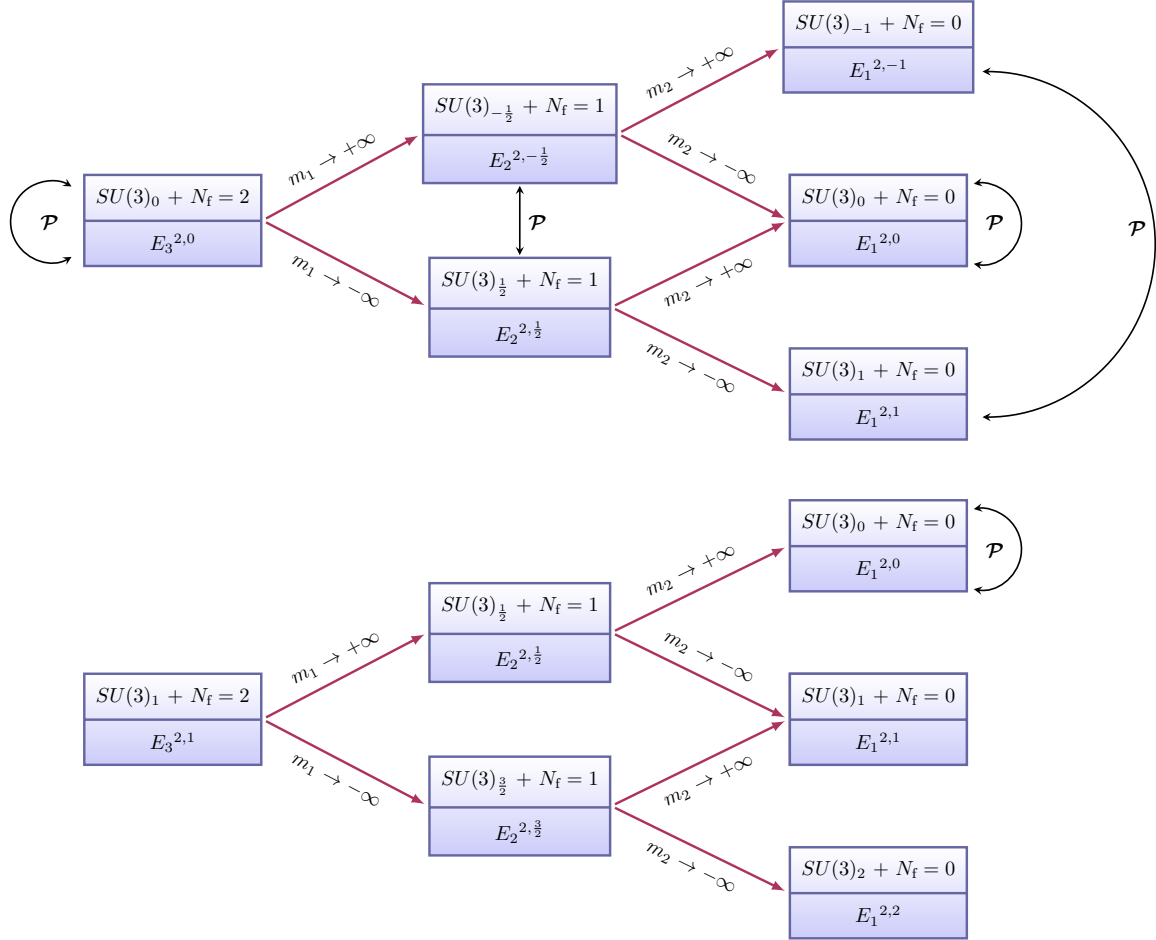


Figure 1. RG flows connecting the different rank-two toric singularities discussed in this paper, the corresponding gauge-theory phases, and their relations under parity (denoted by \mathcal{P}). Non-gauge-theoretic phases are not shown in the figure, but do arise as discussed in the main text. **Top:** Rank-two theories stemming from the $E_3^{2,0}$ (“beetle”) singularity. **Bottom:** Rank-two theories stemming from the $E_3^{2,1}$ singularity. There is a \mathcal{P} -transformed version of this flow, which is not shown here.

relating some of the toric singularities that appear in this paper, specifically among their distinct gauge-theory deformations. A recurrent theme in this paper is that theories with large flavor symmetry can flow to theories with lower flavor symmetry, an operation, which, in geometric engineering, can be understood as a combination of flop transitions in the extended parameter space of the Calabi-Yau geometry, followed by the decoupling of certain divisors in the geometry by blowing up the Kähler volumes of certain compact curves (thereby making them non-compact). As we explain in various examples, this can be understood as a geometric version of renormalization group

(RG) flow, because the operation of decoupling divisors corresponds (rather directly in gauge-theory phases) to integrating out some massive degrees of freedom. We remark here that starting from the two geometries on the extreme left in the two RG flows indicated in Figure 1, that is, the toric geometries labeled $E_3^{2,0}$ and $E_3^{2,1}$, one can obtain all other isolated toric rank-two singularities, including three singularities which have no Lagrangian description.

On the Coulomb branch, a 5d $\mathcal{N} = 1$ gauge theory is characterized by a one-loop exact cubic prepotential [1, 6] $\mathcal{F}_{\text{ft}}(\varphi; h_{0,s}, m_\alpha)$, which is a function of the Coulomb branch vevs φ , masses m_α and (inverse) gauge couplings $h_{0,s}$. In the M-theory engineering, the geometric prepotential is given by a triple intersection form on the CY_3 -fold $\widehat{\mathbf{X}}_\ell$ [46, 47], denoted by $\mathcal{F}_{\text{geo}}(\nu_a, \mu_j)$, where ν_a and μ_j are Kähler moduli of $\widehat{\mathbf{X}}_\ell$. In [10], the issue of matching geometry to field theory after turning on generic mass parameters and gauge couplings was discussed, such that the prepotentials in both descriptions match: $\mathcal{F}_{\text{ft}}(\varphi; h_{0,s}, m_\alpha) = \mathcal{F}_{\text{geo}}(\nu_a, \mu_j)$, once an appropriate map between geometry and field theory is determined. Under this map, the Kähler parameter μ_j are interpreted as mass deformations of $\mathcal{T}_{\mathbf{X}}$, whereas the Kähler moduli ν_a are, in general, some combinations of Coulomb branch vevs and mass deformations. In [10], several rank-one examples of $\mathcal{T}_{\mathbf{X}}$, and a particular rank-two example (which the authors named the “beetle geometry”) were discussed, along with their mass deformations which led to gauge-theory phases.

A crucial new ingredient introduced in [10] was a type IIA background for the five-dimensional theory, obtained by a circle reduction of the M-theory setup. Specifically, this involves the choice of an abelian subgroup $U(1)_M \subset U(1)^3$ of the toric action on $\widehat{\mathbf{X}}_\ell$, and a subsequent reduction to type IIA string theory along this $U(1)_M$, treated as the “M-theory circle” [48–51], resulting in the duality:

$$\text{M-theory on } \mathbb{R}^{1,4} \times \widehat{\mathbf{X}}_\ell \longleftrightarrow \text{Type IIA string theory on } \mathbb{R}^{1,4} \times \mathcal{M}_5, \quad (1.3)$$

where the transverse five-dimensional space $\mathcal{M}_5 \cong \widehat{\mathbf{X}}_\ell/U(1)_M$, is, in fact, a resolved A_{M-1} singularity (a hyperKähler ALE space) fibered over the real line (parametrized by $r_0 \in \mathbb{R}$). The ALE resolution contains exceptional \mathbb{P}^1 s or “2-cycles,” which are wrapped at specific values of r_0 by D6-branes, which engineer gauge groups if they wrap compact 2-cycles (with inverse gauge couplings $\frac{1}{g^2} = \text{vol}(\mathbb{P}^1)$), and flavor groups if they wrap non-compact 2-cycles [52]. However, the existence of such a type IIA description in the first place relies on whether the toric diagram of $\widehat{\mathbf{X}}_\ell$ admits a “vertical reduction.” By identifying a toric diagram as an undirected graph as we briefly explain in this paper, this requirement can be reinterpreted as a condition on the collapsibility of a graph under a sequence of edge reductions. Remarkably, this criterion also distinguishes between toric diagrams that correspond to gauge-theory phases and those that do not.

The details of the fibration, which can be recovered from the “Type IIA reduction” of the gauged linear sigma model (GLSM) associated with the toric $\widehat{\mathbf{X}}$ [48, 53], are specified by volumes of exceptional \mathbb{P}^1 s in the ALE resolution, which are piecewise linear functions of $\{r_0\} \simeq \mathbb{R}$, from which one can extract BPS masses of W-bosons, perturbative hypermultiplets, instantons, and tensions of monopole strings, etc. We carry out this type IIA analysis of [10] for rank-two isolated toric singularities.

A subtle point that arises in the study of mass deformations is the parity anomaly [54–57]. In [10] this issue was revisited in the context of 5d $\mathcal{N} = 1$ gauge theories, and used to motivate a slightly modified version of the Coulomb-branch prepotential, one that is consistent with the requirement of predicting only integer-quantized (mixed) Chern-Simons levels on the Coulomb branch. This also plays a role in the analysis of this paper, as we use the modified prepotential which is consistent with the so-called “ $U(1)_{-\frac{1}{2}}$ quantization scheme,” for the effective Chern-Simons levels [57–59]. This is a fine point and while it may not play a role in classifying SCFTs, it is nevertheless worth emphasizing and will be important for future studies of gauging flavor symmetries.

The number of distinct ($SL(2, \mathbb{Z})$ -inequivalent) two-dimensional toric diagrams increases rapidly with the rank. A natural extension will be to address higher-rank toric singularities. We anticipate that a classification of toric diagrams of rank > 2 will be more involved, although restricting to isolated singularities as a first-order step should make the problem tractable. We expect graph-theoretic techniques to be even more useful in these higher-rank cases. It might also be interesting to interpret the type IIA geometry in terms of calibrated solutions in low-energy supergravity, potentially including orientifolds to describe gauge theories with SO/Sp gauge groups. But this will require leaving the toric realm, and we leave this as another avenue for future work.

This paper is organized as follows. In section 2, we give a brief review of 5d $\mathcal{N} = 1$ theories and geometric engineering, commenting on various features such as the prepotential, the parity anomaly, the BPS states on the Coulomb branch, and the M-theory and type-IIA approaches. We also briefly motivate the use of graph theoretic-methods for operations such as enumerating crepant resolutions and characterizing allowed type IIA reductions. In section 3, we discuss in detail each of the rank-two isolated toric singularities. For every singularity with a gauge-theory phase, we derive the corresponding type IIA description, and use it to match the M-theory description with the field theory description. Along the way, we also discuss the role of walls in moduli space, and geometric transitions to non-Lagrangian phases. We also give several examples of RG flows in the extended parameter space of these toric geometries, which lead to geometries (theories) with fewer external vertices (lower flavor symmetry). Finally, the appendices contain results relevant for intermediate computations, including geometric and field-theory prepotentials, instanton masses and triple-intersection numbers.

2 5d $\mathcal{N} = 1$ theories and M-theory on a CY_3 singularity

In this section, we give a brief review of five-dimensional $\mathcal{N} = 1$ supersymmetric field theories and geometric engineering. For more detailed reviews, see [1, 6, 10] and references therein. In this paper, we focus on the Coulomb-branch physics. (See [60–62] for some recent work on the Higgs branch.)

2.1 Review of 5d $\mathcal{N} = 1$ gauge theories

These theories have eight real supercharges.² We will assume that the gauge group \mathbf{G} is compact and connected, and factorizable into a product of simple factors \mathbf{G}_s , i.e. $\mathbf{G} = \prod_s \mathbf{G}_s$. The Lie algebra of \mathbf{G} is $\mathfrak{g} = \text{Lie}(\mathbf{G})$. The two on-shell multiplets of (rigid) 5d $\mathcal{N} = 1$ supersymmetry are:³ (i) the vector multiplet \mathcal{V} , consisting of a *real* scalar φ , a gauge field A_μ , and gaugini λ and $\tilde{\lambda}$, all valued in the adjoint of \mathfrak{g} , and (ii) the hypermultiplet consisting of four real scalars and their fermionic superpartners. The vector multiplet is coupled to matter fields in the hypermultiplets \mathcal{H} in some representation \mathfrak{R} of the gauge group which is in general reducible.⁴ The R-symmetry group in Lorentzian signature is $SU(2)_R$.

The 5d supersymmetry algebra and central charges. The most general (i.e. centrally extended) \mathcal{N} -extended Poincaré superalgebra in $d = 1 + 4$ dimensions has an $Sp(\mathcal{N}) \cong USp(2\mathcal{N})$ R-symmetry, and has the form [63, 64]:

$$\{Q_\alpha^A, Q_\beta^B\} = (\gamma^\mu C)_{\alpha\beta} P_\mu \Omega^{AB} + (\gamma^\mu C)_{\alpha\beta} Z_\mu^{\circ[AB]} + C_{\alpha\beta} Z^{[AB]} + (\gamma^{\mu\nu} C)_{\alpha\beta} Z_{\mu\nu}^{(AB)}, \quad (2.1)$$

where α, β here are spinor indices (only for the purposes of this equation, and not to be confused with their use elsewhere in this paper), μ, ν are five-dimensional space-time indices, C is the charge conjugation matrix, Ω denotes the symplectic form, and (crucially) Z 's denote *real* central charges. The indices A, B range over $A, B = 1, \dots, 2\mathcal{N}$. Here $Z_\mu^{\circ[AB]}$ and $Z^{[AB]}$ are antisymmetric, and $Z_\mu^{\circ[AB]}$ is symplectic traceless: $\Omega_{AB} Z_\mu^{\circ[AB]} = 0$. The central charges $Z_\mu^{\circ[AB]}$ and $Z_{\mu\nu}^{(AB)}$ contribute to strings and membranes, respectively, whereas $Z^{[AB]}$ contributes to particle states that enter (2.11) (see below). For the purposes of this paper, since we focus on 5d SCFTs, we restrict to $\mathcal{N} = 1$ in (2.1).

²Recall that the minimal spinor of $\text{Spin}(1, 4)$ is a *symplectic* Majorana spinor.

³The tensor multiplet plays no role in our discussion, but on the Coulomb branch one can, of course, dualize a tensor to an abelian vector.

⁴In this paper, since we restrict to rank-2 theories with unitary gauge groups, the gauge group will, in fact, be $\mathbf{G} = SU(3)$ or $\mathbf{G} = U(3)$, and \mathfrak{R} will be the fundamental representation of \mathbf{G} .

Flavor symmetries. Five-dimensional gauge theories have a nontrivial global symmetry $\mathbf{G}_F \times SU(2)_R$, where the $SU(2)_R$ is the R-symmetry group introduced above, and \mathbf{G}_F is the “flavor” symmetry group, which in turn, can be further decomposed as $\mathbf{G}_F = \mathbf{G}_{\mathcal{H}} \times \prod_s U(1)_{T_s}$, that is, a group ($\mathbf{G}_{\mathcal{H}}$) that hypermultiplets transform under, and a product of “ $U(1)$ topological factors,”⁵ one for each simple factor \mathbf{G}_s in \mathbf{G} . More precisely, each hypermultiplet transforms under a representation of $\mathbf{G}_{\mathcal{H}} \times \mathbf{G}$.

5d parity anomaly, Chern-Simons terms and the $U(1)_{-\frac{1}{2}}$ quantization scheme.

A detailed discussion of the 5d parity anomaly can be found in [10]. (See also [57, 65] for original discussions in the three-dimensional setting.) Five-dimensional gauge theories suffer from a “parity anomaly,” which is the statement that parity and gauge invariance cannot simultaneously be preserved. Here, the term “gauge invariance” is used in a general sense to include all potential background gauge symmetries, including flavor symmetries. If we preserve background gauge invariance (so that a gauge field can be made dynamical), we must accept non-conservation of parity.

There are three sources of parity violation: the first is an explicit Chern-Simons term in the low-energy effective action, which for a $U(1)$ gauge field A_μ in five dimensions, is of the form,

$$S_{\text{CS}} = \frac{ik}{24\pi^2} \int_{\mathcal{M}_5} (A \wedge F \wedge F + \dots) . \quad (2.2)$$

on an oriented Riemannian five-manifold \mathcal{M}_5 , where the integrand is understood to include terms needed for a supersymmetric completion. Such a CS term is well-defined only if the CS level k is integer quantized, $k \in \mathbb{Z}$.⁶ The second source is a parity-odd contact term in the three-point function of the conserved current j^μ of a $U(1)$ symmetry acting on a fermion ψ charged under a background $U(1)$ gauge field.⁷ An explicit CS (2.2) shifts the *effective* CS level κ to $\kappa + k$. But since k is integer-quantized, only the non-integer part of the Chern-Simons contact term, $\kappa \pmod{1}$, is physical and it is what probes the presence of a parity-violating term in the effective action. For a collection of Dirac fermions ψ^i with $U(1)$ charges $Q_i \in \mathbb{Z}$, we find that,

$$\kappa = -\frac{1}{2} \sum_i Q_i^3 + k . \quad (2.3)$$

⁵These are due to the “topological symmetry” which is associated with a conserved current $j_{T_s} = \frac{1}{8\pi^2} F^{(s)} \wedge F^{(s)}$ (where $F^{(s)} = dA^{(s)} - iA^{(s)} \wedge A^{(s)}$), which is conserved due to the Bianchi identity.

⁶Note that for any simple Lie group with a nonzero cubic index, i.e. for $\mathfrak{g}_s = \text{Lie}(\mathbf{G}_s) = \mathfrak{su}(N)$ with $N > 2$, one can have explicit non-abelian supersymmetric CS terms.

⁷This term is of the form $\frac{i\kappa}{24\pi^2} \epsilon_{\mu_1\mu_2\mu_3\mu_4\mu_5} p^{\mu_4} q^{\mu_5} \subset \langle j_{\mu_1}(p) j_{\mu_2}(q) j_{\mu_3}(-p-q) \rangle$.

where the integer k is due to a scheme ambiguity which, in this case, corresponds simply to adding an explicit $U(1)$ CS term (2.2) with integer coefficient k to the action [59]. For every Dirac fermion in the gauge theory, we should specify a “quantization scheme” that is consistent with gauge invariance: this requires specifying all the CS contact terms κ , for both dynamical and background gauge fields, which corresponds to a scheme choice for k in (2.3), to remove the integer-valued ambiguity. One such scheme is the so-called “ $U(1)_{-\frac{1}{2}}$ quantization scheme,”⁸ [57] which declares,

$$\kappa_\psi = -\frac{1}{2}, \quad \text{for a massless free fermion.} \quad (2.4)$$

We choose this quantization scheme for every 5d $\mathcal{N} = 1$ hypermultiplet. The final source of parity violation is a mass term for a Dirac fermion ψ in the Lagrangian, $\delta\mathcal{L}_m = im\bar{\psi}\psi$ (for $m \in \mathbb{R}$), which explicitly breaks parity. In the limit $|m| \rightarrow \infty$, one can integrate out ψ . As shown in [7, 66], this shifts the parity-odd contact term by $\delta\kappa = -\frac{1}{2}\text{sign}(m)$. The generalization of (2.3) to a collection of *massive* Dirac fermions of masses $m_i \in \mathbb{R}$ and charges $Q_i \in \mathbb{Z}$ is:

$$\kappa_\psi = -\frac{1}{2} \sum_i Q_i^3 \text{sign}(m_i). \quad (2.5)$$

The notation “ \mathbf{G}_κ ” where \mathbf{G} is the gauge group and $\kappa \in \frac{1}{2}\mathbb{Z}$ is frequently used in the literature, and here κ denotes the effective Chern-Simons level as in (2.5).

2.2 The prepotential on the Coulomb branch

We consider the low-energy effective field theory on the Coulomb branch, where vacuum expectation values of the adjoint scalar, $\langle \boldsymbol{\varphi} \rangle = \text{diag}(\varphi_a) = (\varphi_1, \dots, \varphi_{\text{rk}(\mathbf{G})})$ break the gauge group \mathbf{G} down to a maximal torus \mathbf{H} times the Weyl group:

$$\mathbf{G} \longrightarrow \mathbf{H} \rtimes W_{\mathbf{G}}, \quad \mathbf{H} \cong \prod_{a=1}^{\text{rk}(\mathbf{G})} U(1)_a. \quad (2.6)$$

Here, $\boldsymbol{\varphi} = (\varphi_a)$ denotes the set of low-energy Coulomb-branch scalars which reside in abelian vector multiplets \mathcal{V}_a , and $\boldsymbol{\mu} = (m, h_0)$ denotes the set of real flavor masses and inverse gauge couplings.

The low-energy effective field theory on the Coulomb branch is an $\mathcal{N} = 1$ supersymmetric gauge theory that is completely determined by a one-loop exact *cubic* prepotential $\mathcal{F}(\boldsymbol{\varphi}, \boldsymbol{\mu})$ [1, 6, 46, 47]. The one-loop contribution arises from integrating

⁸Any other quantization scheme is related to this one by a shift of κ by an integer.

out W-bosons and massive hypermultiplets at a generic point on the Coulomb branch. The widely prevalent expression for the prepotential is due to [6]; we refer to it as the “IMS prepotential.” However, this prepotential can lead to non-integer mixed flavor-gauge effective CS levels. To cure this discrepancy, the authors of [10] proposed an alternate expression for the prepotential which corrects the IMS expression essentially by adding explicit “half-integer CS levels” on the Coulomb branch in order to cancel the parity anomalies by restoring background gauge invariance under the flavor group. The prepotential proposed in [10] is:

$$\begin{aligned} \mathcal{F}(\boldsymbol{\varphi}, \boldsymbol{\mu}) = & \frac{1}{2} h_{0,s} K_s^{ab} \varphi_a \varphi_b + \frac{k^{abc}}{6} \varphi_a \varphi_b \varphi_c + \frac{1}{6} \sum_{\alpha \in \Delta} \Theta(\alpha(\varphi)) (\alpha(\varphi))^3 \\ & - \frac{1}{6} \sum_{\omega} \sum_{\rho \in \mathfrak{R}} \Theta(\rho(\varphi) + \omega(m)) (\rho(\varphi) + \omega(m))^3, \end{aligned} \quad (2.7)$$

where a sum over repeated indices (s , and a, b, c) is understood, and our notation is summarized in Table 1.

s	: index ranging over the simple gauge group factors
a, b, c	: indices ranging over $\text{rk}(\mathbf{G})$, i.e. $1 \leq a \leq \text{rk}(\mathbf{G})$
$h_{0,s} = \frac{8\pi^2}{g_s}$: inverse gauge coupling for gauge group factor \mathbf{G}_s
K_s^{ab}	: Killing forms of the simple factors \mathfrak{g}_s
d_s^{abc}	: cubic Casimir of \mathfrak{g}_s
$k^{abc} = k_s d_s^{abc}$: Chern-Simons coefficient in the prepotential
$\alpha = (\alpha^a)$: a typical root of \mathfrak{g}
Δ	: set of nonzero roots (adjoint weights) of \mathfrak{g}
$\alpha(\varphi) = \alpha^a \varphi_a$: natural pairing between Coulomb vevs and adjoint weights
ω^α	: flavor weights (weights of the $\text{repn.}(\mathbf{G}_{\mathcal{H}})$)
$\omega(m) = \omega^\alpha m_\alpha$: natural pairing between hyper masses and flavor weights
ρ^a	: gauge weights (weights of $\text{repn.}(\mathbf{G})$ that the hyper transforms under)
$\rho(\varphi) = \rho^a \varphi_a$: natural pairing between Coulomb vevs and gauge weights

Table 1. Notation for symbols appearing in the prepotential.

By contrast, the IMS prepotential reads:

$$\begin{aligned} \mathcal{F}_{\text{IMS}}(\boldsymbol{\varphi}, \boldsymbol{\mu}) = & \frac{1}{2} h_{0,s} K_s^{ab} \varphi_a \varphi_b + \frac{k_{\text{eff}}^{abc}}{6} \varphi_a \varphi_b \varphi_c + \frac{1}{12} \sum_{\alpha \in \Delta} (\alpha(\varphi))^3 \\ & - \frac{1}{12} \sum_{\omega} \sum_{\rho \in \mathfrak{R}} (\rho(\varphi) + \omega(m))^3 \end{aligned} \quad (2.8)$$

The function $\Theta(x)$ appearing in (2.7) is the Heaviside step function defined by:

$$\Theta(x) = \begin{cases} 1, & \text{if } x \geq 0, \\ 0, & \text{if } x < 0. \end{cases} \quad (2.9)$$

The prepotential (2.7) yields the correct result for a hypermultiplet in the “ $U(1)_{-\frac{1}{2}}$ quantization,” that was introduced above. For a single hypermultiplet coupled to a $U(1)$ vector multiplet containing the real scalar φ , the contribution to the prepotential is $\mathcal{F}_{\mathcal{H}} = -\frac{1}{6}\Theta(\varphi)\varphi^3$. A $U(1)$ Chern-Simons term at level k contributes, on the other hand, $\mathcal{F}_{U(1)_k}(\varphi) = \frac{k}{6}\varphi^3$. Therefore the hypermultiplet contribution $\mathcal{F}_{\mathcal{H}}$ reproduces the correct decoupling limits for both signs of the real mass φ . Comparing (2.7) and (2.8), one finds that terms of order φ^3 are the same once one correctly maps the CS levels, via $k_{\text{eff}}^{abc} = k^{abc} - \frac{1}{2}\sum_{\rho,\omega}\rho^a\rho^b\rho^c$, but there is a difference in the lower-order terms (i.e. terms of order φ^2 and φ). Specifically, at a generic point on the Coulomb branch, the theory is gapped and therefore the Chern-Simons contact terms κ should all be integer-quantized. This must be true not just for the gauge CS levels, but also for mixed (gauge)²–flavor, (gauge)–(flavor)² and (flavor)³ CS levels, etc. More explicitly, *all* the following Chern-Simons levels must be integer quantized at a generic point on the Coulomb branch:

$$\left. \begin{aligned} \kappa^{abc} &= \partial_{\varphi_a}\partial_{\varphi_b}\partial_{\varphi_c}\mathcal{F}, & \kappa^{ab\alpha} &= \partial_{\varphi_a}\partial_{\varphi_b}\partial_{m_\alpha}\mathcal{F}, & \kappa^{\alpha\beta} &= \partial_{\varphi_a}\partial_{m_\alpha}\partial_{m_\beta}\mathcal{F}, \\ \kappa^{abs} &= \partial_{\varphi_a}\partial_{\varphi_b}\partial_{h_{0,s}}\mathcal{F}, & \kappa^{ass'} &= \partial_{\varphi_a}\partial_{h_{0,s}}\partial_{h_{0,s'}}\mathcal{F}, & \kappa^{\alpha\beta\gamma} &= \partial_{m_\alpha}\partial_{m_\beta}\partial_{m_\gamma}\mathcal{F}, \\ \kappa^{\alpha\beta s} &= \partial_{m_\alpha}\partial_{m_\beta}\partial_{h_{0,s}}\mathcal{F}, & \kappa^{\alpha ss'} &= \partial_{m_\alpha}\partial_{h_{0,s}}\partial_{h_{0,s'}}\mathcal{F}, & \kappa^{ss's''} &= \partial_{h_{0,s}}\partial_{h_{0,s'}}\partial_{h_{0,s''}}\mathcal{F}, \\ \kappa^{\alpha\alpha s} &= \partial_{\varphi_a}\partial_{m_\alpha}\partial_{h_{0,s}}\mathcal{F} \end{aligned} \right\} \in \mathbb{Z}. \quad (2.10)$$

One finds that (2.7) indeed produces integer-quantized effective CS levels but (2.8) does not. For a detailed discussion including a derivation of (2.7), see [10]. Henceforth, we will work exclusively with (2.7).

2.3 BPS objects on the Coulomb branch

On the Coulomb branch of 5d $\mathcal{N} = 1$ gauge theories, there are half-BPS particles and strings, which saturate suitable BPS bounds relating their masses (or tensions) to central charges in the supersymmetry algebra.

BPS particles. The masses of BPS particles are given by the absolute value of the (real) central charge of the 5d $\mathcal{N} = 1$ Poincaré superalgebra (2.1):

$$M = |Q^a\varphi_a + Q_F^\alpha m_\alpha + Q_F^s h_{0,s}|. \quad (2.11)$$

where Q^a are gauge charges, Q_F^α are the $\mathbf{G}_{\mathcal{H}}$ flavor charges and Q_F^s are $U(1)_{T_s}$ instanton charges. All charges are integer-quantized. (Also see Table 1.) The three categories of BPS particles of interest here are:

- **W-bosons** W_α , associated with the roots $\alpha \in \mathfrak{g}$ of the gauge algebra, with masses:

$$M(W_\alpha) = \alpha(\varphi) . \quad (2.12)$$

- **Hypermultiplets** $\mathcal{H}_{\rho,\omega}$, transforming in a representation of $\mathbf{G} \times \mathbf{G}_{\mathcal{H}}$ with gauge charges $Q^a = \rho^a$ and flavor charges $Q_F^\alpha = \omega^\alpha$, with masses:

$$M(\mathcal{H}_{\rho,\omega}) = \rho(\varphi) + \omega(m) . \quad (2.13)$$

- **Instantonic particles**: these are BPS particles charged under topological symmetries such that $Q_F^s \neq 0$ in (2.11). They are really solitonic particles in five dimensions, being uplifts of four-dimensional \mathbf{G} -instantons. The procedure to compute the instanton masses is outlined in Appendix A. The results of these computations appear in Tables 4 and 6 for the models discussed in this paper.

BPS monopole strings. The 5d $\mathcal{N} = 1$ gauge theory has real codimension-3 objects which are BPS monopole strings, which are five-dimensional uplifts of 4d $\mathcal{N} = 2$ monopoles. The tension of a monopole string is given by the first derivative of the prepotential with respect to the Coulomb modulus [1]:

$$T_a(\varphi, \boldsymbol{\mu}) = \frac{\partial \mathcal{F}}{\partial \varphi_a} , \quad \text{for } a = 1, \dots, \text{rk}(\mathbf{G}) . \quad (2.14)$$

2.4 M-theory on a CY_3 singularity

In this paper, we consider geometric engineering of 5d $\mathcal{N} = 1$ theories in the space transverse to M-theory on a local Calabi-Yau three-fold (CY_3) \mathbf{X} , an isolated canonical singularity. This is motivated by the conjectured correspondence,

$$\text{M-theory on } \mathbb{R}^{1,4} \times \mathbf{X} \quad \longleftrightarrow \quad \mathcal{T}_{\mathbf{X}} \text{ SCFT on } \mathbb{R}^{1,4} . \quad (2.15)$$

We give a brief recap of some relevant terminology from singularity theory.⁹ For an irreducible variety \mathbf{X} , a resolution of singularities of \mathbf{X} is a proper morphism $\pi : \widehat{\mathbf{X}} \rightarrow \mathbf{X}$ such that $\widehat{\mathbf{X}}$ is smooth and irreducible, and π induces an isomorphism of varieties $\pi^{-1}(\mathbf{X}/\widehat{\mathbf{X}}) = \mathbf{X}/\widehat{\mathbf{X}}$. A projective normal variety \mathbf{X} such that its canonical class $K_{\mathbf{X}}$ is \mathbb{Q} -Cartier has the property that $K_{\widehat{\mathbf{X}}} = \pi^* K_{\mathbf{X}} + \sum_i a_i \mathbf{E}_i$ where the sum (over i) is over irreducible exceptional divisors, and the a_i 's are rational numbers called the discrepancies. Such a variety is called \mathbb{Q} -Gorenstein. The singular variety \mathbf{X} is said to

⁹We refer the mathematically inclined reader to [13, 67–70] and references therein.

have canonical singularities if $a_i \geq 0$ for all i , in which case it is called a Gorenstein canonical singularity. ¹⁰

In the case of a generic CY_3 singularity \mathbf{X} , a crepant resolution exists:

$$\pi : \widehat{\mathbf{X}} \longrightarrow \mathbf{X}, \quad \pi^* K_{\mathbf{X}} = K_{\widehat{\mathbf{X}}}, \quad (2.16)$$

yielding a smooth local CY threefold $\widehat{\mathbf{X}}$. ¹¹ A 5d $\mathcal{N} = 1$ field theory can be obtained in the decoupling limit of an M-theory compactification on a *compact* CY_3 threefold Y , by scaling the volume of Y to infinity, while keeping finite the volumes of a collection of holomorphic 2-cycles and holomorphic 4-cycles which intersect within Y . This makes the five-dimensional Planck mass infinitely large, thereby decoupling gravity. The requirement of intersecting 2- and 4-cycles ensures that we get an interacting SCFT from the local model $\widehat{\mathbf{X}}$.

Recall that divisors are complex codimension-1 hypersurfaces (elements of $H_4(\widehat{\mathbf{X}}, \mathbb{Z})$), whereas compact curves are complex dimension-1 hypersurfaces (elements of $H_2(\widehat{\mathbf{X}}, \mathbb{Z})$). The exceptional set $\pi^{-1}(0)$ (with $0 \in \mathbf{X}$ denoting the isolated singularity) contains a certain number, say $n_4 \equiv r \geq 0$ of compact divisors, called the “rank” of \mathbf{X} . This number is the “rank” of the SCFT Coulomb branch, $r = \dim \mathcal{M}_{\mathbf{X}}^C$. In addition to compact divisors, the resolved space $\widehat{\mathbf{X}}$ contains compact curves which may intersect the exceptional divisors non-trivially. Let \mathcal{C}^a be a basis of compact holomorphic 2-cycles in $H_2(\widehat{\mathbf{X}}, \mathbb{Z})$. Note that the two-cycles \mathcal{C}^a are Poincaré dual to either compact divisors (in the exceptional set) or to non-compact divisors. Let $n_2 \equiv r + f = \dim H_2(\widehat{\mathbf{X}}, \mathbb{Z})$, with $f \geq 0$ being a nonnegative integer. Then, r is the number of compact divisors and f is the number of non-compact divisors.

Let D_k denote a typical divisor (compact or noncompact). We choose some basis of n_2 divisors $\{D_k\}_{k=1}^{n_2}$ and collect the intersection numbers of divisors and curves in a (square) matrix denoted by \mathbf{Q}^a_k :

$$\mathbf{Q}^a_k \equiv \mathcal{C}^a \cdot D_k, \quad \det \mathbf{Q} \neq 0. \quad (2.17)$$

Let J denote the Kähler form of $\widehat{\mathbf{X}}$ (a representative of the cohomology class $H^{1,1}(\widehat{\mathbf{X}})$) and let S denote the Poincaré dual Kähler class, ¹² which can be written as a linear

¹⁰The case of strict equality $a_i > 0$ for all i is called a terminal singularity, in which case the variety \mathbf{X} is called a Gorenstein terminal singularity. Terminal singularities imply that any subsequent resolution changes the canonical class.

¹¹A singular Calabi-Yau is always Gorenstein. Its singularities are either Gorenstein canonical or \mathbb{Q} -factorial Gorenstein terminal. See, for example, [71].

¹²As $\widehat{\mathbf{X}}$ is local, invoking Poincaré duality entails the use of cohomology with compact support [72].

combination of divisors over \mathbb{R} :

$$S = \sum_{k=1}^{n_2} \lambda^k D_k = \sum_{j=1}^f \mu^j D_j + \sum_{a=1}^r \nu^a \mathbf{E}_a . \quad (2.18)$$

Here we have decomposed $\{D_k\}_{k=1}^{n_2}$ into a set of r compact divisors denoted by \mathbf{E}_a (where $a = 1, \dots, r$), and f non-compact divisors, denoted by D_j (where $j = 1, \dots, f$). The Kähler volumes of a compact curve \mathcal{C}^a in $\widehat{\mathbf{X}}$ are given by:

$$\xi^a(\mu, \nu) = \int_{\mathcal{C}^a} J = \mathcal{C}^a \cdot S = \mathbf{Q}^a_k \lambda^k = \mathbf{Q}^a_j \mu^j + \mathbf{Q}^a_a \nu^a \geq 0 . \quad (2.19)$$

Incidentally, the inequalities of the form (2.19) for all basis curves are also sometimes called the Nef conditions [13] in the literature. The curves \mathcal{C}^a generators of the Mori cone. It is clear that the parameters $\mu^k \in \mathbb{R}$ and $\nu^a \in \mathbb{R}$ in (2.18) are, respectively, the Kähler moduli of two-cycles dual to non-compact four-cycles and compact four-cycles. They play an important role in developing the geometry–field-theory dictionary. In particular, μ ’s are mass parameters and couplings (which we collectively refer to as “Kähler parameters,” for they are nondynamical), whereas ν ’s involve a combination of dynamical fields (the Coulomb branch scalar vevs, i.e. φ ’s) and in general, also the masses and couplings. ¹³

The low-energy 5d $\mathcal{N} = 1$ field theory, for generic values of the Kähler parameters, is an abelian theory with gauge group $U(1)^r \cong H^2(\widehat{\mathbf{X}}, \mathbb{R})/H^2(\widehat{\mathbf{X}}, \mathbb{Z})$. In the geometric engineering picture, the $U(1)$ gauge fields arise from periods of the M-theory 3-form $C_{(3)}$ over the curves \mathcal{C}^a dual to compact divisors, i.e. $A_{U(1)}^{(a)} = \int_{\mathcal{C}^a} C_{(3)}$ (where $a = 1, \dots, r$). The exact prepotential for this abelian gauge theory can be computed from the geometry using the following expression: ¹⁴

$$\mathcal{F}(\mu, \nu) = -\frac{1}{6} \int_{\widehat{\mathbf{X}}} J \wedge J \wedge J = -\frac{1}{6} S \cdot S \cdot S . \quad (2.20)$$

The prepotential involves triple-intersection numbers of $\widehat{\mathbf{X}}$, specifically those of the form (dropping the dot for brevity) $D_i D_j \mathbf{E}_a$, $D_i \mathbf{E}_a \mathbf{E}_b$, $\mathbf{E}_a \mathbf{E}_b \mathbf{E}_c$, and $D_i D_j D_k$. But since $\widehat{\mathbf{X}}$ is noncompact, the triple-intersection numbers involving three noncompact divisors ($D_i D_j D_k$) are not well-defined. In subsequent computations of the geometric prepotential (2.20), we ignore such contributions to the prepotential, and we refer to the result as the “compact part” of the prepotential. We refer the reader to Appendix B of [10] for a more detailed discussion of this point.

¹³The important basis-independent feature is that the μ ’s *never* depend on Coulomb branch scalars.

¹⁴The minus sign is simply a matter of convention, chosen in [10].

BPS states from geometry. The BPS states from geometric engineering are:

- Electrically charged BPS particles, from M2-branes wrapping holomorphic (compact) 2-cycles \mathcal{C}^a . These have masses given by the Kähler volumes (2.19), and
- (Dual) magnetically charged BPS monopole strings, from M5-branes wrapping holomorphic surfaces (compact 4-cycles) \mathbf{E}_a . These have tensions by the Kähler volumes of the compact divisors:

$$T_a(\mu, \nu) \equiv -\partial_{\nu^a} \mathcal{F}(\mu, \nu) = \frac{1}{2} \int_{\mathbf{E}_a} J \wedge J = \text{vol}(\mathbf{E}_a) . \quad (2.21)$$

The extended parameter space. Given an isolated canonical CY₃ singularity \mathbf{X} , there can be several birationally equivalent resolutions $\pi_\ell : \widehat{\mathbf{X}}_\ell \rightarrow \mathbf{X}$, each of which is a local Calabi-Yau 3-fold with the same singular limit. The collection of all such $\widehat{\mathbf{X}}_\ell$ constitutes, for a given singularity \mathbf{X} , the set of all crepant resolutions. For a particular $\widehat{\mathbf{X}}_\ell$, the Kähler cone is given by the set of all positive Kähler forms:

$$\mathcal{K}(\widehat{\mathbf{X}}_\ell \setminus \mathbf{X}) = \left\{ [J] \in H^{1,1}(\widehat{\mathbf{X}}_\ell) \cap H^2(\widehat{\mathbf{X}}_\ell, \mathbb{R}) \mid \int_{\mathcal{C}} J = S \cdot \mathcal{C} > 0 \ \forall \text{ hol. curves } \mathcal{C} \in \widehat{\mathbf{X}}_\ell \right\} \quad (2.22)$$

The parameter space of all massive deformations of 5d SCFTs obtained from M-theory is given by the extended Kähler cone, which is the closure of all compatible Kähler cones: $\mathcal{P}_{\mathcal{T}\mathbf{X}} = \widehat{\mathcal{K}}(\mathbf{X}) = \left\{ \bigcup_\ell \mathcal{K}(\widehat{\mathbf{X}}_\ell \setminus \mathbf{X}) \right\}^c$. Pairs of Kähler cones – corresponding to birationally equivalent pairs of Calabi-Yau spaces – are glued along common faces in the interior of $\widehat{\mathcal{K}}(\mathbf{X})$. The boundaries of $\widehat{\mathcal{K}}(\mathbf{X})$ are of the following type [7]:

- Boundaries of Kähler cones of individual crepant resolutions: these are boundaries of $\mathcal{K}(\widehat{\mathbf{X}}_\ell \setminus \mathbf{X})$, where the threefold $\widehat{\mathbf{X}}_\ell$ becomes singular. This happens when a 2-cycle in $\widehat{\mathbf{X}}_\ell$ shrinks to zero size and grows to negative volume in a birational Kähler cone, signaling a flop transition. This corresponds to a BPS particle becoming massless. At such points, the prepotential (2.20) becomes non-smooth.
- Exterior boundaries of $\widehat{\mathcal{K}}(\mathbf{X})$ where a 4-cycle \mathbf{E}_a can collapse to either (i) a 2-cycle, or (ii) a point.

The “origin of moduli space” is the origin of $\widehat{\mathcal{K}}(\mathbf{X})$, which is also the SCFT point. It corresponds to the singular geometry \mathbf{X} , and is given by the connected union of 4-cycles (divisors) collapsing to a point.

Toric geometry and type IIA reduction. In this paper, we will further assume that the isolated canonical singularity \mathbf{X} is also toric. This allows us to exploit the computational machinery of toric geometry (see [43, 44, 69, 71, 73–76] for useful reviews). This restriction admittedly ignores many interesting cases by confining attention to a small subset of singularities. We leave a study of non-toric singularities for future work.

In particular this implies that a resolution $\widehat{\mathbf{X}}$ of such a singularity is described by a two-dimensional toric diagram. This is specified as the convex hull of a set of lattice points $\mathbf{w}_i = (w_i^x, w_i^y) \in \mathbb{Z}^2$ (here $i = 1, \dots, n$, where n is the number of vertices), which contains a number $r \geq 0$ of internal points, denoting compact divisors. The $n_E \equiv n - r$ external points denote noncompact divisors. Edges in the toric diagram connecting two vertices denote curves in the geometry.

The toric variety $\widehat{\mathbf{X}}$ can be described using a gauged linear sigma model (GLSM) [53]. The key idea here is to realize the toric variety as the moduli space of vacua of a certain 2d $\mathcal{N} = (2, 2)$ supersymmetric gauge theory. The defining data for this construction is (i) a set of $U(1)$ charges $Q_i^{\mathbf{a}}$ (where $i = 1, \dots, n$, and $\mathbf{a} = 1, \dots, n - 3$ labels a set of linearly independent compact curves – the Mori cone generators), and (ii) a set of Fayet-Iliopololous (FI) parameters $\{\xi_{\mathbf{a}}\}$ for the auxiliary gauge groups $U(1)_{\mathbf{a}}$. Then, the toric CY₃ variety is defined as a Kähler quotient,

$$\widehat{\mathbf{X}} \cong \mathbb{C}^n //_{\xi} U(1)^{n-3} = \left\{ z_i \in \mathbb{C}^n \left| \sum_i Q_i^{\mathbf{a}} |z_i|^2 = \xi_{\mathbf{a}} \right. \right\} / U(1)^{n-3}, \quad n \equiv n_E + r, \quad (2.23)$$

which we recognize as the familiar quotienting of a set of “D-term equations” by some $U(1)$ actions. Different resolutions of the singularity – which are related by flop transitions – differ in their sets of $U(1)$ charges $Q_i^{\mathbf{a}}$, which always obey the “Calabi-Yau condition,” namely, $\sum_{i=1}^n Q_i^{\mathbf{a}} = 0 \forall \mathbf{a} = 1, \dots, n - 3$. Arranged as a matrix of charges, the CY condition implies that the sum all charges in any row vanishes.

Assuming that the 2d toric diagram satisfies certain conditions (which we will revisit below), it is possible to collapse or project it down to a 1d toric diagram for the corresponding geometry in type IIA string theory. This is known as a “vertical reduction,” which was extensively discussed in [10], which we refer the interested reader to.¹⁵ The idea behind this method is to use a $U(1)_M \subset U(1)^3$ isometry of \mathbf{X} as an M-theory circle to view the $\widehat{\mathbf{X}}$ as a circle fibration over a five-dimensional base \mathcal{M}_5 (that is, $U(1)_M \hookrightarrow \widehat{\mathbf{X}} \longrightarrow \mathcal{M}_5$), such that the base itself is a fibration of an ALE space over the real line parametrized by r_0 :

$$\widehat{\mathbf{Y}}(r_0) \longrightarrow \mathcal{M}_5 \longrightarrow \mathbb{R} \cong \{r_0\}. \quad (2.24)$$

¹⁵This method relies on a technique that was originally introduced in [48] and developed in [49–51, 77, 78] for M-theory on Calabi-Yau fourfold singularities.

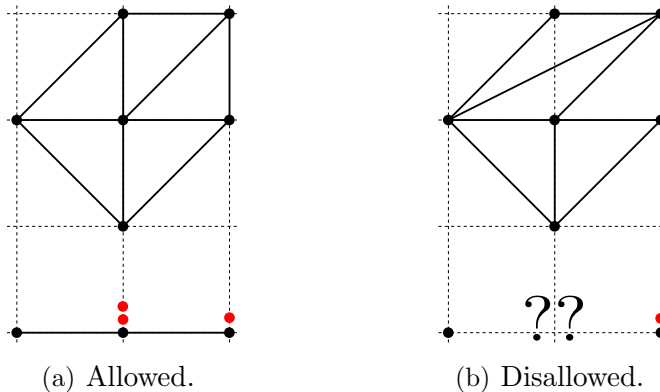


Figure 2. Left: An example of an allowed vertical reduction of a 2d toric diagram, which gives rise to a resolved A_1 singularity visualized by the 1d toric diagram below. **Right:** An example of a disallowed vertical reduction, due to the presence of an edge that would collide with either one of the vertices along the vertical direction under such a reduction.

The complex two-dimensional space $\widehat{Y}(r_0)$, being toric, is the resolution of an A-type toric singularity, a hyperKähler ALE space. The volumes of exceptional \mathbb{P}^1 s in the resolution, denoted by $\chi_s(r_0)$, are piecewise-linear functions of r_0 , the slopes of which jump at the locations of gauge- and flavor- D6-branes. The slope of $\chi_s(r_0)$ jumps by 2 when we cross a gauge D6-brane, and by 1 when we cross a flavor D6-brane. We refer to these functions as the “IIA profiles”. From plots of these functions, one can infer various properties of the field theory and geometry. Let us briefly recall the dictionary developed in [10]:¹⁶

- **Effective Chern-Simons levels:** Due to the presence of a Wess-Zumino term on the worldvolume of gauge D6-branes [48], there is an effective 5d Chern-Simons level k_s for a probe D6-brane wrapping an exceptional \mathbb{P}^1_s . This can be computed directly from the slope of the IIA profile [10, 51] $\chi_s(r_0)$ as follows. First, for every exceptional curve \mathbb{P}^1_s , define the asymptotic slopes,

$$\chi'_{s,\pm} = \lim_{r_0 \rightarrow \pm\infty} \chi'_s(r_0) . \quad (2.25)$$

Then the effective Chern-Simons level $k_{s,\text{eff}}$ is given as the negative average of the asymptotic slopes:

$$k_{s,\text{eff}} = -\frac{1}{2}(\chi'_{s,-} + \chi'_{s,+}) . \quad (2.26)$$

¹⁶In addition, there are bifundamental hypermultiplets for quiver gauge theories realized by open strings stretched between two gauge D6-branes that wrap *adjacent* exceptional curves, but we do not encounter them in this paper.

This “effective CS level” is in general half-integer, and equals the contact term κ including half-integer contributions from matter fields, consistent with (2.5).

- **W-bosons of the $SU(n_s)$ gauge group**, given by open strings stretched between two gauge D6-branes at $r_0 = \xi_{s,(a_i)}$ and $r_0 = \xi_{s,(a_j)}$, have masses:

$$M(W_{s;i,j}) = |\xi_{s,(a_i)} - \xi_{s,(a_j)}| . \quad (2.27)$$

- **Fundamental hypermultiplets**, given by open strings stretched between a gauge D6-brane wrapping a compact 2-cycle at $r_0 = \xi_{s,(a_i)}$ and a flavor D6-brane wrapping a non-compact 2-cycle at $r_0 = \xi_{s,(f)}$, have masses:

$$M(\mathcal{H}_{s;i,\text{flavor}}) = |\xi_{s,(a_i)} - \xi_{s,(f)}| . \quad (2.28)$$

- **Tension of monopole strings**, given by the area under the IIA profile between the locations of two adjacent gauge D6-branes,

$$T_{s,(a)} = \int_{\xi_{s,(a)}}^{\xi_{s,(a+1)}} dr_0 \chi(r_0) , \quad (2.29)$$

which must match the first-derivatives of the gauge theory prepotential (2.14) in the field-theory description.

2.5 Graph-theoretic perspective

The setting described in the previous subsection, especially the criterion in Figure 2, strongly motivates the use of graph-theoretic techniques to study these geometries. In this work, we implement the idea of associating a graph to a toric diagram under study, with the aim of exploiting well-known notions and algorithms in the graph-theory literature. We introduce the relevant terminology briefly in this section, for readers unfamiliar with graph theory, but we focus only on the few features that are relevant to toric geometry. For comprehensive reviews and applications, we refer the reader to [79–81] and references therein.

A 2d toric diagram can be represented as an *undirected graph* (with no loops) in \mathbb{Z}^2 . A graph $G = (V, E)$ is specified by a set V containing vertices and a set E containing edges. An edge $e \in E$ connecting vertices $i, j \in V$ can be specified as a tuple $e = (i, j)$ of vertices. For an undirected graph, the set of tuples is unordered, i.e. the tuples (i, j) and (j, i) are considered to be equivalent. Therefore, for an undirected graph, the adjacency matrix, which is a map from $A_G : V \times V \rightarrow \{0, 1\}$, defined by

$$A_G(i, j) = \begin{cases} 1, & \text{if } \exists \text{ edge } e = (i, j) \in E \\ 0, & \text{otherwise ,} \end{cases} \quad (2.30)$$

is symmetric. The no loops condition further implies that all diagonal entries are 0, so it is sufficient to work with the upper (or lower) triangular part of the matrix, which is specified by $|V|(|V| - 1)/2$ entries. The adjacency matrix is typically sparse. The spectral properties of the adjacency matrix contain useful information about the graph. One can show that the number of edges is given by,

$$|E| = \frac{1}{2} \text{tr}(A_G^2) . \quad (2.31)$$

This counts all edges, including the non-compact curves that make up the toric skeleton (that is, the boundary of the convex hull of V). A cycle in a graph is defined as a non-empty path in which only the first and last path repeat. The number of triangles (3-cycles) in the toric diagram is given [82] by,

$$\mathcal{N}_\Delta = \frac{1}{6} \text{tr}(A_G^3) . \quad (2.32)$$

Clearly, a simplex in a toric diagram is a cycle of length 3, but not every cycle of length 3 is a simplex. (Recall that a simplex in toric geometry must have a minimal simplicial volume of $\frac{1}{2}$.)

In graph theory, the “shape” of a graph usually does not matter, only the connectivity does. However, in toric geometry, the “shape” (up to $SL(2, \mathbb{Z})$ equivalence) does matter, since the locations of the divisors (vertices) critically dictate whether a given toric diagram corresponds to a crepant resolution, and also whether or not some curves can flop. In the previous section, we discussed the “vertical reduction” of the toric diagram. This has a natural interpretation in graph theory, where different ways of reducing the toric diagram can be viewed as different instances of an *edge reduction*. This takes two vertices connected by an edge and eliminates the edge by mapping both vertices to a third vertex (which can be regarded as the fusion of the two vertices). Formally, if $A_G(u, v) = 1$ for a pair of vertices $u, v \in V$ (so that they are connected by an edge) and given a third vertex $w \in V$, we define a function $f : V \rightarrow V$ via its action on the vertices of V by,

$$f_{u,v,w}(x) = \begin{cases} x, & x \in V \setminus \{u, v\}, \\ w, & \text{if } A_G(u, v) = 1 \text{ and } x \in \{u, v\} . \end{cases} \quad (2.33)$$

In this language, the allowed vertical reduction of Figure 2 corresponds to a sequence of (vertical) edge reductions such that at each step there is no obstruction due to an internal edge crossing an internal vertex. This systematizes the study of toric graphs and generalizes well to higher-rank examples.

A related motivation for viewing a toric diagram as a graph is the fact that different crepant resolutions (related by flops) differ only in their connectivities and so a

combinatorial enumeration of crepant resolutions translates to a similar enumeration problem for graphs. The number of crepant resolutions grows very quickly with the rank, and although we restrict our attention in this paper – for reasons of simplicity and brevity – only to *isolated* toric singularities at rank-two, a graph-based enumeration algorithm works even for nonisolated singularities at rank > 2 . It might also be interesting to relate other ideas from spectral graph theory [80] to toric geometry in the context of studying 5d SCFTs. These are possible avenues for future work. In the remainder of this paper, we focus on the isolated toric rank-two case.

3 Rank-two isolated toric CY_3 singularities

An exhaustive list of rank-2 toric diagrams, i.e. toric diagrams with 2 interior points, was given by Xie and Yau in [13], based on earlier work by Wei and Ding [45] which classified convex polygons with two interior points. Their list consists of 44 singularities, of which only 10 describe isolated toric singularities, i.e. toric diagrams with no lattice point on the boundary (except if it is a vertex). These 10 cases are listed in Figure 3.

The rank-2 singularities \mathbf{X} are labeled as:

$$E_f^{2,\kappa_{\text{eff}}} , \tag{3.1}$$

where $f \equiv E - 3$ denotes the rank of the flavor symmetry of the theory $\mathcal{T}_{\mathbf{X}}$ (here E is the number of external points in the toric diagram), the first superscript (2) denotes the rank of the singularity (the number of internal points), and the second superscript κ_{eff} is the effective Chern-Simons level when a gauge-theory description exists or is ‘NL’ when the theory admits no Lagrangian interpretation.

In the remainder of this section, we consider each singularity that admits a gauge theory description, and examine its crepant resolutions, comparing the geometric description (using the M-theory and the type IIA interpretations) with the gauge-theory description. Along the way, we comment on various features of each model, including the BPS states and walls in moduli space, and also remark on resolutions that admit no gauge-theory interpretation. We use M-theory/type IIA duality to characterize the existence or non-existence of a “gauge-theory phase” of the resolved toric Calabi-Yau geometry based on whether or not the toric diagram admits a vertical reduction as explained in the previous section. ¹⁷

¹⁷Another approach [6, 16] is to find a ruling of the exceptional set $\pi^{-1}(0) \subset \widehat{\mathbf{X}}$, that is, a set of surfaces E which have the form of a fibration of \mathbb{P}^1 over a curve \mathcal{C} (i.e. $\mathbb{P}^1 \hookrightarrow E \rightarrow \mathcal{C}$), such that M2-branes wrapping \mathcal{C} are identified with W-bosons.

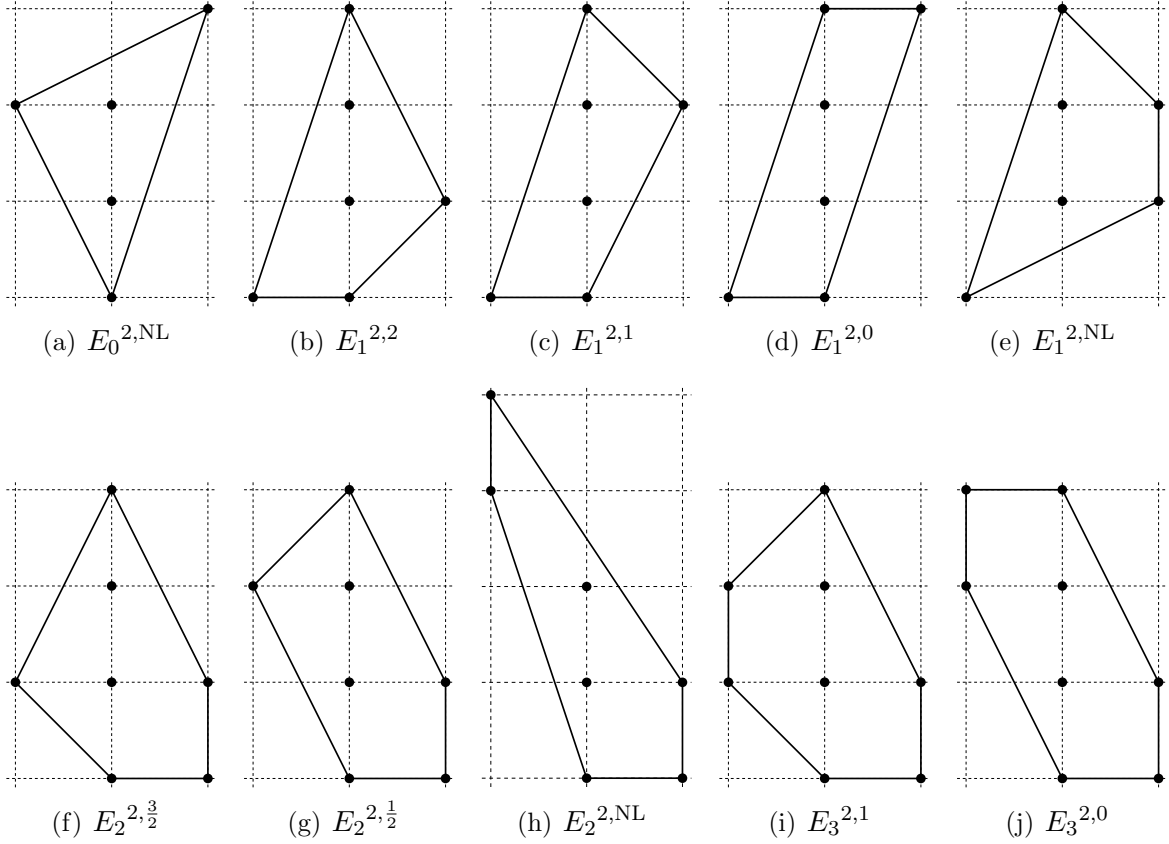


Figure 3. The 10 $SL(2, \mathbb{Z})$ -inequivalent isolated toric rank-2 singularities.

Non-gauge-theoretic singularities. Before proceeding, let us comment on the non-gauge-theoretic singularities $E_\ell^{2,\text{NL}}$ for $\ell = 0, 1, 2$, which admit no vertical reduction. Let $\mathcal{C}(E_\ell^{2,\text{NL}})$ denote the set of crepant resolutions of $E_\ell^{2,\text{NL}}$, with a typical crepant resolution denoted by $\mathcal{R}_\ell^{\text{NL}} \in \mathcal{C}(E_\ell^{2,\text{NL}})$. Also, let $\mathcal{C}_{\text{vert}}^{(2)}$ be the space of all rank-2 crepant resolutions that admit a vertical reduction. There is a natural action of $g \in SL(2, \mathbb{Z})$ action on every \mathcal{R}_ℓ , denoted by $g \cdot \mathcal{R}_\ell$ (this simply applies an $SL(2, \mathbb{Z})$ transformation given by g on the toric vertices of \mathcal{R}_ℓ). The fact that these singularities are non-gauge-theoretic is equivalent to saying that there exists no $SL(2, \mathbb{Z})$ transformation that yields a resolution with a vertical reduction:

$$\forall g \in SL(2, \mathbb{Z}) \text{ and } \forall \mathcal{R}_\ell^{\text{NL}} \in \mathcal{C}(E_\ell^{2,\text{NL}}), \quad g \cdot \mathcal{R}_\ell^{\text{NL}} \notin \mathcal{C}_{\text{vert}}^{(2)}, \quad \text{for } \ell = 0, 1, 2. \quad (3.2)$$

The $E_2^{2,\text{NL}}$ and $E_3^{3,\text{NL}}$ singularities each admit an interpretation as a gauge theory coupled to a “non-Lagrangian sector,” due to the existence of a ruling (see footnote 17). But $E_0^{2,\text{NL}}$ does not admit such a ruling. (In this case, a ruling is equivalent to having a

line with three points.) In fact, resolutions of these non-gauge-theoretic singularities can be arrived at by starting from resolutions of gauge-theoretic singularities $E_{\rho}^{2, \kappa_{\text{eff}}}$ (that is, the singularities whose crepant resolutions do admit a gauge theory interpretation) by a combination of flop transitions followed by decoupling divisors in the geometry by sending the volumes of certain compact curves to infinity. We interpret this as a “generalized renormalization group (RG) flow,” in the extended parameter space of the Calabi-Yau geometry.

Parity. Parity \mathcal{P} acts on the toric diagram by the application of the central element $C_0 = S^2 \in SL(2, \mathbb{Z})$. If the effective Chern-Simons level k_{eff} of a gauge-theory phase vanishes, the toric diagram is \mathcal{P} -invariant. In Figure 1, this action of parity on the gauge-theory phases is indicated by arrows relating various geometries. Note that parity flips the sign of the effective Chern-Simons level k_{eff} .

RG flows at rank-two. As we remark in more detail in various examples below and as also mentioned in the introduction, there are many RG flows that relate different geometries and field theories. The crucial point to note here is that starting from the two singularities labeled $E_3^{2,1}$ and $E_3^{2,0}$ one can recover all isolated toric singularities of rank-two shown in Figure 3, by a combination of flops and divisor decouplings, which we refer to as RG flow. For example, Figure 1 already shows how the various rank-2 gauge-theory phases arise starting from these bigger geometries.

Vertical reductions. For every toric rank-two singularity of Figure 3 that admits a crepant resolution with a vertical reduction (that is, whenever a gauge-theory phase exists), the type IIA geometry takes the form of a resolved A_1 singularity fibered over the $x^9 = r_0$ direction, with a set of D6-branes wrapping the exceptional \mathbb{P}^1 s in the resolution. The fibration, as discussed in Section 2.4, is characterized by a piecewise linear function $\chi(r_0)$, the precise form of which depends on the specific details of the resolution. We refer to this function loosely as the “IIA profile”. For a review of the vertical reduction method, see [10]. Recall that the vertical reduction is defined by the choice of an auxiliary “ $U(1)_M$ line” in the GLSM charge matrix, which specifies a redundant parametrization of the GLSM. The integer charges Q_i^M ($i = 1, \dots, n$, where n is the number of toric vertices) of this line are required to satisfy $\sum_{i=1}^n Q_i^M = 0$ and $\sum_{i=1}^n w_i^y Q_i^M = 1$ where $\mathbf{w} = (w_i^x, w_i^y) \in \mathbb{Z}^2$ are the coordinates of the toric vertices. In all the geometries considered in this paper, the nonzero $U(1)_M$ charges satisfying these conditions are given by $Q_{\mathbf{E}_1}^M = -1$ and $Q_{\mathbf{E}_2}^M = 1$ (and $Q_i^M = 0$ for $i \neq \mathbf{E}_1, \mathbf{E}_2$), where $\mathbf{E}_{1,2}$ denote the two compact divisors in any rank-two toric diagram (which are the two interior points). In every case, we begin by briefly outlining the toric geometry, listing the linear relations among divisors and curve classes, the GLSM charge matrix, the

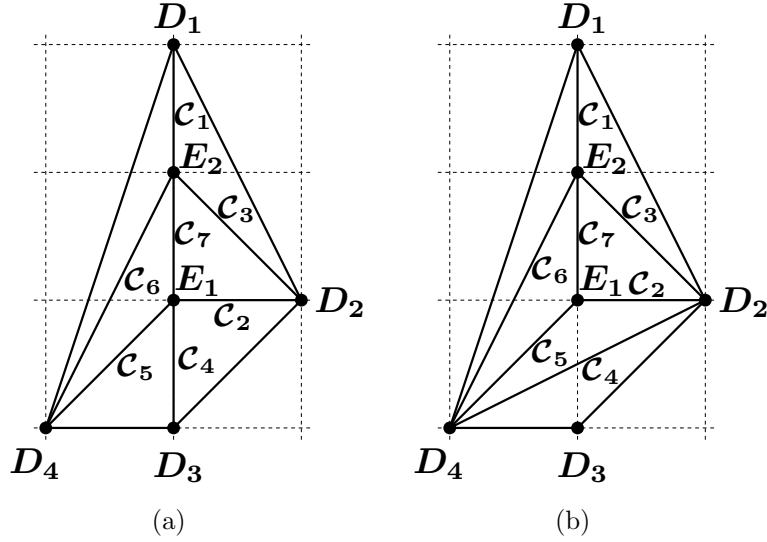


Figure 4. The two crepant resolutions of the $E_1^{2,2}$ singularity. Resolution (a) admits a vertical reduction.

intersection numbers, and the geometric prepotential, followed by an analysis of the IIA profile leading to a map between geometry and field theory parameters. To keep the discussion brief, we spell out only the relevant details.

3.1 The $E_1^{2,2}$ singularity and $SU(3)_2$ gauge theory

In this section, we consider the $E_1^{2,2}$ singularity of Figure 3(b). There are two crepant resolutions, shown in Figure 4, related by a flop of the curve \mathcal{C}_4 . Let us focus on resolution (a). There are four non-compact toric divisors D_i ($i = 1, \dots, 4$), and two compact toric divisors \mathbf{E}_1 and \mathbf{E}_2 with the following linear relations:

$$D_2 \simeq D_4, \quad \mathbf{E}_1 \simeq D_1 - 3D_2 - 2D_3, \quad \mathbf{E}_2 \simeq -2D_1 + D_2 + D_3. \quad (3.3)$$

The curves \mathcal{C} are given as intersections of pairs of divisors according to:

$$\begin{aligned} \mathcal{C}_1 &= \mathbf{E}_2 \cdot D_1, & \mathcal{C}_2 &= \mathbf{E}_1 \cdot D_2, & \mathcal{C}_3 &= \mathbf{E}_2 \cdot D_2, & \mathcal{C}_4 &= \mathbf{E}_1 \cdot D_3, \\ \mathcal{C}_5 &= \mathbf{E}_1 \cdot D_4, & \mathcal{C}_6 &= \mathbf{E}_2 \cdot D_4, & \mathcal{C}_7 &= \mathbf{E}_2 \cdot \mathbf{E}_1. \end{aligned} \quad (3.4)$$

The linear relations among curve classes are

$$\mathcal{C}_1 \simeq \mathcal{C}_2 + 3\mathcal{C}_3 + \mathcal{C}_4, \quad \mathcal{C}_5 \simeq \mathcal{C}_2, \quad \mathcal{C}_6 \simeq \mathcal{C}_3, \quad \mathcal{C}_7 \simeq \mathcal{C}_2 + \mathcal{C}_4. \quad (3.5)$$

We may take $\{\mathcal{C}_2, \mathcal{C}_3, \mathcal{C}_4\}$ as generators of the Mori cone. Thus, the GLSM charge matrix is:

$$\begin{array}{c|cccccc|c}
 & D_1 & D_2 & D_3 & D_4 & \mathbf{E}_1 & \mathbf{E}_2 & \text{vol}(\mathcal{C}) \\
\hline
\mathcal{C}_2 & 0 & 0 & 1 & 0 & -2 & 1 & \xi_2 \\
\mathcal{C}_3 & 1 & 0 & 0 & 0 & 1 & -2 & \xi_3 \\
\mathcal{C}_4 & 0 & 1 & -1 & 1 & -1 & 0 & \xi_4 \\
\hline
U(1)_M & 0 & 0 & 0 & 0 & -1 & 1 & r_0
\end{array} \tag{3.6}$$

The FI terms $\xi_2 \geq 0$, $\xi_3 \geq 0$, and $\xi_4 \geq 0$ are, respectively, the volumes of the compact curves \mathcal{C}_2 , \mathcal{C}_3 and \mathcal{C}_4 . In (3.6) we have shown also the last line (“ $U(1)_M$ line”) which defines the GLSM of the vertical reduction, which we shall describe shortly.

Geometric prepotential. The geometric prepotential can be computed from M-theory as follows. The Kähler cone can be parametrized by

$$S = \mu_4 D_4 + \nu_1 \mathbf{E}_1 + \nu_2 \mathbf{E}_2 . \tag{3.7}$$

By (2.19) the parameters (μ_1, ν_1, ν_2) are related to the FI parameters as:

$$\xi_2 = -2\nu_1 + \nu_2 \geq 0, \quad \xi_3 = \nu_1 - 2\nu_2 \geq 0, \quad \xi_4 = \mu_4 - \nu_1 \geq 0 . \tag{3.8}$$

Using the charge matrix (the entries of which immediately give the intersection numbers between divisors and curves) and the linear equivalences among divisors, it is straightforward to compute the relevant triple-intersection numbers:

$$\begin{aligned}
D_4 \mathbf{E}_1 \mathbf{E}_2 = 1, \quad D_4^2 \mathbf{E}_1 = 0, \quad D_4^2 \mathbf{E}_2 = 0, \quad D_4 \mathbf{E}_1^2 = -2, \quad D_4 \mathbf{E}_2^2 = -2, \\
\mathbf{E}_1^2 \mathbf{E}_2 = -3, \quad \mathbf{E}_1 \mathbf{E}_2^2 = 1, \quad \mathbf{E}_1^3 = 8, \quad \mathbf{E}_2^3 = 8 .
\end{aligned} \tag{3.9}$$

The value of D_4^3 , the triple-intersection number for the noncompact divisor is ambiguous and regulator-dependent. Its coefficient, μ_4 , does not depend on Coulomb moduli (and thus its value does not affect subsequent analysis of BPS states), so we may as well drop this term.¹⁸ The compact part of the prepotential (i.e. D_4^3 -independent part) is determined to be:

$$\mathcal{F}(\nu_1, \nu_2; \mu_4) = -\frac{1}{6} S^3 = -\frac{4}{3}(\nu_1^3 + \nu_2^3) + \frac{3}{2}\nu_1^2\nu_2 - \frac{1}{2}\nu_1\nu_2^2 - \mu_4\nu_1\nu_2 + \mu_4(\nu_1^2 + \nu_2^2) . \tag{3.10}$$

To relate to the non-abelian gauge theory description, we need to discuss the type-IIA string theory reduction of this geometry.

¹⁸The regulator dependence was explored and discussed in some detail in [10], where a method based on the Jeffrey-Kirwan residue was proposed to compute it.

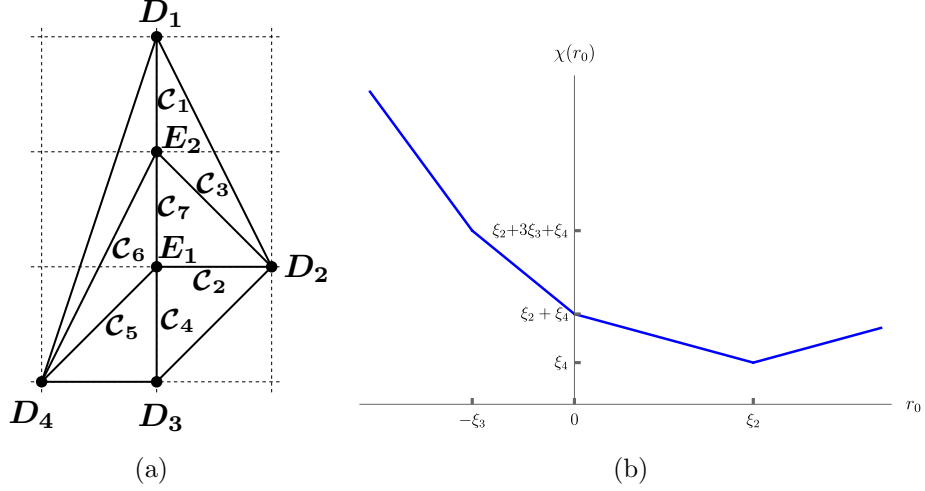


Figure 5. Resolution (a) of the $E_1^{2,2}$ singularity and its vertical reduction.

Type IIA reduction and gauge theory description. The vertical reduction of the toric diagram of Figure 4(a) is represented in the GLSM approach via the $U(1)_M$ charges in the last line of (3.6). The type IIA string background is a resolved A_1 singularity fibered over the $x^9 = r_0$ direction. The four vertical points in the toric diagram give rise to three D6-branes wrapping the exceptional \mathbb{P}^1 in the resolved A_1 singularity. This yields an $SU(3)$ gauge theory, as we explain below.

The volume of the exceptional \mathbb{P}^1 varies as a function of r_0 , and is denoted by $\chi(r_0)$. This is a piecewise-linear function, which is determined to be:

$$\chi(r_0) = \begin{cases} -5r_0 + \xi_2 - 2\xi_3 + \xi_4, & \text{for } r_0 \leq -\xi_3 \\ -3r_0 + \xi_2 + \xi_4, & \text{for } -\xi_3 \leq r_0 \leq 0 \\ -r_0 + \xi_2 + \xi_4, & \text{for } 0 \leq r_0 \leq \xi_2 \\ +r_0 - \xi_2 + \xi_4, & \text{for } r_0 \geq \xi_2 . \end{cases} \quad (3.11)$$

From a sketch of this function, shown in Figure 5(b), we can infer several features of the geometry. First of all, at each of the three kinks of the function where the slope changes by 2, namely, at $r_0 = -\xi_3$, $r_0 = 0$ and $r_0 = +\xi_2$, there is a gauge D6-brane. When ξ_2 and ξ_3 are zero, the three wrapped D6-branes realize a 5d $SU(3)$ gauge group at $r_0 = 0$. The inverse coupling of the $SU(3)$ gauge group is given by the size of the \mathbb{P}^1 at $r_0 = 0$, which is $h_0 = \xi_4$ when $\xi_2 = \xi_3 = 0$. The effective Chern-Simons level is given by (2.26), which yields:

$$\kappa_{s,\text{eff}} = -\frac{1}{2}(1 - 5) = +2 . \quad (3.12)$$

Using (A.3), the gauge theory prepotential for $SU(3)_{k=2}$ gauge theory is given by:

$$\mathcal{F}_{SU(3)_{k=2}} = h_0(\varphi_1^2 + \varphi_2^2 - \varphi_1\varphi_2) + \frac{1}{2}\varphi_1^2\varphi_2 - \frac{3}{2}\varphi_1\varphi_2^2 + \frac{4}{3}(\varphi_1^3 + \varphi_2^3) . \quad (3.13)$$

Finite FI parameters (i.e. finite volumes of the compact curves in the toric diagram) correspond to separating the D6-branes along the r_0 direction, which is equivalent to flowing onto the Coulomb branch. Open strings stretched between the gauge D6-branes yield W-bosons and their superpartners. In this case, the simple root W-bosons have masses given by (2.27), which yields,

$$M(W_1) = 2\varphi_2 - \varphi_1 = \xi_2, \quad M(W_2) = 2\varphi_1 - \varphi_2 = \xi_3 . \quad (3.14)$$

We note the appearance of the Cartan matrix of $\mathfrak{su}(3)$ in the field-theoretic expressions for the W-boson masses, consistent with (2.12).

Instantons are engineered by D2-branes wrapping the gauge D6-branes, i.e. D2-branes wrapping the D6-branes at $r_0 = -\xi_3$, $r_0 = 0$ and $r_0 = \xi_2$. These states have masses given by the volumes of the exceptional \mathbb{P}^1 's at these values of r_0 :

$$\begin{aligned} M(\mathcal{I}_1) &= h_0 + \varphi_2 = \xi_4 , \\ M(\mathcal{I}_2) &= h_0 - \varphi_1 + 3\varphi_2 = \xi_2 + \xi_4 , \\ M(\mathcal{I}_3) &= h_0 + 5\varphi_1 = \xi_2 + 3\xi_3 + \xi_4 . \end{aligned} \quad (3.15)$$

The field-theoretic expressions for the instanton masses can be obtained using (A.1). We note that \mathcal{I}_1 is the instanton state of lowest mass, whereas the other instanton states can be viewed as bound states of this ‘‘elementary instanton’’ with other perturbative particles, e.g. $M(\mathcal{I}_2) = M(\mathcal{I}_1) + M(W_2)$, $M(\mathcal{I}_3) = M(\mathcal{I}_1) + M(W_1) + M(W_2)$, etc.

Using the expressions for the Kähler volumes of the curves in terms of the FI terms (3.8) and the expressions for the W-boson and instanton masses, we can complete the map between geometric quantities and field theory quantities. Specifically, we find:

$$\mu_1 = -3h_0, \quad \nu_1 = -h_0 - \varphi_2, \quad \nu_2 = -2h_0 - \varphi_1 . \quad (3.16)$$

Plugging (3.16) into (3.10), we find that the geometric prepotential (3.10) indeed matches the field theory prepotential (3.13).

As a final consistency check, we can compute the monopole string tensions from field theory via the first derivatives of the prepotential with respect to the Coulomb moduli (cf. (2.14)). Using (3.13), these are:

$$T_{1,\text{ft}} = \frac{\partial \mathcal{F}_{SU(3)_2}}{\partial \varphi_1} = 2h_0\varphi_1 + 4\varphi_1^2 - h_0\varphi_2 + \varphi_1\varphi_2 - \frac{3\varphi_2^2}{2} , \quad (3.17)$$

$$T_{2,\text{ft}} = \frac{\partial \mathcal{F}_{SU(3)_2}}{\partial \varphi_2} = -h_0 \varphi_1 + \frac{1}{2} \varphi_1^2 + 2h_0 \varphi_2 - 3\varphi_1 \varphi_2 + 4\varphi_2^2 . \quad (3.18)$$

whereas from geometry, these are given by the area under the $\chi(r_0)$ curve between the locations of gauge D6-branes (cf. (2.29)):

$$T_{1,\text{geo}} = \int_{-\xi_3}^0 \chi(r_0) dr_0 = \xi_3 \left(\frac{3}{2} \xi_3 + \xi_2 + \xi_4 \right) , \quad T_{2,\text{geo}} = \int_0^{\xi_2} \chi(r_0) dr_0 = \xi_2 \left(\frac{1}{2} \xi_2 + \xi_4 \right) . \quad (3.19)$$

Using the map $\xi_2 = 2\varphi_2 - \varphi_1$, $\xi_3 = 2\varphi_1 - \varphi_2$ and $\xi_4 = h_0 + \varphi_2$, we find that $T_{i,\text{geo}} = T_{i,\text{ft}}$ for $i = 1, 2$.

Magnetic walls. The tensions vanish at the loci defined by:

$$(I) : \{ \xi_3 = 0 \} \cup \left\{ \frac{3}{2} \xi_3 + \xi_2 + \xi_4 = 0 \right\} , \quad \text{and, } (II) : \{ \xi_2 = 0 \} \cup \left\{ \frac{1}{2} \xi_2 + \xi_4 = 0 \right\} . \quad (3.20)$$

The loci $\{ \xi_3 = 0 \} \subset (I)$ and $\{ \xi_2 = 0 \} \subset (II)$, respectively correspond to hard walls along which the W-bosons W_2 and W_1 become massless. The loci $\{ \frac{3}{2} \xi_3 + \xi_2 + \xi_4 = 0 \} \subset (I)$ and $\{ \frac{1}{2} \xi_2 + \xi_4 = 0 \} \subset (II)$ are not part of the Kähler chamber of this resolution. So there are no magnetic walls. But away from hard walls, the BPS instanton \mathcal{I}_1 can become massless at $\xi_4 = 0$ (corresponding to a flop of the curve \mathcal{C}_4), resulting in a traversable instantonic wall. In this case, the theory flows to a chamber (resolution (b)) that does not have a gauge theory interpretation.

Parity. Since the effective Chern-Simons level (3.12) is nonvanishing, the theory breaks parity. This is consistent with the fact that the toric diagram of $E_1^{2,2}$ is not invariant under $C_0 = S^2$, the central element of $SL(2, \mathbb{Z})$.

Resolution (b) and RG flow. Resolution (b) of the $E_1^{2,2}$ singularity, shown in Figure 4(b), can be obtained by a flop of the instantonic curve \mathcal{C}_4 in resolution (a). It does not admit a vertical reduction. This is consistent with the fact that the $SU(3)_2$ gauge theory has only one chamber that is geometrically engineered by resolution (a). However, note that in this resolution, one can decouple the divisor D_3 by sending the volume of the curve \mathcal{C}_4 to infinity as shown in Figure 3.4. This leads to the $SL(2, \mathbb{Z})$ -transformed version of the unique crepant singularity of the $E_0^{2,\text{NL}}$ singularity (see Figure 3(a)). We interpret this decoupling as a generalized renormalization group (RG) flow in the extended parameter space of the geometry. Physically, this amounts to sending the mass of the instanton particle \mathcal{I}_1 in the gauge theory description of resolution (a) to zero (signaling a flop of \mathcal{C}_4) and then blowing it up (in the opposite direction) in the Kähler cone of resolution (b), by sending the coupling to infinity.

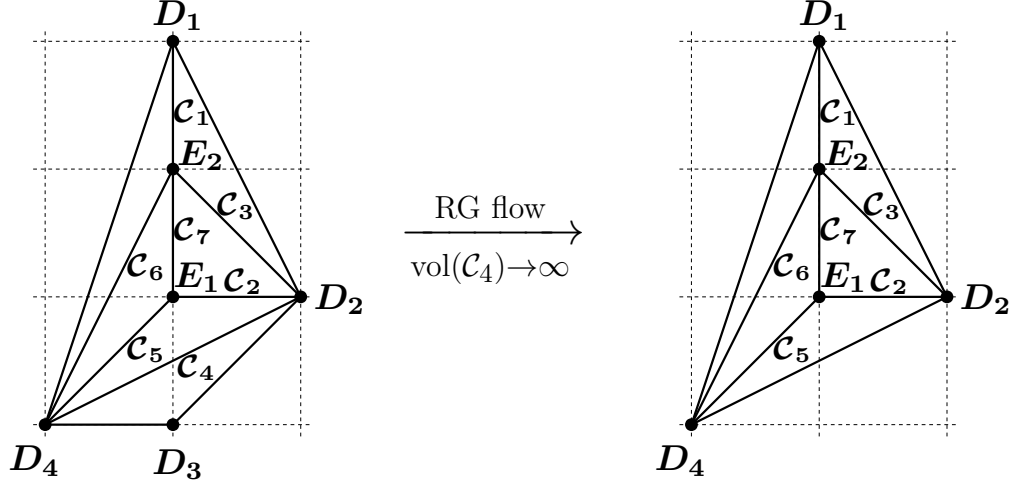


Figure 6. Decoupling the divisor D_3 leads to the unique crepant resolution of the $E_0^{2,\text{NL}}$ singularity.

As we will see in subsequent examples, such a generalized RG flow, which involves some combination of flops (which are reversible operations) and decouplings (which are not reversible), frequently relates theories obtained by resolutions of distinct isolated toric singularities. In terms of geometry, one can “flow” to a toric diagram with fewer external points. Since the rank of the flavor symmetry is $f = E - 3$ where E is the number of external points, such a flow reduces the flavor symmetry of the theory. This parallels the field-theoretic operation of integrating out massive degrees of freedom.

3.2 The $E_1^{2,1}$ singularity and $SU(3)_1$ gauge theory

This geometry has exactly one crepant resolution, shown in Figure 7. The linear relations among divisors are:

$$D_4 \simeq D_2, \quad \mathbf{E}_1 \simeq D_1 - 2D_2 - 2D_3, \quad \mathbf{E}_2 \simeq -2D_1 + D_3. \quad (3.21)$$

The compact curves \mathcal{C} are given by the intersection pairings of the divisors they connect in the toric diagram (for example, $\mathcal{C}_1 = \mathbf{E}_2 \cdot D_1$, $\mathcal{C}_7 = \mathbf{E}_2 \cdot \mathbf{E}_1$ etc.), and can be read off from the toric diagram. The linear relations among curve classes are:

$$\mathcal{C}_1 \simeq 2\mathcal{C}_3 + \mathcal{C}_4, \quad \mathcal{C}_5 \simeq \mathcal{C}_2, \quad \mathcal{C}_6 \simeq \mathcal{C}_3, \quad \mathcal{C}_7 \simeq \mathcal{C}_4. \quad (3.22)$$

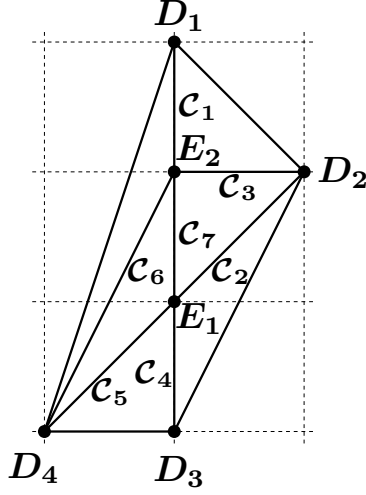


Figure 7. The unique crepant resolution of the $E_1^{2,1}$ singularity. This admits a vertical reduction.

We take $\{\mathcal{C}_2, \mathcal{C}_3, \mathcal{C}_4\}$ as generators of the Mori cone. The GLSM charge matrix is:

	D_1	D_2	D_3	D_4	\mathbf{E}_1	\mathbf{E}_2	$\text{vol}(\mathcal{C})$	
\mathcal{C}_2	0	0	1	0	-2	1	ξ_2	(3.23)
\mathcal{C}_3	1	0	0	0	1	-2	ξ_3	
\mathcal{C}_4	0	1	0	1	-2	0	ξ_4	
$U(1)_M$	0	0	0	0	-1	1	r_0	

Geometric prepotential. We parametrize the Kähler cone by $S = \mu_4 D_4 + \nu_1 \mathbf{E}_1 + \nu_2 \mathbf{E}_2$. The parameters (μ_4, ν_1, ν_2) are related to the FI parameters as:

$$\xi_2 = -2\nu_1 + \nu_2 \geq 0, \quad \xi_3 = \nu_1 - 2\nu_2 \geq 0, \quad \xi_4 = \mu_4 - 2\nu_1 \geq 0. \quad (3.24)$$

The relevant triple-intersection numbers are:

$$\begin{aligned} D_4 \mathbf{E}_1 \mathbf{E}_2 = 1, \quad D_4^2 \mathbf{E}_1 = 0, \quad D_4^2 \mathbf{E}_2 = 0, \quad D_4 \mathbf{E}_1^2 = -2, \quad D_4 \mathbf{E}_2^2 = -2, \\ \mathbf{E}_1^2 \mathbf{E}_2 = -2, \quad \mathbf{E}_1 \mathbf{E}_2^2 = 0, \quad \mathbf{E}_1^3 = 8, \quad \mathbf{E}_2^3 = 8. \end{aligned} \quad (3.25)$$

So the compact part of the prepotential is:

$$\mathcal{F}(\nu_1, \nu_2; \mu_4) = -\frac{1}{6} S^3 = -\frac{4}{3} \nu_1^3 - \frac{4}{3} \nu_2^3 + \nu_1^2 \nu_2 + \mu_4 (\nu_1^2 + \nu_2^2 - \nu_1 \nu_2). \quad (3.26)$$

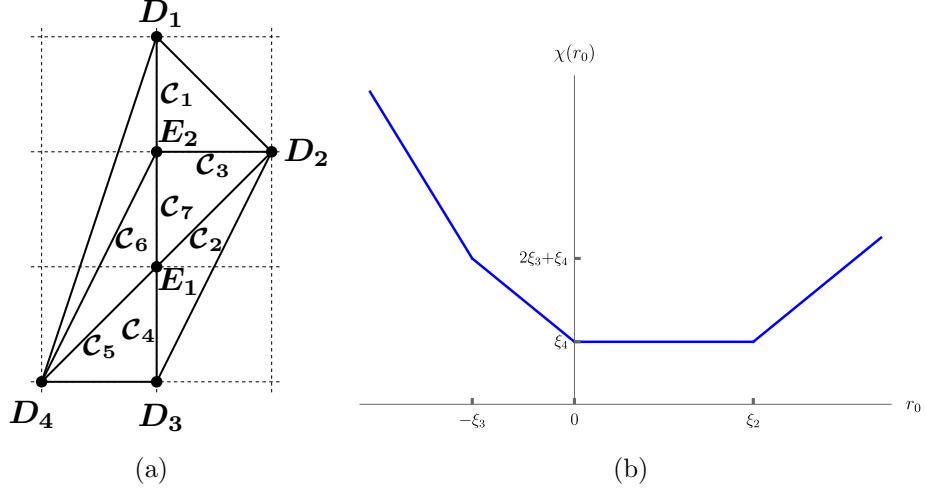


Figure 8. Resolution (a) of the $E_1^{2,1}$ singularity and its vertical reduction.

Type IIA reduction and gauge theory description. The type IIA profile is:

$$\chi(r_0) = \begin{cases} -4r_0 - 2\xi_3 + \xi_4, & \text{for } r_0 \leq -\xi_3 \\ -2r_0 + \xi_4, & \text{for } -\xi_3 \leq r_0 \leq 0 \\ \xi_4, & \text{for } 0 \leq r_0 \leq \xi_2 \\ +2r_0 - 2\xi_2 + \xi_4, & \text{for } r_0 \geq \xi_2 . \end{cases} \quad (3.27)$$

This function is sketched in Figure 8(b). At the points $r_0 = -\xi_3$, $r_0 = 0$ and $r_0 = \xi_2$, there are gauge D6-branes wrapping exceptional \mathbb{P}^1 's. When $\xi_2 = \xi_3 = 0$, the three gauged D6-branes wrapping the exceptional \mathbb{P}^1 at $r_0 = 0$ engineer an $SU(3)$ gauge theory with gauge coupling $h_0 = \xi_4$. The effective CS level is given by $\kappa_{s,\text{eff}} = -\frac{1}{2}(-4 + 2) = +1$. Using (A.3), the prepotential for the $SU(3)_{k=1}$ gauge theory is given by:

$$\mathcal{F}_{SU(3)_1} = h_0(\varphi_1^2 + \varphi_2^2 - \varphi_1\varphi_2) - \varphi_1\varphi_2^2 + \frac{4}{3}(\varphi_1^3 + \varphi_2^3) . \quad (3.28)$$

The simple-root W-bosons have masses given by:

$$M(W_1) = 2\varphi_2 - \varphi_1 = \xi_2, \quad M(W_2) = 2\varphi_1 - \varphi_2 = \xi_3 . \quad (3.29)$$

whereas the instantons have masses given by:

$$M(\mathcal{I}_1) = h_0 + 4\varphi_1 = 2\xi_3 + \xi_4, \quad M(\mathcal{I}_2) = M(\mathcal{I}_3) = h_0 + 2\varphi_2 = \xi_4 . \quad (3.30)$$

From the Kähler volumes (3.24) and the masses of W-bosons and instantons, we find:

$$\mu_4 = h_0, \quad \nu_1 = -\varphi_2, \quad \nu_2 = -\varphi_1 . \quad (3.31)$$

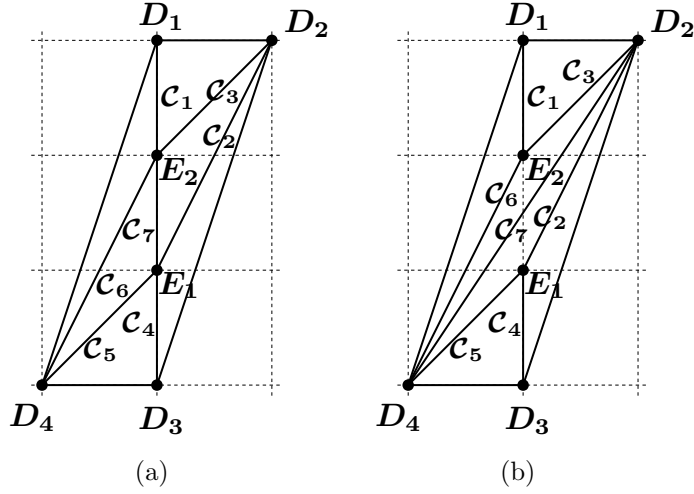


Figure 9. The two resolutions of the $E_1^{2,0}$ singularity. Resolution (a) admits a vertical reduction.

Plugging (3.31) into (3.26), we recover the field theory prepotential (3.28).

The monopole string tensions from field theory are given by:

$$T_{1,\text{ft}} = \frac{\partial \mathcal{F}_{SU(3)_1}}{\partial \varphi_1} = 4\varphi_1^2 + h_0(2\varphi_1 - \varphi_2) - 2\varphi_1\varphi_2, \quad (3.32)$$

$$T_{2,\text{ft}} = \frac{\partial \mathcal{F}_{SU(3)_1}}{\partial \varphi_2} = 4\varphi_2^2 + h_0(2\varphi_2 - \varphi_1) - \varphi_1^2. \quad (3.33)$$

whereas from geometry, they are given by:

$$T_{1,\text{geo}} = \int_{-\xi_3}^0 \chi(r_0) dr_0 = \xi_3(\xi_3 + \xi_4), \quad T_{2,\text{geo}} = \int_0^{\xi_2} \chi(r_0) dr_0 = \xi_2\xi_4. \quad (3.34)$$

Using the map $\xi_2 = 2\varphi_2 - \varphi_1$, $\xi_3 = 2\varphi_1 - \varphi_2$ and $\xi_4 = h_0 + 2\varphi_2$, we find that indeed $T_{i,\text{geo}} = T_{i,\text{ft}}$ for $i = 1, 2$. The tensions vanish along hard-walls where the W-bosons W_1 or W_2 become massless, or along the hard instanton wall $\xi_4 = 0$ where the instanton \mathcal{I}_2 would become massless, which is not possible in this Kähler chamber (the corresponding curve \mathcal{C}_4 cannot flop in this geometry). There are no walls in this geometry, except the hard walls along the boundary of the Kähler cone.

3.3 The $E_1^{2,0}$ singularity and $SU(3)_0$ gauge theory

This geometry has two crepant resolutions, shown in Figure 9, related by a flop of the curve \mathcal{C}_7 . Only resolution (a) admits a vertical reduction, so we consider it first. The linear relations among divisors are:

$$D_2 \simeq D_4, \quad \mathbf{E}_1 \simeq D_1 - D_2 - 2D_3, \quad \mathbf{E}_2 \simeq -2D_1 - D_2 + D_3. \quad (3.35)$$

The linear relations among curve classes are:

$$\mathcal{C}_1 \simeq \mathcal{C}_3 + \mathcal{C}_7, \quad \mathcal{C}_4 \simeq \mathcal{C}_2 + \mathcal{C}_7, \quad \mathcal{C}_5 \simeq \mathcal{C}_2, \quad \mathcal{C}_6 \simeq \mathcal{C}_3. \quad (3.36)$$

We take $\{\mathcal{C}_2, \mathcal{C}_3, \mathcal{C}_7\}$ as generators of the Mori cone. The GLSM charge matrix is:

	D_1	D_2	D_3	D_4	\mathbf{E}_1	\mathbf{E}_2	$\text{vol}(\mathcal{C})$
\mathcal{C}_2	0	0	1	0	-2	1	ξ_2
\mathcal{C}_3	1	0	0	0	1	-2	ξ_3
\mathcal{C}_7	0	1	0	1	-1	-1	ξ_7
$U(1)_M$	0	0	0	0	-1	1	r_0

(3.37)

Geometric prepotential. We parameterize the Kähler cone by $S = \mu_4 D_4 + \nu_1 \mathbf{E}_1 + \nu_2 \mathbf{E}_2$. The parameters (μ_4, ν_1, ν_2) are related to the FI parameters by

$$\xi_2 = -2\nu_1 + \nu_2 \geq 0, \quad \xi_3 = \nu_1 - 2\nu_2 \geq 0, \quad \xi_7 = \mu_4 - \nu_1 - \nu_2 \geq 0. \quad (3.38)$$

The relevant triple-intersection numbers are:

$$\begin{aligned} D_4 \mathbf{E}_1 \mathbf{E}_2 = 1, \quad D_4^2 \mathbf{E}_1 = 0, \quad D_4^2 \mathbf{E}_2 = 0, \quad D_4 \mathbf{E}_1^2 = -2, \quad D_4 \mathbf{E}_2^2 = -2, \\ \mathbf{E}_1^2 \mathbf{E}_2 = -1, \quad \mathbf{E}_1 \mathbf{E}_2^2 = -1, \quad \mathbf{E}_1^3 = 8, \quad \mathbf{E}_2^3 = 8. \end{aligned} \quad (3.39)$$

Therefore, the compact part of the prepotential is determined to be:

$$\mathcal{F}(\nu_1, \nu_2; \mu_4) = -\frac{1}{6} S^3 = -\frac{4}{3}(\nu_1^3 + \nu_2^3) + \frac{1}{2}(\nu_1^2 \nu_2 + \nu_1 \nu_2^2) + \mu_4(\nu_1^2 + \nu_2^2 - \nu_1 \nu_2). \quad (3.40)$$

Type IIA reduction and gauge theory description. The IIA profile function is:

$$\chi(r_0) = \begin{cases} -3r_0 - 2\xi_3 + \xi_7, & \text{for } r_0 \leq -\xi_3 \\ -r_0 + \xi_7, & \text{for } -\xi_3 \leq r_0 \leq 0 \\ +r_0 + \xi_7, & \text{for } 0 \leq r_0 \leq \xi_2 \\ +3r_0 - 2\xi_2 + \xi_7, & \text{for } r_0 \geq \xi_2. \end{cases} \quad (3.41)$$

This function is sketched in Figure 10, where we have chosen $\xi_2 > \xi_3$ without loss of generality to plot the function. At the points $r_0 = -\xi_3$, $r_0 = 0$ and $r_0 = \xi_2$, there are gauge D6-branes wrapping exceptional \mathbb{P}^1 's in the resolution of the singularity. When $\xi_2 = \xi_3 = 0$, an $SU(3)$ gauge theory is realized with gauge coupling $h_0 = \xi_7$. The effective Chern-Simons level now vanishes: $\kappa_{s,\text{eff}} = -\frac{1}{2}(-3 + 3) = 0$. Using (A.3), the prepotential for the $SU(3)_{k=0}$ gauge theory is given by:

$$\mathcal{F}_{SU(3)_0} = \frac{4}{3}(\varphi_1^3 + \varphi_2^3) - \frac{1}{2}(\varphi_1^2 \varphi_2 + \varphi_1 \varphi_2^2) + h_0(\varphi_1^2 + \varphi_2^2 - \varphi_1 \varphi_2). \quad (3.42)$$

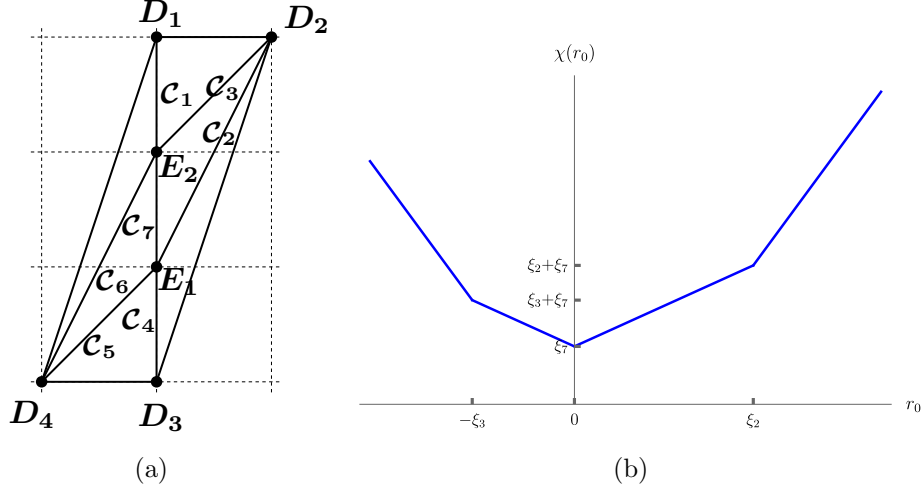


Figure 10. Resolution (a) of the $E_1^{2,0}$ singularity and its vertical reduction.

The simple-root W-bosons have masses given by:

$$M(W_1) = 2\varphi_2 - \varphi_1 = \xi_2, \quad M(W_2) = 2\varphi_1 - \varphi_2 = \xi_3. \quad (3.43)$$

whereas the instantons have masses given by:

$$M(\mathcal{I}_1) = h_0 + \varphi_1 + \varphi_2 = \xi_7, \quad M(\mathcal{I}_2) = h_0 + 3\varphi_2 = \xi_2 + \xi_7, \quad M(\mathcal{I}_3) = h_0 + 3\varphi_1 = \xi_3 + \xi_7. \quad (3.44)$$

From the Kähler volumes (3.38) of the compact curves and the masses of W-bosons and instantons, the map between geometry and field theory is determined to be:

$$\mu_4 = h_0, \quad \nu_1 = -\varphi_2, \quad \nu_2 = -\varphi_1. \quad (3.45)$$

Plugging (3.45) into (3.40), we recover the field theory prepotential (3.42), up to φ -independent terms.

The monopole string tensions in field theory are given by:

$$T_{1,\text{ft}} = \frac{\partial \mathcal{F}_{SU(3)_0}}{\partial \varphi_1} = 4\varphi_1^2 + h_0(2\varphi_1 - \varphi_2) - \varphi_1\varphi_2 - \frac{1}{2}\varphi_2^2, \quad (3.46)$$

$$T_{2,\text{ft}} = \frac{\partial \mathcal{F}_{SU(3)_0}}{\partial \varphi_2} = 4\varphi_2^2 + h_0(2\varphi_2 - \varphi_1) - \varphi_1\varphi_2. \quad (3.47)$$

whereas from geometry, they are given by:

$$T_{1,\text{geo}} = \int_{-\xi_3}^0 \chi(r_0) dr_0 = \frac{1}{2}\xi_3(\xi_3 + 2\xi_7), \quad T_{2,\text{geo}} = \int_0^{\xi_2} \chi(r_0) dr_0 = \frac{1}{2}\xi_2(\xi_2 + 2\xi_7). \quad (3.48)$$

Using the map $\xi_2 = 2\varphi_2 - \varphi_1$, $\xi_3 = 2\varphi_1 - \varphi_2$ and $\xi_7 = h_0 + \varphi_1 + \varphi_2$, we find that $T_{i,\text{geo}} = T_{i,\text{ft}}$ for $i = 1, 2$. The vanishing tension loci $\{xi_3 = 0\}$ and $\{xi_2 = 0\}$ respectively correspond to hard walls where the W-bosons W_2 and W_1 become massless, whereas the loci $\{\xi_3 + 2\xi_7 = 0\}$ and $\{\xi_2 + 2\xi_7 = 0\}$ do not belong to the Kähler chamber of this resolution. Away from any hard wall, the instanton particle \mathcal{I}_1 can become massless at $\xi_7 = 0$ (signaling a flop of the curve \mathcal{C}_7). This is a traversable instantonic wall, crossing which leads to a non-gauge-theoretic chamber (resolution (b)).

Parity. The effective Chern-Simons level vanishes, as observed above, and so the theory conserves parity. This is reflected by the symmetry of the toric diagram under the central element $C_0 = S^2 \subset SL(2, \mathbb{Z})$.

Resolution (b). We remark that resolution (b) of the $E_1^{2,0}$, upon an $SL(2, \mathbb{Z})$ transformation, is seen to represent a coupling of two rank-1 E_0 non-Lagrangian singularities [1, 10] (cf. the discussion around Figure 27).

3.4 The $E_2^{2, \frac{3}{2}}$ singularity and $SU(3)_{\frac{3}{2}} N_f = 1$ gauge theory

The $E_2^{2, \frac{3}{2}}$ singularity (Figure 3(f)) admits 7 crepant resolutions, shown in Figures 11. The first four resolutions, Figure 11(a)-11(d), admit vertical reductions to type IIA, which correspond to chambers of the $SU(3)_{\frac{3}{2}} N_f = 1$ gauge theory, as we illustrate below. Resolutions (e), (f), and (g) do not admit a gauge-theory interpretation.

Resolution (a). Consider the crepant resolution of Figure 11(a), with curves and divisors shown in Figure 12(a). There are five non-compact toric divisors D_i ($i = 1, \dots, 5$), and two compact toric divisors \mathbf{E}_1 and \mathbf{E}_2 with the following linear relations:

$$D_1 \simeq D_3 + D_4, \quad \mathbf{E}_1 \simeq D_2 - 2D_3 - 3D_4 - 2D_5, \quad \mathbf{E}_2 \simeq -2D_2 + D_4 + D_5. \quad (3.49)$$

The linear relations among curve classes are:

$$\mathcal{C}_1 \simeq \mathcal{C}_4 + \mathcal{C}_6, \quad \mathcal{C}_3 \simeq 2\mathcal{C}_2 + \mathcal{C}_6 + \mathcal{C}_7, \quad \mathcal{C}_5 \simeq \mathcal{C}_2. \quad (3.50)$$

We take $\{\mathcal{C}_2, \mathcal{C}_4, \mathcal{C}_6, \mathcal{C}_7\}$ as generators of the Mori cone. The GLSM charge matrix is:

	D_1	D_2	D_3	D_4	D_5	\mathbf{E}_1	\mathbf{E}_2	$\text{vol}(\mathcal{C})$
\mathcal{C}_2	0	1	0	0	0	1	-2	ξ_2
\mathcal{C}_4	0	0	-1	1	0	-1	1	ξ_4
\mathcal{C}_6	0	0	1	-1	1	-1	0	ξ_6
\mathcal{C}_7	1	0	0	1	-1	-1	0	ξ_7
$U(1)_M$	0	0	0	0	0	-1	1	r_0

(3.51)

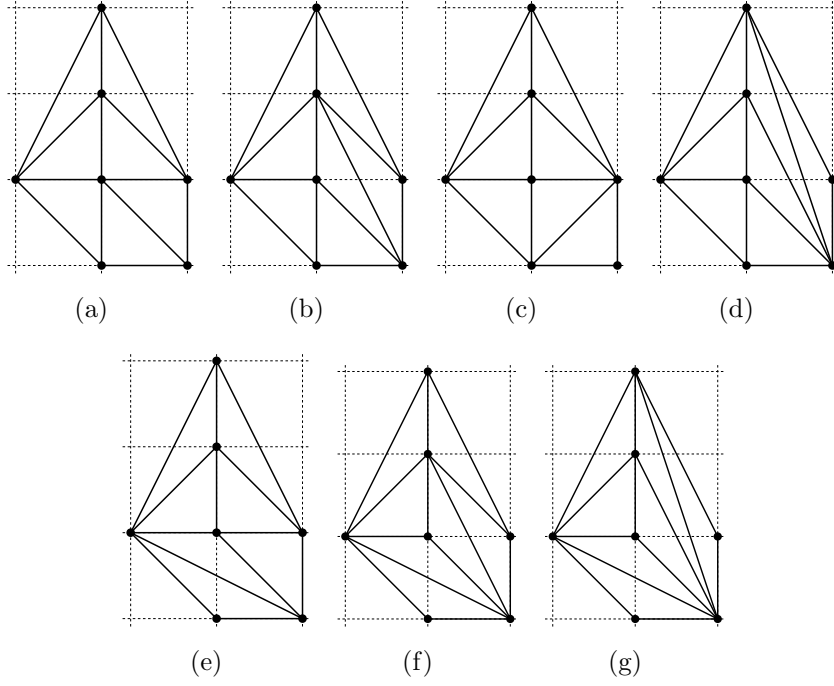


Figure 11. The 7 crepant singularities of the $E_2^{2, \frac{3}{2}}$ singularity. The first four, (a)-(d) admit a vertical reduction, corresponding to chambers of the $SU(3)_{\frac{3}{2}} N_f = 1$ gauge theory.

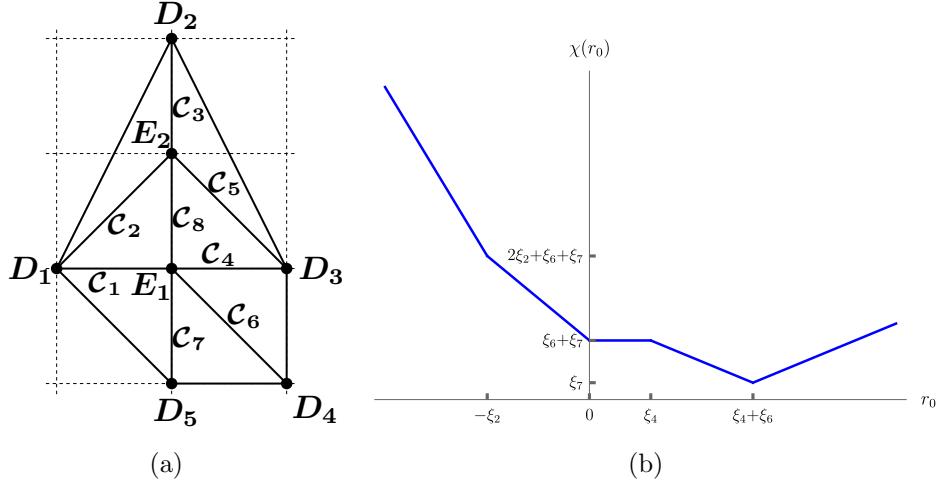


Figure 12. Resolution (a) of the $E_2^{2, \frac{3}{2}}$ singularity and its vertical reduction.

Geometric prepotential. We parametrize the Kähler cone by:

$$S = \mu_1 D_1 + \mu_2 D_2 + \nu_1 \mathbf{E}_1 + \nu_2 \mathbf{E}_2 . \tag{3.52}$$

The parameters $(\mu_1, \mu_2, \nu_1, \nu_2)$ are related to the FI parameters by:

$$\xi_2 = \mu_2 + \nu_1 - 2\nu_2 \geq 0, \quad \xi_4 = -\nu_1 + \nu_2 \geq 0, \quad \xi_6 = -\nu_1 \geq 0, \quad \xi_7 = \mu_1 - \nu_1 \geq 0. \quad (3.53)$$

The relevant triple-intersection numbers are:

$$\begin{aligned} D_1 \mathbf{E}_1 \mathbf{E}_2 &= 1, & D_2 \mathbf{E}_1 \mathbf{E}_2 &= 0, & D_1 D_2 \mathbf{E}_1 &= 0, & D_1 D_2 \mathbf{E}_2 &= 1, \\ D_1 \mathbf{E}_1^2 &= -2, & D_2 \mathbf{E}_1^2 &= 0, & D_1 \mathbf{E}_2^2 &= -2, & D_2 \mathbf{E}_2^2 &= -4, \\ D_1^2 \mathbf{E}_1 &= 0, & D_1^2 \mathbf{E}_2 &= 0, & D_2^2 \mathbf{E}_1 &= 0, & D_2^2 \mathbf{E}_2 &= 2, \\ \mathbf{E}_1^2 \mathbf{E}_2 &= -2, & \mathbf{E}_1 \mathbf{E}_2^2 &= 0, & \mathbf{E}_1^3 &= 7, & \mathbf{E}_2^3 &= 8. \end{aligned} \quad (3.54)$$

Therefore, the compact part of the prepotential is:

$$\begin{aligned} \mathcal{F}_{(a)}(\nu_1, \nu_2; \mu_1, \mu_2) &= -\frac{1}{6} S^3 = -\frac{7}{6} \nu_1^3 - \frac{4}{3} \nu_2^3 + \nu_1^2 \nu_2 + \mu_1 \nu_1^2 - \mu_1 \nu_1 \nu_2 + (\mu_1 + 2\mu_2) \nu_2^2 \\ &\quad - \mu_2^2 \nu_2 - \mu_1 \mu_2 \nu_2. \end{aligned} \quad (3.55)$$

Type IIA reduction and gauge theory description. The type IIA background is a resolved A_1 singularity fibered over the $x^9 = r_0$ direction. There are three D6-branes wrapping the exceptional \mathbb{P}^1 in the resolved A_1 singularity, resulting in an $SU(3)$ gauge theory. There is also a D6-brane wrapping a noncompact divisor in the resolved ALE space, which corresponds to one fundamental flavor. The volume of the exceptional \mathbb{P}^1 is given by the following piecewise linear function:

$$\chi(r_0) = \begin{cases} -4r_0 - 2\xi_2 + \xi_6 + \xi_7, & \text{for } r_0 \leq -\xi_2 \\ -2r_0 + \xi_6 + \xi_7, & \text{for } -\xi_2 \leq r_0 \leq 0 \\ \xi_6 + \xi_7, & \text{for } 0 \leq r_0 \leq \xi_4 \\ -r_0 + \xi_4 + \xi_6 + \xi_7, & \text{for } \xi_4 \leq r_0 \leq \xi_4 + \xi_6 \\ +r_0 - \xi_4 - \xi_6 + \xi_7, & \text{for } r_0 \geq \xi_4 + \xi_6. \end{cases} \quad (3.56)$$

This function is sketched in Figure 12(b). At the points $r_0 = -\xi_2$, $r_0 = 0$ and $r_0 = \xi_4 + \xi_6$, there are gauge D6-branes wrapping \mathbb{P}^1 's in the resolution of the singularity. When $\xi_2 = \xi_4 = \xi_6 = 0$, an $SU(3)$ gauge theory is realized with coupling $h_0 = \xi_7$. There is a flavor D6-brane at $r_0 = \xi_4$. The effective Chern-Simons level is given by $\kappa_{s,\text{eff}} = -\frac{1}{2}(-4+1) = \frac{3}{2}$, which is interpreted as a bare CS level of 2 plus the contribution $-\frac{1}{2}$ due to the single hypermultiplet (cf. (2.5)). The simple-root W-bosons have masses given by:

$$M(W_1) = \xi_2 = 2\varphi_1 - \varphi_2, \quad M(W_2) = \xi_4 + \xi_6 = 2\varphi_2 - \varphi_1, \quad (3.57)$$

This resolution corresponds to gauge theory chamber 3 (cf. Table 4 and (A.7)), with instanton masses given by:

$$\begin{aligned} M(\mathcal{I}_1) &= \chi(r_0 = -\xi_2) = 2\xi_2 + \xi_6 + \xi_7 = h_0 + 4\varphi_1 - m , \\ M(\mathcal{I}_2) &= \chi(r_0 = 0) = \xi_6 + \xi_7 = h_0 + 2\varphi_2 - m , \\ M(\mathcal{I}_3) &= \chi(r_0 = \xi_4 + \xi_6) = \xi_7 = h_0 + \varphi_2 . \end{aligned} \quad (3.58)$$

The masses of hypermultiplets (due to open strings stretched between gauge and flavor branes) are:

$$M(\mathcal{H}_1) = \xi_6 = \varphi_2 - m , \quad M(\mathcal{H}_2) = \xi_4 = -\varphi_1 + \varphi_2 + m , \quad M(\mathcal{H}_3) = \xi_2 + \xi_4 = \varphi_1 + m . \quad (3.59)$$

From the Kähler volumes (3.53) of the compact curves and masses of W-bosons and instantons, the map between geometry and field theory variables is determined to be:

$$\mu_1 = h_0 + m, \quad \mu_2 = 3m, \quad \nu_1 = -\varphi_2 + m, \quad \nu_2 = -\varphi_1 + 2m . \quad (3.60)$$

Plugging (3.60) into (3.55), we recover the field theory prepotential,

$$\mathcal{F}_{SU(3)_2, N_f=1}^{\text{chamber 3}} = \frac{4}{3}\varphi_1^3 + \frac{7}{6}\varphi_2^3 - \varphi_1\varphi_2^2 + \left(h_0 - \frac{m}{2}\right)\varphi_1^2 + h_0\varphi_2^2 - h_0\varphi_1\varphi_2 - \frac{m^2}{2}\varphi_1 , \quad (3.61)$$

up to φ -independent terms (i.e. terms independent of φ_1 and φ_2 , as discussed in previous examples). From field theory, the monopole string tensions are given by:

$$T_{1,\text{ft}} = \frac{\partial \mathcal{F}_{SU(3)_2, N_f=1}^{\text{chamber 3}}}{\partial \varphi_1} = 4\varphi_1^2 + 2(h_0 - m)\varphi_1 + (m - h_0)\varphi_2 - \varphi_2^2 , \quad (3.62)$$

$$T_{2,\text{ft}} = \frac{\partial \mathcal{F}_{SU(3)_2, N_f=1}^{\text{chamber 3}}}{\partial \varphi_2} = \frac{7}{2}\varphi_2^2 + (m - h_0)\varphi_1 + (2h_0 - m)\varphi_2 - 2\varphi_1\varphi_2 - \frac{m^2}{2} , \quad (3.63)$$

whereas from geometry, they are given by:

$$T_{1,\text{geo}} = \int_{-\xi_2}^0 \chi(r_0) dr_0 = \xi_2(\xi_2 + \xi_6 + \xi_7) , \quad (3.64)$$

$$T_{2,\text{geo}} = \int_0^{\xi_4 + \xi_6} \chi(r_0) dr_0 = \frac{\xi_6^2}{2} + \xi_4\xi_6 + \xi_6\xi_7 + \xi_4\xi_7 . \quad (3.65)$$

Using the map $\xi_2 = 2\varphi_1 - \varphi_2$, $\xi_4 = -\varphi_1 + \varphi_2 + m$, $\xi_6 = \varphi_2 - m$ and $\xi_7 = h_0 + \varphi_2$, we find that $T_{i,\text{ft}} = T_{i,\text{geo}}$ for $i = 1, 2$. The tensions vanish at loci given by:

$$(I) : \{\xi_2 = 0\} \cup \{\xi_2 + \xi_6 + \xi_7 = 0\}, \quad \text{and} \quad (II) : \left\{ \frac{\xi_6^2}{2} + \xi_4\xi_6 + \xi_6\xi_7 + \xi_4\xi_7 = 0 \right\} . \quad (3.66)$$

The loci $\{\xi_2 = 0\} \subset (I)$ coincides with the boundary of the Weyl chamber where the W-boson W_1 becomes massless, indicating a hard wall. The component $\{\xi_2 + \xi_6 + \xi_7 = 0\} \subset (I)$ is not part of the Kähler chamber of resolution (a). As for the second component (II), the solutions of the quadratic equation for ξ_6 , defining the vanishing locus are:

$$\xi_6 \stackrel{(II)}{=} -\xi_4 - \xi_7 \pm \sqrt{\xi_4^2 + \xi_7^2}, \quad (3.67)$$

which always lead to negative values of ξ_6 in resolution (a) (for both sign choices), which is unphysical in this Kähler chamber, and are hence rejected. Note that away from any hard wall, the BPS perturbative hypermultiplets \mathcal{H}_1 or \mathcal{H}_2 can become massless at $\xi_6 = 0$ or $\xi_4 = 0$ respectively (signaling flops of the curves \mathcal{C}_6 or \mathcal{C}_4). These are traversable walls that lead, respectively to gauge theory resolutions (c) and (b) respectively. Also away from any hard wall, the BPS instanton \mathcal{I}_3 can become massless at $\xi_7 = 0$ (signaling a flop of \mathcal{C}_7), which corresponds to a traversable instantonic wall that leads to a non-gauge-theoretic chamber (resolution (e)).

Parity. Since the effective Chern-Simons level is nonvanishing, this theory breaks parity. In geometry, this is reflected by the non-invariance of the toric diagram under the central element $C_0 = S^2$ of $SL(2, \mathbb{Z})$. This is true, of course, of all the crepant resolutions of $E_2^{2, \frac{3}{2}}$ as the CS level does not change under flops.

Resolution (b). Consider the crepant resolution of Figure 11(b), with curves and divisors shown in Figure 13(a). The linear equivalences among divisors remain un-

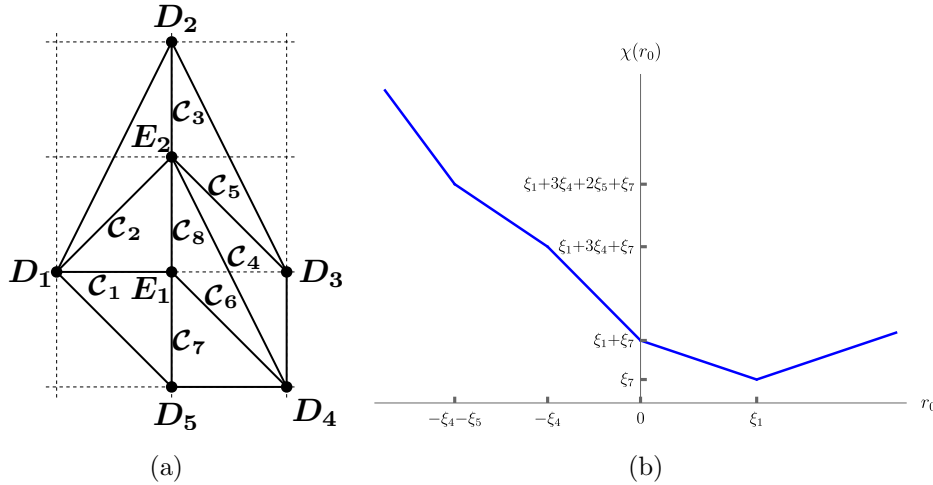


Figure 13. Resolution (b) of the $E_2^{2, \frac{3}{2}}$ singularity and its vertical reduction.

changed, as in (3.49). The linear relations among curve classes are:

$$\mathcal{C}_2 \simeq \mathcal{C}_4 + \mathcal{C}_5, \quad \mathcal{C}_3 \simeq \mathcal{C}_1 + 3\mathcal{C}_4 + 2\mathcal{C}_5 + \mathcal{C}_7, \quad \mathcal{C}_6 \simeq \mathcal{C}_1, \quad \mathcal{C}_8 \simeq \mathcal{C}_1 + \mathcal{C}_7. \quad (3.68)$$

We take $\{\mathcal{C}_1, \mathcal{C}_4, \mathcal{C}_5, \mathcal{C}_7\}$ as generators of the Mori cone. The GLSM charge matrix is

	D_1	D_2	D_3	D_4	D_5	\mathbf{E}_1	\mathbf{E}_2	$\text{vol}(\mathcal{C})$
\mathcal{C}_1	0	0	0	0	1	-2	1	ξ_1
\mathcal{C}_4	0	0	1	-1	0	1	-1	ξ_4
\mathcal{C}_5	0	1	-1	1	0	0	-1	ξ_5
\mathcal{C}_7	1	0	0	1	-1	-1	0	ξ_7
$U(1)_M$	0	0	0	0	0	-1	1	r_0

(3.69)

The Kähler cone is parametrized by (3.52). The parameters $(\mu_1, \mu_2, \nu_1, \nu_2)$ are now related to the FI parameters by:

$$\xi_1 = -2\nu_1 + \nu_2 \geq 0, \quad \xi_4 = \nu_1 - \nu_2 \geq 0, \quad \xi_5 = \mu_2 - \nu_2 \geq 0, \quad \xi_7 = \mu_1 - \nu_1 \geq 0. \quad (3.70)$$

The relevant triple-intersection numbers are:

$$\begin{aligned}
D_1 \mathbf{E}_1 \mathbf{E}_2 &= 1, & D_2 \mathbf{E}_1 \mathbf{E}_2 &= 0, & D_1 D_2 \mathbf{E}_1 &= 0, & D_1 D_2 \mathbf{E}_2 &= 1, \\
D_1 \mathbf{E}_1^2 &= -2, & D_2 \mathbf{E}_1^2 &= 0, & D_1 \mathbf{E}_2^2 &= -2, & D_2 \mathbf{E}_2^2 &= -4, \\
D_1^2 \mathbf{E}_1 &= 0, & D_1^2 \mathbf{E}_2 &= 0, & D_2^2 \mathbf{E}_1 &= 0, & D_2^2 \mathbf{E}_2 &= 2, \\
\mathbf{E}_1^2 \mathbf{E}_2 &= -3, & \mathbf{E}_1 \mathbf{E}_2^2 &= 1, & \mathbf{E}_1^3 &= 8, & \mathbf{E}_2^3 &= 7.
\end{aligned} \quad (3.71)$$

Therefore, the compact part of the prepotential is:

$$\begin{aligned}
\mathcal{F}_{(b)}(\nu_1, \nu_2; \mu_1, \mu_2) &= -\frac{1}{6} S^3 = -\frac{4}{3} \nu_1^3 - \frac{7}{6} \nu_2^3 + \frac{3}{2} \nu_1^2 \nu_2 - \frac{1}{2} \nu_1 \nu_2^2 + \mu_1 \nu_1^2 + (\mu_1 + 2\mu_2) \nu_2^2, \\
&\quad - \mu_1 \nu_1 \nu_2 - \mu_2^2 \nu_2 - \mu_1 \mu_2 \nu_2.
\end{aligned} \quad (3.72)$$

The type IIA profile is:

$$\chi(r_0) = \begin{cases} -4r_0 + \xi_1 - \xi_4 - 2\xi_5 + \xi_7, & \text{for } r_0 \leq -\xi_4 - \xi_5 \\ -2r_0 + \xi_1 + \xi_4 + \xi_7, & \text{for } -\xi_4 - \xi_5 \leq r_0 \leq -\xi_4 \\ -3r_0 + \xi_1 + \xi_7, & \text{for } -\xi_4 \leq r_0 \leq 0 \\ -r_0 + \xi_1 + \xi_7, & \text{for } 0 \leq r_0 \leq \xi_1 \\ +r_0 - \xi_1 + \xi_7, & \text{for } r_0 \geq \xi_1. \end{cases} \quad (3.73)$$

This function is sketched in Figure 13(b). At the points $r_0 = -\xi_4 - \xi_5$, $r_0 = 0$ and $r_0 = \xi_1$, there are gauge D6-branes wrapping \mathbb{P}^1 's in the resolution of the singularity. There is a flavor D6-brane at $r_0 = -\xi_4$. The simple-root W-bosons have masses given by:

$$M(W_1) = \xi_4 + \xi_5 = 2\varphi_1 - \varphi_2, \quad M(W_2) = \xi_1 = 2\varphi_2 - \varphi_1. \quad (3.74)$$

This resolution corresponds to gauge theory chamber 2 (cf. Table 4 and (A.6)) with instanton masses given by:

$$\begin{aligned}
M(\mathcal{I}_1) &= \chi(r_0 = -\xi_4 - \xi_6) = \xi_1 + 3\xi_4 + 2\xi_5 + \xi_7 = h_0 + 4\varphi_1 - m , \\
M(\mathcal{I}_2) &= \chi(r_0 = 0) = \xi_1 + \xi_7 = h_0 - \varphi_1 + 3\varphi_2 , \\
M(\mathcal{I}_3) &= \chi(r_0 = \xi_1) = \xi_7 = h_0 + \varphi_2 .
\end{aligned} \tag{3.75}$$

The masses of hypermultiplets are:

$$M(\mathcal{H}_1) = \xi_4 = \varphi_1 - \varphi_2 - m , \quad M(\mathcal{H}_2) = \xi_5 = \varphi_1 + m , \quad M(\mathcal{H}_3) = \xi_1 + \xi_4 = \varphi_2 - m . \tag{3.76}$$

One can verify that the map (3.56) still holds, and plugging it into (3.72), we recover the field theory prepotential,

$$\begin{aligned}
\mathcal{F}_{SU(3)_2, N_f=1}^{\text{chamber 2}} &= \frac{7}{6}\varphi_1^3 + \frac{4}{3}\varphi_2^3 + \frac{1}{2}\varphi_1^2\varphi_2 - \frac{3}{2}\varphi_1\varphi_2^2 + \left(h_0 - \frac{m}{2}\right)\varphi_1^2 + h_0\varphi_2^2 \\
&\quad - h_0\varphi_1\varphi_2 - \frac{m^2}{2}\varphi_1 ,
\end{aligned} \tag{3.77}$$

up to φ -independent terms. The monopole string tensions are given from $\chi(r_0)$ by:

$$T_{1,\text{geo}} = \int_{-\xi_4-\xi_5}^0 \chi(r_0) dr_0 = \frac{3\xi_4^2}{2} + \xi_4(3\xi_5 + \xi_7) + \xi_1(\xi_4 + \xi_5) + \xi_5(\xi_5 + \xi_7) , \tag{3.78}$$

$$T_{2,\text{geo}} = \int_0^{\xi_1} \chi(r_0) dr_0 = \frac{\xi_1^2}{2} + \xi_1\xi_7 . \tag{3.79}$$

One can verify, using the map $\xi_1 = 2\varphi_2 - \varphi_1$, $\xi_4 = \varphi_1 - \varphi_2 - m$, $\xi_5 = \varphi_1 + m$ and $\xi_7 = h_0 + \varphi_2$, that $T_{i,\text{ft}} = T_{i,\text{geo}}$ for $i = 1, 2$. The tensions vanish at loci given by:

$$\begin{aligned}
(I) &: \{\xi_1 = 0\} \cup \{\xi_1 + 2\xi_7 = 0\}, \text{ and } , \\
(II) &: \left\{ \frac{3}{2}\xi_4^2 + \xi_4(3\xi_5 + \xi_7) + \xi_1(\xi_4 + \xi_5) + \xi_5(\xi_5 + \xi_7) = 0 \right\} .
\end{aligned} \tag{3.80}$$

Along the submanifold $\{\xi_1 = 0\} \subset (I)$, the W-boson W_2 becomes massless, signaling a hard wall. Also $\{\xi_1 + 2\xi_7 = 0\}$ is not part of the Kähler chamber of resolution (b). As for the condition (II), the solutions to the quadratic equation for ξ_4 are:

$$\xi_4 = -\xi_5 - \frac{1}{3} \left(\xi_1 + \xi_7 \pm \sqrt{(\xi_1 + \xi_7)^2 + 3\xi_5^2} \right) . \tag{3.81}$$

Both sign choices lead to a negative value of ξ_4 , which is inconsistent in this Kähler chamber. Also note that the curve \mathcal{C}_5 cannot flop in this chamber, so ξ_5 cannot vanish.

Away from any hard wall, the perturbative BPS hypermultiplet \mathcal{H}_1 can become massless at $\xi_4 = 0$ (signaling a flop of \mathcal{C}_4), indicating a traversable wall that leads back to gauge theory resolution (a). Alternatively, the BPS instanton \mathcal{I}_3 can become massless at $\xi_7 = 0$ (signaling a flop of \mathcal{C}_7), corresponding to a traversable instantonic wall that leads to non-gauge-theoretic resolution (f).

Resolution (c). Consider the crepant resolution of Figure 11(c), with curves and divisors shown in Figure 14(a). The linear relations among curve classes are:

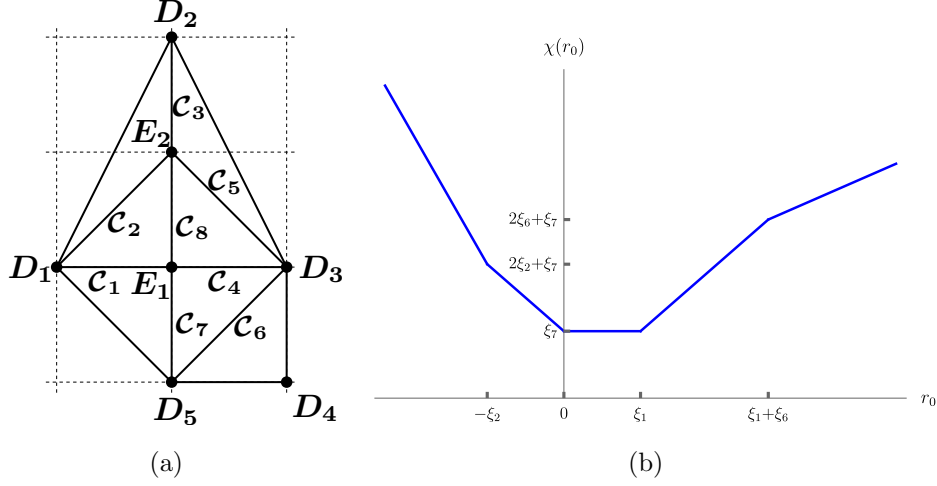


Figure 14. Resolution (c) of the $E_2^{2, \frac{3}{2}}$ singularity and its vertical reduction.

$$\mathcal{C}_3 \simeq 2\mathcal{C}_2 + \mathcal{C}_7, \quad \mathcal{C}_4 \simeq \mathcal{C}_1, \quad \mathcal{C}_5 \simeq \mathcal{C}_2, \quad \mathcal{C}_8 \simeq \mathcal{C}_7. \quad (3.82)$$

We take $\{\mathcal{C}_1, \mathcal{C}_2, \mathcal{C}_6, \mathcal{C}_7\}$ as generators of the Mori cone. The GLSM charge matrix is:

	D_1	D_2	D_3	D_4	D_5	\mathbf{E}_1	\mathbf{E}_2	$\text{vol}(\mathcal{C})$
\mathcal{C}_1	0	0	0	0	1	-2	1	ξ_1
\mathcal{C}_2	0	1	0	0	0	1	-2	ξ_2
\mathcal{C}_6	0	0	-1	1	-1	1	0	ξ_6
\mathcal{C}_7	1	0	1	0	0	-2	0	ξ_7
$U(1)_M$	0	0	0	0	0	-1	1	r_0

(3.83)

The parameters $(\mu_1, \mu_2, \nu_1, \nu_2)$ are related to the FI parameters by:

$$\xi_1 = -2\nu_1 + \nu_2 \geq 0, \quad \xi_2 = \mu_2 + \nu_1 - 2\nu_2 \geq 0, \quad \xi_6 = \nu_1 \geq 0, \quad \xi_7 = \mu_1 - 2\nu_1 \geq 0. \quad (3.84)$$

The relevant triple-intersection numbers are:

$$\begin{aligned}
D_1 \mathbf{E}_1 \mathbf{E}_2 &= 1, & D_2 \mathbf{E}_1 \mathbf{E}_2 &= 0, & D_1 D_2 \mathbf{E}_1 &= 0, & D_1 D_2 \mathbf{E}_2 &= 1, \\
D_1 \mathbf{E}_1^2 &= -2, & D_2 \mathbf{E}_1^2 &= 0, & D_1 \mathbf{E}_2^2 &= -2, & D_2 \mathbf{E}_2^2 &= -4, \\
D_1^2 \mathbf{E}_1 &= 0, & D_1^2 \mathbf{E}_2 &= 0, & D_2^2 \mathbf{E}_1 &= 0, & D_2^2 \mathbf{E}_2 &= 2, \\
\mathbf{E}_1^2 \mathbf{E}_2 &= -2, & \mathbf{E}_1 \mathbf{E}_2^2 &= 0, & \mathbf{E}_1^3 &= 8, & \mathbf{E}_2^3 &= 8.
\end{aligned} \tag{3.85}$$

Therefore, the compact part of the prepotential is:

$$\begin{aligned}
\mathcal{F}_{(c)}(\nu_1, \nu_2; \mu_1, \mu_2) &= -\frac{1}{6} S^3 = -\frac{4}{3}(\nu_1^3 + \nu_2^3) + \nu_1^2 \nu_2 + \mu_1 \nu_1^2 + (\mu_1 + 2\mu_2) \nu_2^2 \\
&\quad - \mu_1 \nu_1 \nu_2 - \mu_2 (\mu_1 + \mu_2) \nu_2.
\end{aligned} \tag{3.86}$$

The type IIA profile is:

$$\chi(r_0) = \begin{cases} -4r_0 - 2\xi_2 + \xi_7, & \text{for } r_0 \leq -\xi_2 \\ -2r_0 + \xi_7, & \text{for } -\xi_2 \leq r_0 \leq 0 \\ \xi_7, & \text{for } 0 \leq r_0 \leq \xi_1 \\ +2r_0 - 2\xi_1 + \xi_7, & \text{for } \xi_1 \leq r_0 \leq \xi_1 + \xi_6 \\ +r_0 - \xi_1 + \xi_6 + \xi_7, & \text{for } r_0 \geq \xi_1 + \xi_6. \end{cases} \tag{3.87}$$

This function is sketched in Figure 14(b). At the points $r_0 = -\xi_2$, $r_0 = 0$ and $r_0 = \xi_1$, there are gauge D6-branes wrapping \mathbb{P}^1 's in the resolution of the singularity. There is a flavor D6-brane at $r_0 = \xi_1 + \xi_6$. The simple-root W-bosons have masses given by:

$$M(W_1) = \xi_2 = 2\varphi_1 - \varphi_2, \quad M(W_2) = \xi_1 = 2\varphi_2 - \varphi_1. \tag{3.88}$$

This resolution corresponds to gauge theory chamber 4 (cf. Table 4 and (A.8)), with instanton masses given by:

$$\begin{aligned}
M(\mathcal{I}_1) &= \chi(r_0 = -\xi_2) = 2\xi_2 + \xi_7 = h_0 + 4\varphi_1 - m, \\
M(\mathcal{I}_2) &= \chi(r_0 = 0) = \xi_7 = h_0 + 2\varphi_2 - m, \\
M(\mathcal{I}_3) &= \chi(r_0 = \xi_1) = \xi_7 = h_0 + 2\varphi_2 - m.
\end{aligned} \tag{3.89}$$

The masses of hypermultiplets are:

$$\begin{aligned}
M(\mathcal{H}_1) &= \xi_6 = -\varphi_2 + m, \\
M(\mathcal{H}_2) &= \xi_1 + \xi_6 = -\varphi_1 + \varphi_2 + m, \\
M(\mathcal{H}_3) &= \xi_1 + \xi_2 + \xi_6 = \varphi_1 + m.
\end{aligned} \tag{3.90}$$

Plugging the map between $(\boldsymbol{\nu}, \boldsymbol{\mu})$ parameters and field-theory parameters given by (3.60), into (3.86), we recover the field theory prepotential,

$$\mathcal{F}_{SU(3)_2, N_f=1}^{\text{chamber 4}} = \frac{4}{3}(\varphi_1^3 + \varphi_2^3) - \varphi_1 \varphi_2^2 + (h_0 - m) \varphi_1^2 + (h_0 - m) \varphi_2^2 + (m - h_0) \varphi_1 \varphi_2, \tag{3.91}$$

up to φ -independent terms. The monopole string tensions from $\chi(r_0)$ are given by:

$$T_{1,\text{geo}} = \int_{-\xi_2}^0 \chi(r_0) dr_0 = \xi_2(\xi_2 + \xi_7), \quad T_{2,\text{geo}} = \int_0^{\xi_1} \chi(r_0) dr_0 = \xi_1\xi_7, \quad (3.92)$$

Using the map $\xi_1 = 2\varphi_2 - \varphi_1$, $\xi_2 = 2\varphi_1 - \varphi_2$, $\xi_6 = -\varphi_2 + m$ and $\xi_7 = h_0 + 2\varphi_2 - m$, one can verify that $T_{i,\text{ft}} = T_{i,\text{geo}}$ for $i = 1, 2$. It is easy to see that subloci of vanishing tension lie along hard walls where either W-boson becomes massless, or along hard walls that are not in this Kähler chamber. Away from a hard wall, \mathcal{H}_1 can become massless signaling a flop of \mathcal{C}_6 leading back to resolution (a).

Resolution (d). Consider the crepant resolution of Figure 11(d), with curves and divisors shown in Figure 15(a). The linear relations among curve classes are:

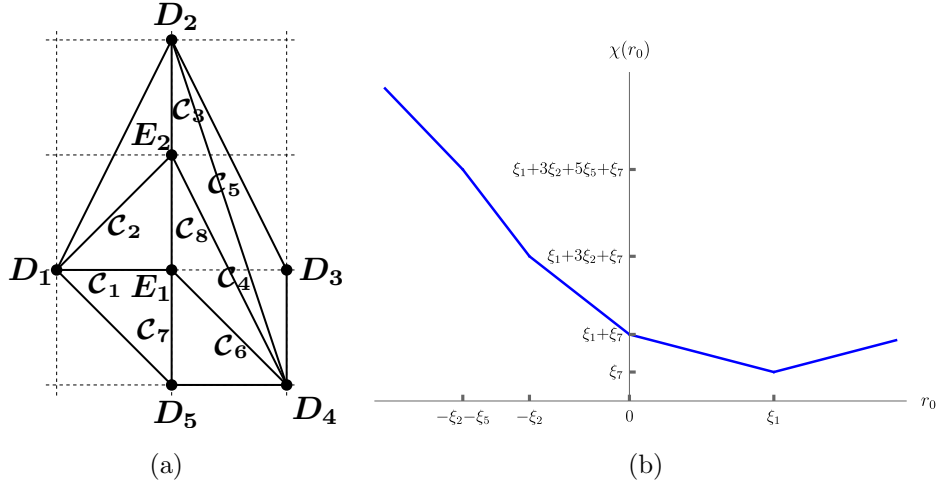


Figure 15. Resolution (d) of the $E_2^{2, \frac{3}{2}}$ singularity and its vertical reduction.

$$\mathcal{C}_3 \simeq \mathcal{C}_1 + 3\mathcal{C}_2 + \mathcal{C}_7, \quad \mathcal{C}_4 \simeq \mathcal{C}_2, \quad \mathcal{C}_6 \simeq \mathcal{C}_1, \quad \mathcal{C}_8 \simeq \mathcal{C}_1 + \mathcal{C}_7. \quad (3.93)$$

We take $\{\mathcal{C}_1, \mathcal{C}_2, \mathcal{C}_5, \mathcal{C}_7\}$ as generators of the Mori cone. The GLSM charge matrix is:

	D_1	D_2	D_3	D_4	D_5	\mathbf{E}_1	\mathbf{E}_2	$\text{vol}(\mathcal{C})$
\mathcal{C}_1	0	0	0	0	1	-2	1	ξ_1
\mathcal{C}_2	0	1	0	0	0	1	-2	ξ_2
\mathcal{C}_5	0	-1	1	-1	0	0	1	ξ_5
\mathcal{C}_7	1	0	0	1	-1	-1	0	ξ_7
$U(1)_M$	0	0	0	0	0	-1	1	r_0

(3.94)

The parameters $(\mu_1, \mu_2, \nu_1, \nu_2)$ are related to the FI parameters by:

$$\xi_1 = -2\nu_1 + \nu_2 \geq 0, \quad \xi_2 = \mu_2 + \nu_1 - 2\nu_2 \geq 0, \quad \xi_5 = -\mu_2 + \nu_2 \geq 0, \quad \xi_7 = \mu_1 - \nu_1 \geq 0. \quad (3.95)$$

The relevant triple-intersection numbers are:

$$\begin{aligned} D_1 \mathbf{E}_1 \mathbf{E}_2 &= 1, & D_2 \mathbf{E}_1 \mathbf{E}_2 &= 0, & D_1 D_2 \mathbf{E}_1 &= 0, & D_1 D_2 \mathbf{E}_2 &= 1, \\ D_1 \mathbf{E}_1^2 &= -2, & D_2 \mathbf{E}_1^2 &= 0, & D_1 \mathbf{E}_2^2 &= -2, & D_2 \mathbf{E}_2^2 &= -5, \\ D_1^2 \mathbf{E}_1 &= 0, & D_1^2 \mathbf{E}_2 &= 0, & D_2^2 \mathbf{E}_1 &= 0, & D_2^2 \mathbf{E}_2 &= 3, \\ \mathbf{E}_1^2 \mathbf{E}_2 &= -3, & \mathbf{E}_1 \mathbf{E}_2^2 &= 1, & \mathbf{E}_1^3 &= 8, & \mathbf{E}_2^3 &= 8. \end{aligned} \quad (3.96)$$

Therefore, the compact part of the prepotential is:

$$\begin{aligned} \mathcal{F}_{(d)}(\nu_1, \nu_2; \mu_1, \mu_2) &= -\frac{1}{6} S^3 = -\frac{4}{3}(\nu_1^3 + \nu_2^3) + \frac{3}{2}\nu_1^2\nu_2 - \frac{1}{2}\nu_1\nu_2^2 + \mu_1\nu_1^2 - \mu_1\nu_1\nu_2 \\ &\quad + \left(\mu_1 + \frac{5}{2}\mu_2\right)\nu_2^2 + \left(\frac{3}{2}\mu_2^2 - \mu_1\mu_2\right)\nu_2. \end{aligned} \quad (3.97)$$

The IIA profile is:

$$\chi(r_0) = \begin{cases} -4r_0 + \xi_1 - \xi_2 + \xi_5 + \xi_7, & \text{for } r_0 \leq -\xi_2 - \xi_5 \\ -5r_0 + \xi_1 - 2\xi_2 + \xi_7, & \text{for } -\xi_2 - \xi_5 \leq r_0 \leq -\xi_2 \\ -3r_0 + \xi_1 + \xi_7, & \text{for } -\xi_2 \leq r_0 \leq 0 \\ -r_0 + \xi_1 + \xi_7, & \text{for } \xi_1 \leq r_0 \leq \xi_1 \\ +r_0 - \xi_1 + \xi_7, & \text{for } r_0 \geq \xi_1. \end{cases} \quad (3.98)$$

This function is sketched in Figure 15(b). At the points $r_0 = -\xi_2$, $r_0 = 0$ and $r_0 = \xi_1$, there are gauge D6-branes wrapping \mathbb{P}^1 's in the resolution of the singularity. There is a flavor D6-brane at $r_0 = -\xi_2 - \xi_5$. The simple-root W-bosons have masses given by:

$$M(W_1) = \xi_2 = 2\varphi_1 - \varphi_2, \quad M(W_2) = \xi_1 = 2\varphi_2 - \varphi_1. \quad (3.99)$$

This resolution corresponds to gauge theory chamber 1 (cf. Table 4 and (A.5)), with instanton masses given by:

$$\begin{aligned} M(\mathcal{I}_1) &= \chi(r_0 = -\xi_2) = \xi_1 + 3\xi_2 + \xi_7 = h_0 + 5\varphi_1, \\ M(\mathcal{I}_2) &= \chi(r_0 = 0) = \xi_1 + \xi_7 = h_0 - \varphi_1 + 3\varphi_2, \\ M(\mathcal{I}_3) &= \chi(r_0 = \xi_1) = \xi_7 = h_0 + \varphi_2. \end{aligned} \quad (3.100)$$

The masses of hypermultiplets are:

$$\begin{aligned} M(\mathcal{H}_1) &= \xi_5 = -\varphi_1 - m, \\ M(\mathcal{H}_2) &= \xi_2 + \xi_5 = \varphi_1 - \varphi_2 - m, \\ M(\mathcal{H}_3) &= \xi_1 + \xi_2 + \xi_5 = \varphi_2 - m. \end{aligned} \quad (3.101)$$

Plugging (3.60) into (3.97), we recover the field theory prepotential,

$$\mathcal{F}_{SU(3)_2, N_f=2}^{\text{chamber 1}} = \frac{4}{3}(\varphi_1^3 + \varphi_2^3) - \varphi_1\varphi_2^2 + (h_0 - m)\varphi_1^2 + (h_0 - m)\varphi_2^2 + (m - h_0)\varphi_1\varphi_2, \quad (3.102)$$

up to φ -independent terms. The tensions from $\chi(r_0)$ are given by:

$$T_{1,\text{geo}} = \int_{-\xi_2}^0 \chi(r_0) dr_0 = \xi_2 \left(\frac{3}{2}\xi_2 + \xi_1 + \xi_7 \right), \quad T_{2,\text{geo}} = \int_0^{\xi_1} \chi(r_0) dr_0 = \frac{1}{2}\xi_1(\xi_1 + 2\xi_7). \quad (3.103)$$

Using the map $\xi_1 = 2\varphi_2 - \varphi_1$, $\xi_2 = 2\varphi_1 - \varphi_2$, $\xi_5 = -\varphi_1 - m$ and $\xi_7 = h_0 + \varphi_2$, we find that $T_{i,\text{ft}} = T_{i,\text{geo}}$ for $i = 1, 2$. It is easy to check that in this case too, loci of vanishing tension are either hard walls where W-bosons become massless, or walls that do not lie in this Kähler chamber. There is a perturbative wall corresponding to a flop of \mathcal{C}_5 (when \mathcal{H}_1 becomes massless), but also a traversible instantonic wall at leading to non-gauge theory resolution (g).

Resolutions (e), (f), (g) and RG flow. As noted above, the crepant resolutions in Figures 11(e)-11(g) do not admit vertical reductions. Nevertheless, they have interesting roles to play in the Kähler moduli space of the $E_2^{2, \frac{3}{2}}$ singularity. In resolution (e), one can send the volume of the curve \mathcal{C}_7 to infinity, thereby decoupling the divisor D_5 . This leads to a crepant resolution of the non-Lagrangian $E_1^{2,\text{NL}}$ singularity (see Figure 16).¹⁹ Similarly in resolution (f), one can decouple D_5 by sending $\text{vol}(\mathcal{C}_7)$ to infinity. This results in yet another crepant resolution of the $E_1^{2,\text{NL}}$ singularity, as shown in Figure 17. Finally in resolution (g), one can decouple D_3 and D_5 by sending both $\text{vol}(\mathcal{C}_5)$ and $\text{vol}(\mathcal{C}_7)$ to infinity as shown in Figure 18. This leads to the unique crepant resolution of the $SL(2, \mathbb{Z})$ -transformed version of the $E_0^{2,\text{NL}}$ singularity, which as we stated above, is also non-Lagrangian.

In summary, starting from the non-Lagrangian deformations of the $E_2^{2, \frac{3}{2}}$ singularity, one can obtain the non-Lagrangian deformations of $E_0^{2,\text{NL}}$ and $E_1^{2,\text{NL}}$ via RG flow in parameter space. A careful analysis of the phase boundaries – carried out in the next section – reveals that resolutions (e), (f) and (g) do not survive the limit in which the mass deformations are set to zero (that is, the Coulomb branch of the SCFT).

3.4.1 Sample slicings of the $E_2^{2, \frac{3}{2}}$ moduli space

In Figure 19, we show some sample slices of the moduli space of the $E_2^{2, \frac{3}{2}}$ geometry. The phase diagram of this geometry, parametrized by $(\boldsymbol{\nu}; \boldsymbol{\mu}) \equiv (\nu_1, \nu_2; \mu_1, \mu_2)$ is a four-dimensional region, given by the disjoint union of the regions described by the defining inequalities of 7 Kähler chambers, which are listed in Table 2.

¹⁹More precisely, an $SL(2, \mathbb{Z})$ transformation (using, for instance an S^2TSTS^{-2} transformation) of the toric diagram on the right in Figure 16 brings it into crepant resolution of $E_1^{2,\text{NL}}$ of Figure 3(e).

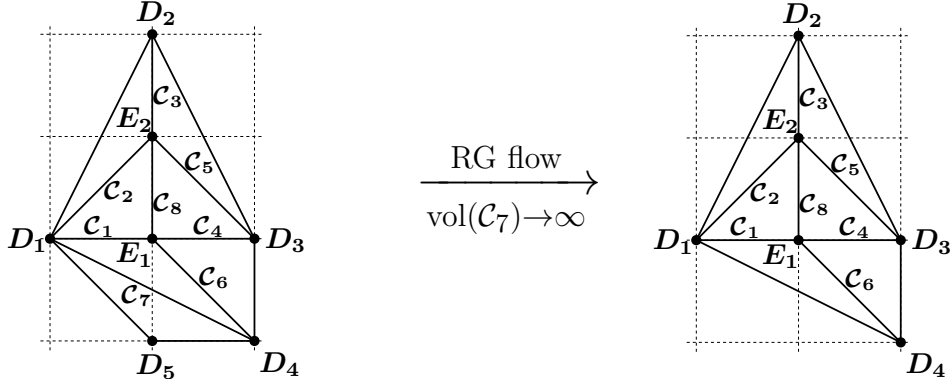


Figure 16. Decoupling a divisor from $E_2^{2,\frac{3}{2}}$ resolution (e) yields an $SL(2, \mathbb{Z})$ -transformed version of a crepant resolution of the $E_1^{2, \text{NL}}$ singularity.

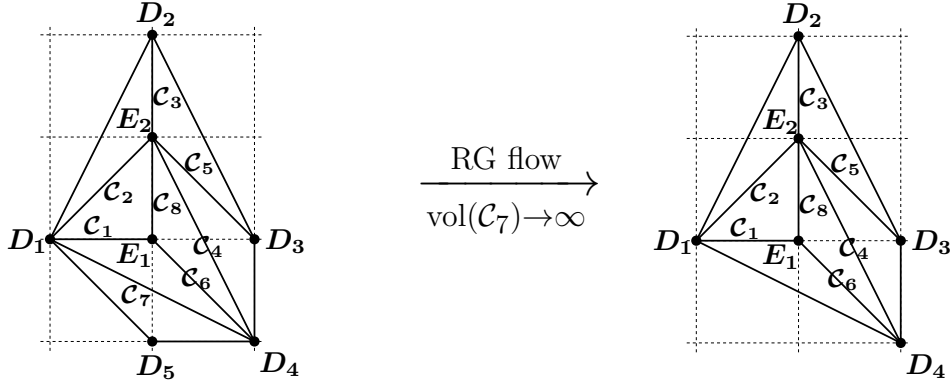


Figure 17. Decoupling a divisor from $E_2^{2,\frac{3}{2}}$ resolution (f) yields an $SL(2, \mathbb{Z})$ -transformed version of a crepant resolution of the $E_1^{2, \text{NL}}$ singularity.

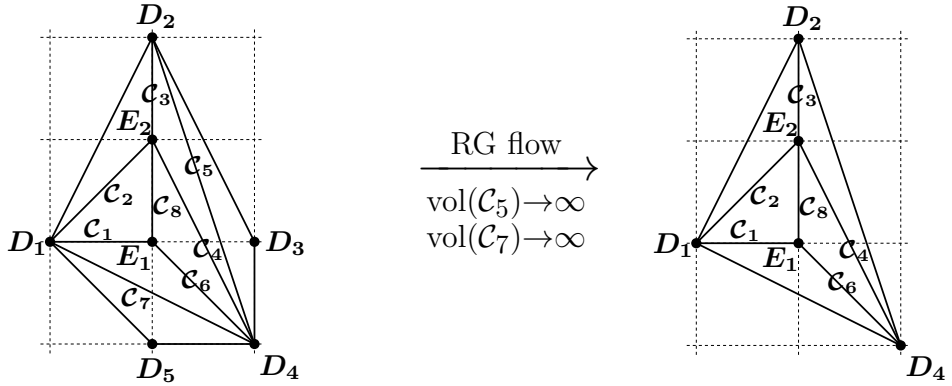


Figure 18. Decoupling two divisors from $E_2^{2,\frac{3}{2}}$ resolution (g) yields an $SL(2, \mathbb{Z})$ -transformed version of the unique crepant resolution of the $E_0^{2, \text{NL}}$ singularity.

(a)	$\{\mu_2 + \nu_1 - 2\nu_2 \geq 0\} \cap \{\nu_2 - \nu_1 \geq 0\} \cap \{-\nu_1 \geq 0\} \cap \{\mu_1 - \nu_1 \geq 0\}$
(b)	$\{\nu_2 - 2\nu_1 \geq 0\} \cap \{\nu_1 - \nu_2 \geq 0\} \cap \{\mu_2 - \nu_2 \geq 0\} \cap \{\mu_1 - \nu_1 \geq 0\}$
(c)	$\{\nu_2 - 2\nu_1 \geq 0\} \cap \{\mu_2 + \nu_1 - 2\nu_2 \geq 0\} \cap \{\nu_1 \geq 0\} \cap \{\mu_1 - 2\nu_1 \geq 0\}$
(d)	$\{\nu_2 - 2\nu_1 \geq 0\} \cap \{\mu_2 + \nu_1 - 2\nu_2 \geq 0\} \cap \{\nu_2 - \mu_2 \geq 0\} \cap \{\mu_1 - \nu_1 \geq 0\}$
(e)	$\{\nu_2 - \nu_1 \geq 0\} \cap \{\mu_2 + \nu_1 - 2\nu_2 \geq 0\} \cap \{\mu_1 - 2\nu_1 \geq 0\} \cap \{\nu_1 - \mu_1 \geq 0\}$
(f)	$\{\mu_1 - 3\nu_1 + \nu_2 \geq 0\} \cap \{\nu_1 - \nu_2 \geq 0\} \cap \{\mu_2 - \nu_2 \geq 0\} \cap \{\nu_1 - \mu_1 \geq 0\}$
(g)	$\{\mu_1 - 3\nu_1 + \nu_2 \geq 0\} \cap \{\mu_2 + \nu_1 - 2\nu_2 \geq 0\} \cap \{\nu_2 - \mu_2 \geq 0\} \cap \{\nu_1 - \mu_1 \geq 0\}$

Table 2. Geometric inequalities (“Nef conditions”) defining the Kähler chambers of the 7 resolutions of the $E_2^{2, \frac{3}{2}}$ geometry.

The phase diagram can be visualized by taking slices at different values of (μ_1, μ_2) , which reveal different chambers. For some values of $(\nu; \mu)$ some regions vanish altogether while other regions collapse to real codimension-one walls in this parameter space (along which flops may occur). The origin $(\nu_1, \nu_2) = (0, 0)$ is denoted by a red dot on the top right of each plot. To make the plots readable, we only highlight chambers that have a finite area in parameter space in the slices that are considered. When $\mu \neq 0$, the origin $\nu_1 = \nu_2 = 0$ is generally *not* the origin of the Coulomb branch of the gauge theory (when such a description exists), since the map (3.60) between ν_1, ν_2 and φ_1, φ_2 for $SU(3) N_f = 2$ involves a contribution from the real mass m . The slicings of Figure 19 can also be used to highlight some geometric features. For instance, resolution (b) is obtained from resolution (a) by flopping curve \mathcal{C}_4 . This corresponds to the volume $\text{vol}(\mathcal{C}_4) = \xi_4 = -\nu_1 + \nu_2$ shrinking to zero size in the Kähler chamber defining resolution (a), before it grows in the birational Kähler chamber of resolution (b). The real codimension-1 wall separating phases (a) and (b) is clearly visible in Figure 19(i). In order to reach resolution (c), one just needs to flop curve \mathcal{C}_6 which has volume $\text{vol}(\mathcal{C}_6) = \xi_6 = -\nu_1$. This vanishes along the vertical line $\nu_1 = 0$ indicating a wall separating regions (a) and (c) in Figure 19(ii). On the other hand, to reach chamber (c) from chamber (b), one needs to perform *two* flops, which necessitates going through the origin, as is also clear from the figure.

Finally, turning on generic mass deformations reveals non-gauge theoretic phases, and, as is clear from Figure 19(iii) and Figure 19(iv), these phases – which also admit no type IIA reduction – are not compatible with the SCFT Coulomb branch. This is consistent with the results of [10].

3.4.2 Probing the Coulomb branch of the 5d SCFT

To probe the Coulomb branch of the 5d SCFT, we set the mass parameters to zero. From (3.60), this implies that $\nu_1 = -\varphi_2$ and $\nu_2 = -\varphi_1$. On the field theory side, we

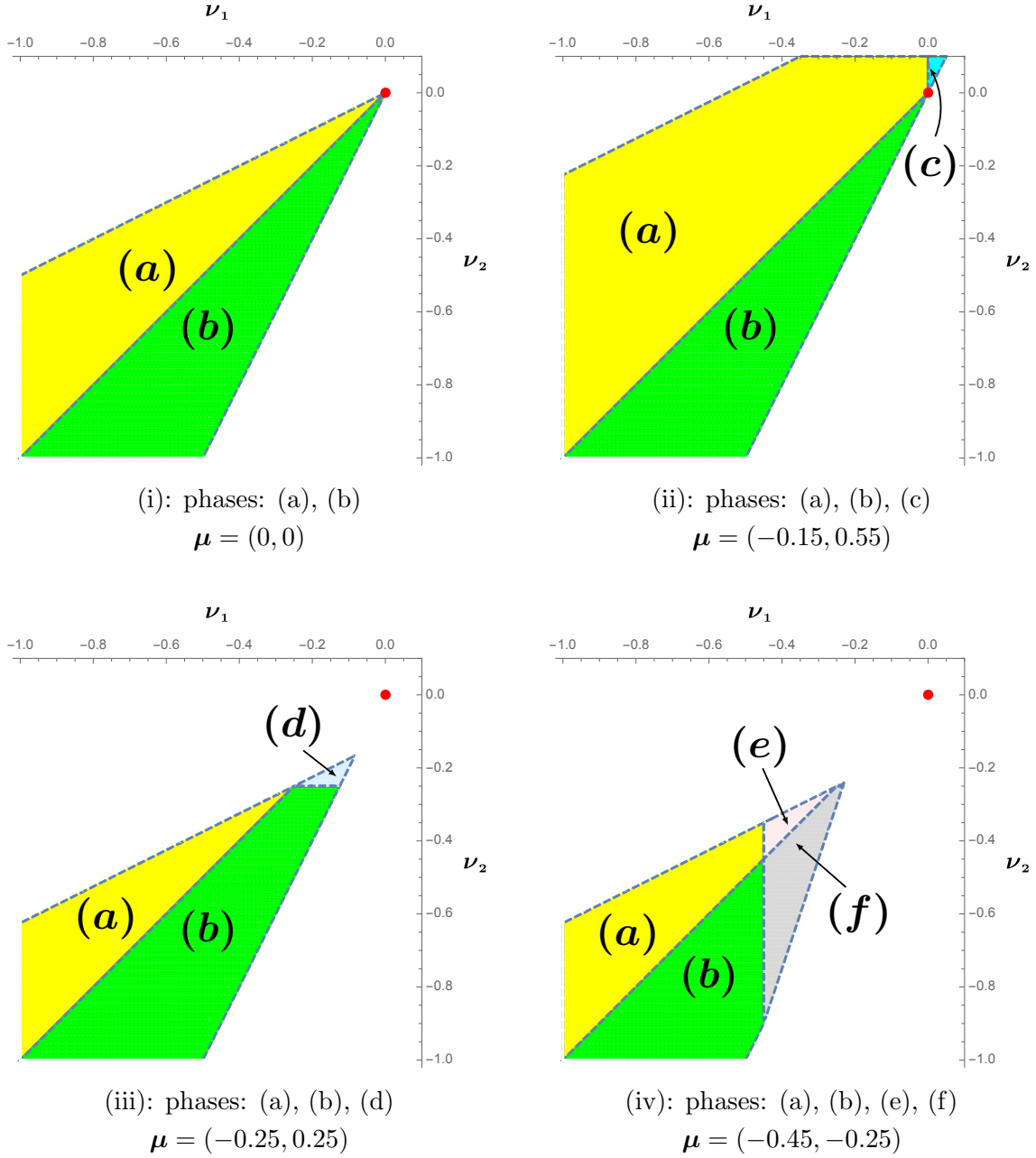


Figure 19. Sample slices of the moduli space of the $E_2^{2, \frac{3}{2}}$ geometry. Turning on different mass deformations reveals more $SU(3)$ $N_f = 1$ phases such as (c) in (ii) and (d) in (iii), but also non-gauge theoretic phases such as (e) and (f) in (iv).

observe that only chambers 2 and 3 of the $SU(3)_{\frac{3}{2}}$ $N_f = 1$ theory (see Appendix A)

survive in this limit, and they are given by:

$$\text{chamber 2 : } \begin{cases} \varphi_1 \geq 0 , \\ -\varphi_2 + \varphi_2 < 0 , \\ -\varphi_2 < 0 , \end{cases} \quad \text{chamber 3 : } \begin{cases} \varphi_1 \geq 0 , \\ -\varphi_2 + \varphi_2 \geq 0 , \\ -\varphi_2 < 0 . \end{cases} \quad (3.104)$$

One can also verify from the Nef conditions in Table 2 that only resolutions (a) and (b) survive in this limit. The Coulomb branch of the SCFT is sketched in Figure 19(i). The red dot on the right in the figure is the conformal point.

3.5 The $E_2^{2, \frac{1}{2}}$ singularity and $SU(3)_{\frac{1}{2}} N_f = 1$ gauge theory

The $E_2^{2, \frac{1}{2}}$ singularity (Figure 3(g)) admits 6 crepant resolutions shown in Figure 20. The first four resolutions, Figures 20(a)-20(d), admit vertical reductions to type IIA, which correspond to chambers of the $SU(3)_1 N_f = 1$ gauge theory, as we illustrate below. Phases (e) and (f) do not admit a Lagrangian description.

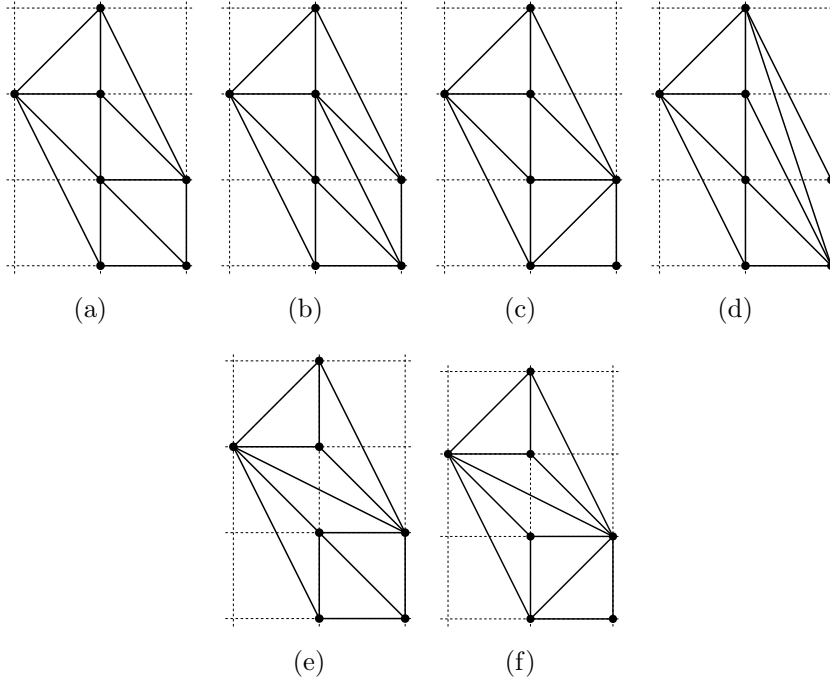


Figure 20. The 6 crepant singularities of the $E_2^{2, \frac{1}{2}}$ singularity. The first four, (a)-(d) admit a vertical reduction, corresponding to chambers of the $SU(3)_1 N_f = 1$ gauge theory.

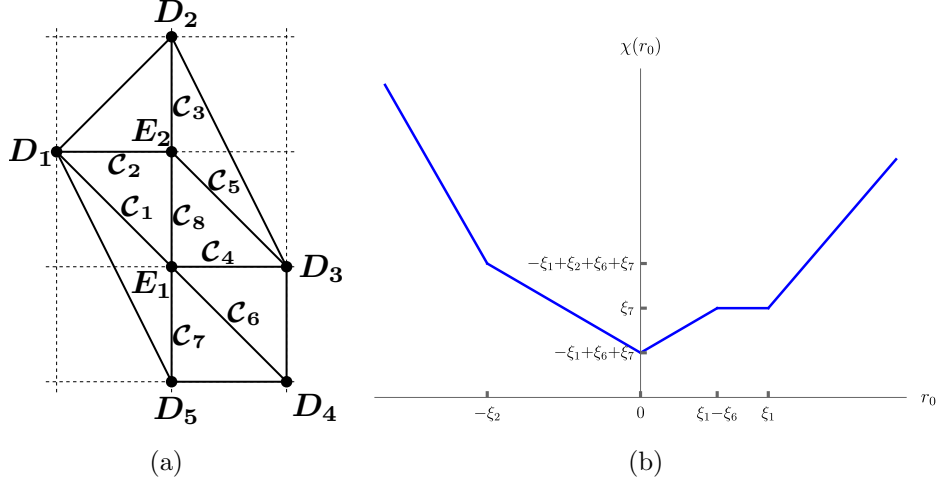


Figure 21. Resolution (a) of the $E_2^{2, \frac{1}{2}}$ singularity and its vertical reduction.

Resolution (a). Consider the crepant resolution of Figure 20(a), with curves and divisors shown in Figure 21(a). There are five non-compact toric divisors D_i ($i = 1, \dots, 5$), and two compact toric divisors \mathbf{E}_1 and \mathbf{E}_2 with the following linear relations:

$$D_1 \simeq D_3 + D_4, \quad \mathbf{E}_1 \simeq D_2 - D_3 - 2D_4 - 2D_5, \quad \mathbf{E}_2 \simeq -D_1 - 2D_2 + D_4 + D_5. \quad (3.105)$$

The compact curves \mathcal{C} are:

$$\begin{aligned} \mathcal{C}_1 &= \mathbf{E}_1 \cdot D_1, & \mathcal{C}_2 &= \mathbf{E}_2 \cdot D_1, & \mathcal{C}_3 &= \mathbf{E}_2 \cdot D_2, & \mathcal{C}_4 &= \mathbf{E}_1 \cdot D_3, \\ \mathcal{C}_5 &= \mathbf{E}_2 \cdot D_3, & \mathcal{C}_6 &= \mathbf{E}_1 \cdot D_4, & \mathcal{C}_7 &= \mathbf{E}_1 \cdot D_5, & \mathcal{C}_8 &= \mathbf{E}_2 \cdot \mathbf{E}_1. \end{aligned} \quad (3.106)$$

The linear relations among curve classes are:

$$\mathcal{C}_3 \simeq -\mathcal{C}_1 + \mathcal{C}_2 + \mathcal{C}_6 + \mathcal{C}_7, \quad \mathcal{C}_4 \simeq \mathcal{C}_1 - \mathcal{C}_6, \quad \mathcal{C}_5 \simeq \mathcal{C}_2, \quad \mathcal{C}_8 \simeq -\mathcal{C}_1 + \mathcal{C}_6 + \mathcal{C}_7. \quad (3.107)$$

We take $\{\mathcal{C}_1, \mathcal{C}_2, \mathcal{C}_6, \mathcal{C}_7\}$ as generators of the Mori cone. The requirement the compact curves $\mathcal{C}_3, \mathcal{C}_4$ and \mathcal{C}_8 have non-negative volume imposes the following additional conditions on the FI parameters in this chamber:

$$-\xi_1 + \xi_2 + \xi_6 + \xi_7 \geq 0, \quad \xi_1 - \xi_6 \geq 0, \quad -\xi_1 + \xi_6 + \xi_7 \geq 0. \quad (3.108)$$

The GLSM charge matrix is:

	D_1	D_2	D_3	D_4	D_5	\mathbf{E}_1	\mathbf{E}_2	$\text{vol}(\mathcal{C})$
\mathcal{C}_1	0	0	0	0	1	-2	1	ξ_1
\mathcal{C}_2	0	1	0	0	0	1	-2	ξ_2
\mathcal{C}_6	0	0	1	-1	1	-1	0	ξ_6
\mathcal{C}_7	1	0	0	1	0	-2	0	ξ_7
$U(1)_M$	0	0	0	0	0	-1	1	r_0

(3.109)

Geometric prepotential. We parametrize the Kähler cone by:

$$S = \mu_1 D_1 + \mu_2 D_2 + \nu_1 \mathbf{E}_1 + \nu_2 \mathbf{E}_2 . \quad (3.110)$$

The parameters $(\mu_1, \mu_2, \nu_1, \nu_2)$ are related to the FI parameters by:

$$\xi_1 = -2\nu_1 + \nu_2 \geq 0, \quad \xi_2 = \mu_2 + \nu_1 - 2\nu_2 \geq 0, \quad \xi_6 = -\nu_1 \geq 0, \quad \xi_7 = \mu_1 - 2\nu_1 \geq 0 . \quad (3.111)$$

The relevant triple-intersection numbers are:

$$\begin{aligned} D_1 \mathbf{E}_1 \mathbf{E}_2 &= 1, & D_2 \mathbf{E}_1 \mathbf{E}_2 &= 0, & D_1 D_2 \mathbf{E}_1 &= 0, & D_1 D_2 \mathbf{E}_2 &= 1, \\ D_1 \mathbf{E}_1^2 &= -2, & D_2 \mathbf{E}_1^2 &= 0, & D_1 \mathbf{E}_2^2 &= -2, & D_2 \mathbf{E}_2^2 &= -3, \\ D_1^2 \mathbf{E}_1 &= 0, & D_1^2 \mathbf{E}_2 &= 0, & D_2^2 \mathbf{E}_1 &= 0, & D_2^2 \mathbf{E}_2 &= 1, \\ \mathbf{E}_1^2 \mathbf{E}_2 &= -1, & \mathbf{E}_1 \mathbf{E}_2^2 &= -1, & \mathbf{E}_1^3 &= 7, & \mathbf{E}_2^3 &= 8. \end{aligned} \quad (3.112)$$

Therefore, the compact part of the prepotential is:

$$\begin{aligned} \mathcal{F}_{(a)}(\nu_1, \nu_2; \mu_1, \mu_2) &= -\frac{1}{6} S^3 = -\frac{7}{6} \nu_1^3 - \frac{4}{3} \nu_2^3 + \frac{1}{2} (\nu_1^2 \nu_2 + \nu_1 \nu_2^2) + \mu_1 \nu_1^2 - \mu_1 \nu_1 \nu_2 \\ &\quad + \left(\mu_1 + \frac{3}{2} \mu_2 \right) \nu_2^2 - \left(\mu_1 \mu_2 + \frac{1}{2} \mu_2^2 \right) \nu_2 . \end{aligned} \quad (3.113)$$

Type IIA reduction and gauge theory description. The type IIA background is again resolved A_1 singularity fibered over the $x^9 = r_0$ direction. There are three D6-branes wrapping the exceptional \mathbb{P}^1 in the resolved A_1 singularity, resulting in an $SU(3)$ gauge theory. There is also a D6-brane wrapping a noncompact divisor in the resolved ALE space, which corresponds to one fundamental flavor. The volume of the exceptional \mathbb{P}^1 is given by the following piecewise linear function:

$$\chi(r_0) = \begin{cases} -3r_0 - \xi_1 - 2\xi_2 + \xi_6 + \xi_7, & \text{for } r_0 \leq -\xi_2 \\ -r_0 - \xi_1 + \xi_6 + \xi_7, & \text{for } -\xi_2 \leq r_0 \leq 0 \\ +r_0 - \xi_1 + \xi_6 + \xi_7, & \text{for } 0 \leq r_0 \leq \xi_1 - \xi_6 \\ \xi_7, & \text{for } \xi_1 - \xi_6 \leq r_0 \leq \xi_1 \\ +2r_0 - 2\xi_1 + \xi_7, & \text{for } r_0 \geq \xi_1 . \end{cases} \quad (3.114)$$

This function is sketched in Figure 21(b). At the points $r_0 = -\xi_2$, $r_0 = 0$ and $r_0 = \xi_1$, there are gauge D6-branes wrapping \mathbb{P}^1 's in the resolution of the singularity. When $\xi_1 = \xi_2 = 0$, an $SU(3)$ gauge theory is realized with coupling $h_0 = \xi_6 + \xi_7$. There is a flavor D6-brane at $r_0 = \xi_1 - \xi_6$. The effective Chern-Simons level is given by $\kappa_{s,\text{eff}} = -\frac{1}{2}(-3+2) = \frac{1}{2}$, which is interpreted as a bare CS level of 1 plus the contribution $-\frac{1}{2}$ due to the single hypermultiplet (cf. (2.5)). The simple-root W-bosons have masses:

$$M(W_1) = \xi_2 = 2\varphi_1 - \varphi_2, \quad M(W_2) = \xi_1 = 2\varphi_2 - \varphi_1 . \quad (3.115)$$

From the instanton masses, one can identify that this resolution corresponds to gauge theory chamber 3 (cf. Table 4 and (A.7)):

$$\begin{aligned}
M(\mathcal{I}_1) &= \chi(r_0 = -\xi_2) = -\xi_1 + \xi_2 + \xi_6 + \xi_7 = h_0 + 3\varphi_1 - m , \\
M(\mathcal{I}_2) &= \chi(r_0 = 0) = -\xi_1 + \xi_6 + \xi_7 = h_0 + \varphi_1 + \varphi_2 - m , \\
M(\mathcal{I}_3) &= \chi(r_0 = \xi_1) = \xi_7 = h_0 + 2\varphi_2 .
\end{aligned} \tag{3.116}$$

The masses of hypermultiplets are:

$$\begin{aligned}
M(\mathcal{H}_1) &= \xi_6 = \varphi_2 - m , \\
M(\mathcal{H}_2) &= \xi_1 - \xi_6 = -\varphi_1 + \varphi_2 + m , \\
M(\mathcal{H}_3) &= \xi_1 + \xi_2 - \xi_6 = \varphi_1 + m .
\end{aligned} \tag{3.117}$$

From the Kähler volumes (3.111) of the compact curves and masses of W-bosons and instantons, the map between geometry and field theory variables is determined to be:

$$\mu_1 = h_0 + 2m, \quad \mu_2 = 3m, \quad \nu_1 = -\varphi_2 + m, \quad \nu_2 = -\varphi_1 + 2m . \tag{3.118}$$

Plugging (3.118) into (3.113), we recover the field theory prepotential,

$$\begin{aligned}
\mathcal{F}_{SU(3)_{\frac{1}{2}}, N_f=1}^{\text{chamber 3}} &= \frac{4}{3}\varphi_1^3 + \frac{7}{6}\varphi_2^3 - \frac{1}{2}(\varphi_1^2\varphi_2 + \varphi_1\varphi_2^2) + (h_0 - m)\varphi_1^2 + \left(h_0 - \frac{m}{2}\right)\varphi_2^2 \\
&\quad + (m - h_0)\varphi_1\varphi_2 - \frac{m^2}{2}\varphi_2 ,
\end{aligned} \tag{3.119}$$

up to φ -independent terms. The monopole string tensions from $\chi(r_0)$ are given by:

$$T_{1,\text{geo}} = \int_{-\xi_2}^0 \chi(r_0) dr_0 = \xi_2 \left(-\xi_1 + \frac{1}{2}\xi_2 + \xi_6 + \xi_7 \right) , \tag{3.120}$$

$$T_{2,\text{geo}} = \int_0^{\xi_1} \chi(r_0) dr_0 = -\frac{\xi_1^2}{2} + \xi_6\xi_1 + \xi_7\xi_1 - \frac{\xi_6^2}{2} . \tag{3.121}$$

Using the map $\xi_1 = 2\varphi_2 - \varphi_1$, $\xi_2 = 2\varphi_1 - \varphi_2$, $\xi_6 = \varphi_2 - m$ and $\xi_7 = h_0 + 2\varphi_2$, one can verify that indeed $T_{i,\text{ft}} = T_{i,\text{geo}}$ for $i = 1, 2$. The tensions vanishes at loci given by:

$$\begin{aligned}
(I) &: \{ \xi_2 = 0 \} \cup \left\{ -\xi_1 + \frac{1}{2}\xi_2 + \xi_6 + \xi_7 = 0 \right\} , \quad \text{and} , \\
(II) &: \left\{ -\frac{\xi_1^2}{2} + \xi_6\xi_1 + \xi_7\xi_1 - \frac{\xi_6^2}{2} = 0 \right\} .
\end{aligned} \tag{3.122}$$

Along the submanifold $\{\xi_2 = 0\} \subset (I)$, the W-boson W_1 becomes massless, signaling a hard wall. The submanifold $\{-\xi_1 + \frac{1}{2}\xi_2 + \xi_6 + \xi_7 = 0\}$ is not part of the Kähler chamber of resolution (a). Solving the quadratic equation in (II), we get two solutions:

$\xi_6 = \xi_1 \pm \sqrt{2\xi_1\xi_7}$. Both sign choices are inconsistent with (3.108), and are hence rejected. Note that away from any hard wall, the perturbative hypermultiplet \mathcal{H}_1 can become massless at $\xi_6 = 0$ (signaling a flop of \mathcal{C}_6), leading to gauge theory resolution (c), or the hypermultiplet \mathcal{H}_2 can become massless along the locus $\xi_4 = \xi_1 - \xi_6 = 0$ (signaling a flop of \mathcal{C}_4), leading to gauge theory resolution (b). Note that the intersection of the loci (II) above with the loci $\{\xi_1 = \xi_6\}$ is $\xi_1\xi_7 = 0$, is inconsistent in this Kähler chamber, as neither the W-boson W_2 (with mass ξ_1) can become massless (except at the hard wall) nor can the curve \mathcal{C}_7 flop in this chamber. This is a reassuring consistency check.

Resolution (b). Consider the crepant resolution of Figure 20(b), with curves and divisors shown in Figure 22(a). The linear relations among the toric divisors are still

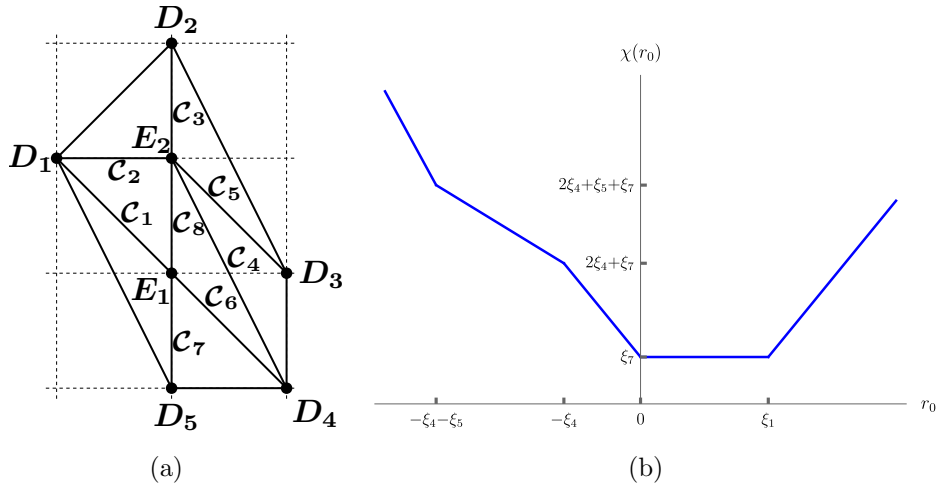


Figure 22. Resolution (b) of the $E_2^{2, \frac{1}{2}}$ singularity and its vertical reduction.

given by (3.105). The compact curves \mathcal{C} can be read off the toric diagram. The linear relations among curve classes are:

$$\mathcal{C}_2 \simeq \mathcal{C}_4 + \mathcal{C}_5, \quad \mathcal{C}_3 \simeq 2\mathcal{C}_4 + \mathcal{C}_5 + \mathcal{C}_7, \quad \mathcal{C}_6 \simeq \mathcal{C}_1, \quad \mathcal{C}_8 \simeq \mathcal{C}_7. \quad (3.123)$$

We take $\{\mathcal{C}_1, \mathcal{C}_4, \mathcal{C}_5, \mathcal{C}_7\}$ as generators of the Mori cone. The GLSM charge matrix is:

	D_1	D_2	D_3	D_4	D_5	\mathbf{E}_1	\mathbf{E}_2	$\text{vol}(\mathcal{C})$
\mathcal{C}_1	0	0	0	0	1	-2	1	ξ_1
\mathcal{C}_4	0	0	1	-1	0	1	-1	ξ_4
\mathcal{C}_5	0	1	-1	1	0	0	-1	ξ_5
\mathcal{C}_7	1	0	0	1	0	-2	0	ξ_7
$U(1)_M$	0	0	0	0	0	-1	1	r_0

(3.124)

The Kähler cone is parametrized by (3.110). The parameters $(\mu_1, \mu_2, \nu_1, \nu_2)$ are related to the FI parameters by:

$$\xi_1 = -2\nu_1 + \nu_2 \geq 0, \quad \xi_4 = \nu_1 - \nu_2 \geq 0, \quad \xi_5 = \mu_2 - \nu_2 \geq 0, \quad \xi_7 = \mu_1 - 2\nu_1 \geq 0. \quad (3.125)$$

The relevant triple-intersection numbers are:

$$\begin{aligned} D_1 \mathbf{E}_1 \mathbf{E}_2 &= 1, & D_2 \mathbf{E}_1 \mathbf{E}_2 &= 0, & D_1 D_2 \mathbf{E}_1 &= 0, & D_1 D_2 \mathbf{E}_2 &= 1, \\ D_1 \mathbf{E}_1^2 &= -2, & D_2 \mathbf{E}_1^2 &= 0, & D_1 \mathbf{E}_2^2 &= -2, & D_2 \mathbf{E}_2^2 &= -3, \\ D_1^2 \mathbf{E}_1 &= 0, & D_1^2 \mathbf{E}_2 &= 0, & D_2^2 \mathbf{E}_1 &= 0, & D_2^2 \mathbf{E}_2 &= 1, \\ \mathbf{E}_1^2 \mathbf{E}_2 &= -2, & \mathbf{E}_1 \mathbf{E}_2^2 &= 0, & \mathbf{E}_1^3 &= 8, & \mathbf{E}_2^3 &= 7. \end{aligned} \quad (3.126)$$

Therefore, the compact part of the prepotential is:

$$\begin{aligned} \mathcal{F}_{(b)}(\nu_1, \nu_2; \mu_1, \mu_2) &= -\frac{1}{6} S^3 = -\frac{4}{3} \nu_1^3 - \frac{7}{6} \nu_2^3 + \nu_1^2 \nu_2 + \mu_1 \nu_1^2 + \left(\mu_1 + \frac{3}{2} \mu_2\right) \nu_2^2 \\ &\quad - \mu_1 \nu_1 \nu_2 - \left(\mu_1 \mu_2 + \frac{1}{2} \mu_2^2\right) \nu_2. \end{aligned} \quad (3.127)$$

The type IIA profile is:

$$\chi(r_0) = \begin{cases} -3r_0 - \xi_4 - 2\xi_5 + \xi_7, & \text{for } r_0 \leq -\xi_4 - \xi_5 \\ -r_0 + \xi_4 + \xi_7, & \text{for } -\xi_4 - \xi_5 \leq r_0 \leq -\xi_4 \\ -2r_0 + \xi_7, & \text{for } -\xi_4 \leq r_0 \leq 0 \\ \xi_7, & \text{for } 0 \leq r_0 \leq \xi_1 \\ +2r_0 - 2\xi_1 + \xi_7, & \text{for } r_0 \geq \xi_1. \end{cases} \quad (3.128)$$

This function is sketched in Figure 22(b). At the points $r_0 = -\xi_4 - \xi_5$, $r_0 = 0$ and $r_0 = \xi_1$, there are gauge D6-branes wrapping \mathbb{P}^1 's in the resolution of the singularity. There is a flavor D6-brane at $r_0 = -\xi_4$. The effective Chern-Simons level is, of course, still $\frac{1}{2}$, as for resolution (a). The simple-root W-bosons have masses given by:

$$M(W_1) = \xi_4 + \xi_5 = 2\varphi_1 - \varphi_2, \quad M(W_2) = \xi_1 = 2\varphi_2 - \varphi_1. \quad (3.129)$$

This resolution corresponds to gauge theory chamber 2 (cf. Table 4 and (A.6)), with instanton masses given by:

$$\begin{aligned} M(\mathcal{I}_1) &= \chi(r_0 = -\xi_4 - \xi_5) = 2\xi_4 + \xi_5 + \xi_7 = h_0 + 3\varphi_1 - m, \\ M(\mathcal{I}_2) &= \chi(r_0 = 0) = \xi_7 = h_0 + 2\varphi_2, \\ M(\mathcal{I}_3) &= \chi(r_0 = \xi_1) = \xi_7 = h_0 + 2\varphi_2. \end{aligned} \quad (3.130)$$

The masses of hypermultiplets are:

$$\begin{aligned} M(\mathcal{H}_1) &= \xi_5 = \varphi_1 + m , \\ M(\mathcal{H}_2) &= \xi_4 = \varphi_1 - \varphi_2 - m , \\ M(\mathcal{H}_3) &= \xi_1 + \xi_4 = \varphi_2 - m . \end{aligned} \tag{3.131}$$

The map between geometry and field theory variables is still given by (3.118), and plugging it into (3.127), we recover the field theory prepotential,

$$\mathcal{F}_{SU(3)_{3/2}, N_f=1}^{\text{chamber 2}} = \frac{7}{6}\varphi_1^3 + \frac{4}{3}\varphi_2^3 - \varphi_1\varphi_2^2 + \left(h_0 - \frac{m}{2}\right)\varphi_1^2 + h_0\varphi_2^2 - h_0\varphi_1\varphi_2 - \frac{m^2}{2}\varphi_2 , \tag{3.132}$$

up to φ -independent terms. The monopole string tensions from $\chi(r_0)$ are given by:

$$T_{1,\text{geo}} = \int_{-\xi_4-\xi_5}^0 \chi(r_0) dr_0 = \xi_4^2 + (2\xi_5 + \xi_7)\xi_4 + \frac{1}{2}\xi_5(\xi_5 + 2\xi_7) , \tag{3.133}$$

$$T_{2,\text{geo}} = \int_0^{\xi_1} \chi(r_0) dr_0 = \xi_1\xi_7 . \tag{3.134}$$

Using the map $\xi_1 = 2\varphi_2 - \varphi_1$, $\xi_4 = \varphi_1 - \varphi_2 - m$, $\xi_5 = \varphi_1 + m$ and $\xi_7 = h_0 + 2\varphi_2$, we find that $T_{i,\text{ft}} = T_{i,\text{geo}}$ for $i = 1, 2$. The tensions vanish at loci given by:

$$(I) : \left\{ \xi_4^2 + (2\xi_5 + \xi_7)\xi_4 + \frac{1}{2}\xi_5(\xi_5 + 2\xi_7) = 0 \right\} , \text{ and } (II) : \{\xi_1 = 0\} \cup \{\xi_7 = 0\} . \tag{3.135}$$

The solution to the quadratic equation from (I) is $\xi_4 = \frac{1}{2}(-2\xi_5 - \xi_7 \pm \sqrt{2\xi_5^2 + \xi_7^2})$. Both sign choices lead to a negative value for ξ_4 in this chamber, and are hence rejected. The loci $\{\xi_1 = 0\} \subset (II)$ and $\{\xi_7 = 0\} \subset (II)$ coincide with hard walls, which are, respectively, loci along which the W-boson W_2 becomes massless and the instanton particles $\mathcal{I}_2, \mathcal{I}_3$ become massless. These are both non-traversable walls. Away from the hard wall, either hypermultiplet \mathcal{H}_1 can become massless at $\xi_5 = 0$ (signaling a flop of \mathcal{C}_5), leading to gauge theory resolution (d), or hypermultiplet \mathcal{H}_2 can become massless at $\xi_4 = 0$ (signaling a flop of \mathcal{C}_4) leading to back to gauge theory resolution (a).

Resolution (c). Consider the crepant resolution of Figure 20(c), with curves and divisors shown in Figure 23(a).

The linear relations among curve classes are:

$$\mathcal{C}_3 \simeq \mathcal{C}_5 + \mathcal{C}_8, \quad \mathcal{C}_4 \simeq \mathcal{C}_1, \quad \mathcal{C}_5 \simeq \mathcal{C}_2, \quad \mathcal{C}_7 \simeq \mathcal{C}_1 + \mathcal{C}_8 . \tag{3.136}$$

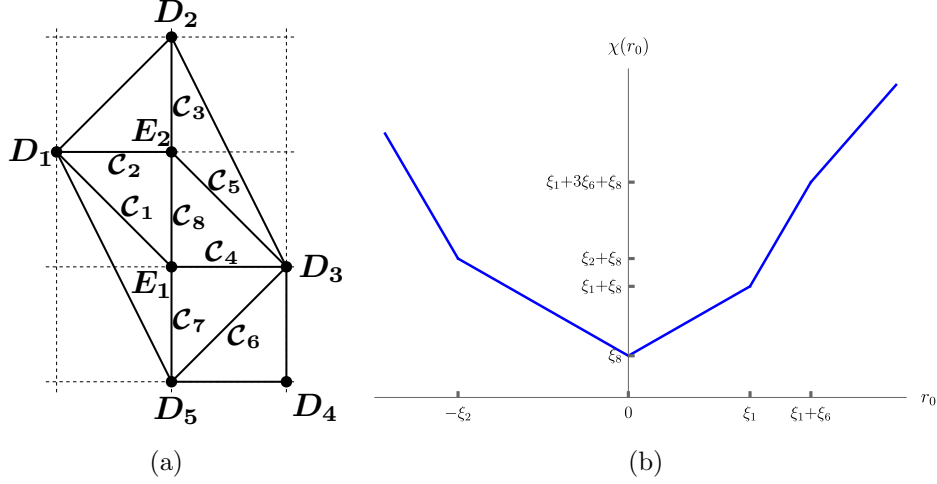


Figure 23. Resolution (c) of the $E_2^{2, \frac{1}{2}}$ singularity and its vertical reduction.

We take $\{\mathcal{C}_1, \mathcal{C}_2, \mathcal{C}_6, \mathcal{C}_8\}$ as generators of the Mori cone. The GLSM charge matrix is:

	D_1	D_2	D_3	D_4	D_5	\mathbf{E}_1	\mathbf{E}_2	$\text{vol}(\mathcal{C})$
\mathcal{C}_1	0	0	0	0	1	-2	1	ξ_1
\mathcal{C}_2	0	1	0	0	0	1	-2	ξ_2
\mathcal{C}_6	0	0	-1	1	-1	1	0	ξ_6
\mathcal{C}_8	1	0	1	0	0	-1	-1	ξ_8
$U(1)_M$	0	0	0	0	0	-1	1	r_0

(3.137)

The Kähler cone is parametrized by (3.110). The parameters $(\mu_1, \mu_2, \nu_1, \nu_2)$ are related to the FI parameters by

$$\xi_1 = -2\nu_1 + \nu_2 \geq 0, \quad \xi_2 = \mu_2 + \nu_1 - 2\nu_2 \geq 0, \quad \xi_6 = \nu_1 \geq 0, \quad \xi_8 = \mu_1 - \nu_1 - \nu_2 \geq 0. \quad (3.138)$$

The relevant triple-intersection numbers are:

$$\begin{aligned} D_1 \mathbf{E}_1 \mathbf{E}_2 &= 1, & D_2 \mathbf{E}_1 \mathbf{E}_2 &= 0, & D_1 D_2 \mathbf{E}_1 &= 0, & D_1 D_2 \mathbf{E}_2 &= 1, \\ D_1 \mathbf{E}_1^2 &= -2, & D_2 \mathbf{E}_1^2 &= 0, & D_1 \mathbf{E}_2^2 &= -2, & D_2 \mathbf{E}_2^2 &= -3, \\ D_1^2 \mathbf{E}_1 &= 0, & D_1^2 \mathbf{E}_2 &= 0, & D_2^2 \mathbf{E}_1 &= 0, & D_2^2 \mathbf{E}_2 &= 1, \\ \mathbf{E}_1^2 \mathbf{E}_2 &= -1, & \mathbf{E}_1 \mathbf{E}_2^2 &= -1, & \mathbf{E}_1^3 &= 8, & \mathbf{E}_2^3 &= 8. \end{aligned} \quad (3.139)$$

Therefore, the compact part of the prepotential is:

$$\mathcal{F}_{(c)}(\nu_1, \nu_2; \mu_1, \mu_2) = -\frac{1}{6} S^3 = -\frac{4}{3} \nu_1^3 - \frac{4}{3} \nu_2^3 + \frac{1}{2} (\nu_1^2 \nu_2 + \nu_1 \nu_2^2) + \mu_1 \nu_1^2 + \left(\mu_1 + \frac{3}{2} \mu_2 \right) \nu_2^2$$

$$- \mu_1 \nu_1 \nu_2 - \left(\mu_1 \mu_2 + \frac{1}{2} \mu_2^2 \right) \nu_2 . \quad (3.140)$$

The IIA profile is:

$$\chi(r_0) = \begin{cases} -3r_0 - 2\xi_2 + \xi_8, & \text{for } r_0 \leq -\xi_2 \\ -r_0 + \xi_8, & \text{for } -\xi_2 \leq r_0 \leq 0 \\ r_0 + \xi_8, & \text{for } 0 \leq r_0 \leq \xi_1 \\ 3r_0 - 2\xi_1 + \xi_8, & \text{for } \xi_1 \leq r_0 \leq \xi_1 + \xi_6 \\ +2r_0 - \xi_1 + \xi_6 + \xi_8, & \text{for } r_0 \geq \xi_1 + \xi_6 . \end{cases} \quad (3.141)$$

This function is sketched in Figure 23(b). At the points $r_0 = -\xi_2$, $r_0 = 0$ and $r_0 = \xi_1$, there are gauge D6-branes wrapping \mathbb{P}^1 's in the resolution of the singularity. There is a flavor D6-brane at $r_0 = \xi_1 + \xi_6$. The effective Chern-Simons level is still $\frac{1}{2}$. The simple-root W -bosons have masses given by:

$$M(W_1) = \xi_2 = 2\varphi_1 - \varphi_2, \quad M(W_2) = \xi_1 = 2\varphi_2 - \varphi_1 . \quad (3.142)$$

This resolution corresponds to gauge theory chamber 4 (cf. Table 4 and (A.8)), with instanton masses given by:

$$\begin{aligned} M(\mathcal{I}_1) &= \chi(r_0 = -\xi_2) = \xi_2 + \xi_8 = h_0 + 3\varphi_1 - m , \\ M(\mathcal{I}_2) &= \chi(r_0 = 0) = \xi_8 = h_0 + \varphi_1 + \varphi_2 - m , \\ M(\mathcal{I}_3) &= \chi(r_0 = \xi_1) = \xi_1 + \xi_8 = h_0 + 3\varphi_2 - m . \end{aligned} \quad (3.143)$$

The masses of hypermultiplets are:

$$\begin{aligned} M(\mathcal{H}_1) &= \xi_6 = -\varphi_2 + m , \\ M(\mathcal{H}_2) &= \xi_1 + \xi_6 = -\varphi_1 + \varphi_2 + m , \\ M(\mathcal{H}_3) &= \xi_1 + \xi_2 + \xi_6 = \varphi_1 + m . \end{aligned} \quad (3.144)$$

The map between geometry and field theory variables is given by (3.118). Plugging (3.118) into (3.140), we recover the field theory prepotential,

$$\begin{aligned} \mathcal{F}_{SU(3)_{3/2}, N_f=1}^{\text{chamber 4}} &= \frac{4}{3} \varphi_1^3 + \frac{4}{3} \varphi_2^3 - \frac{1}{2} (\varphi_1^2 \varphi_2 + \varphi_1 \varphi_2^2) + (h_0 - m) \varphi_1^2 + (h_0 - m) \varphi_2^2 \\ &\quad + (m - h_0) \varphi_1 \varphi_2 , \end{aligned} \quad (3.145)$$

up to φ -independent terms. The monopole string tensions from $\chi(r_0)$ are:

$$T_{1,\text{geo}} = \int_{-\xi_2}^0 \chi(r_0) dr_0 = \frac{1}{2} \xi_2 (\xi_2 + 2\xi_8) , \quad T_{2,\text{geo}} = \int_0^{\xi_1} \chi(r_0) dr_0 = \frac{1}{2} \xi_1 (\xi_1 + 2\xi_8) . \quad (3.146)$$

Using the map $\xi_1 = 2\varphi_2 - \varphi_1$, $\xi_2 = 2\varphi_1 - \varphi_2$, $\xi_6 = -\varphi_2 + m$ and $\xi_8 = h_0 + \varphi_1 + \varphi_2 - m$, one can verify that $T_{i,\text{ft}} = T_{i,\text{geo}}$ for $i = 1, 2$. The loci $\xi_1 = 0$ and $\xi_2 = 0$ correspond, respectively, to hard walls along which the W-bosons W_2 and W_1 become massless, whereas the loci $\{\xi_2 + 2\xi_8 = 0\}$ and $\{\xi_1 + 2\xi_8 = 0\}$ (II) are both not part of the Kähler chamber of resolution (c). Away from any hard wall, the BPS instanton particle \mathcal{I}_2 can become massless at $\xi_8 = 0$ (signaling a flop of \mathcal{C}_8), indicating a traversable instantonic wall which leads to a non-gauge-theoretic chamber (f). Alternatively, away from any hard wall, the perturbative hypermultiplet \mathcal{H}_1 can become massless at $\xi_6 = 0$ (signaling a flop of \mathcal{C}_6), leading back to gauge theory resolution (a).

RG flow and decoupling limits. In this resolution, we can decouple divisor D_4 by sending the volume of the curve \mathcal{C}_6 to infinity. As $M(\mathcal{H}_1) = \xi_6 = -\varphi_2 + m$, this is equivalent to taking the limit $m \rightarrow +\infty$, i.e. integrating out the massive fermion, which results in an $SU(3)_0$ pure gauge theory. From the perspective of geometry, this leads to an $SL(2, \mathbb{Z})$ -transformed version of a resolution of the $E_1^{2,0}$ singularity, as shown in Figure 24. For example, one can apply a $(TS)^2 T^{-1} S^{-1}$ transformation to the toric diagram on the right in Figure 24 to get to resolution (a) of the $E_1^{2,0}$ singularity.

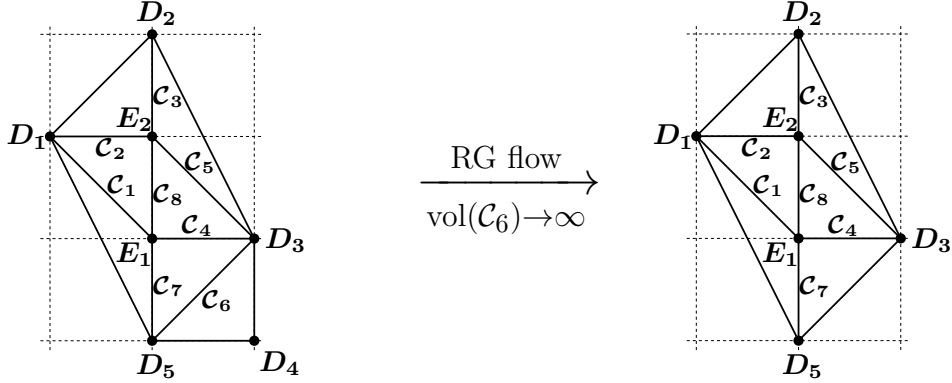


Figure 24. Decoupling the divisor D_4 leads to a crepant resolution of the $E_1^{2,0}$ singularity.

Resolution (d). Consider the crepant resolution of Figure 20(d), with curves and divisors shown in Figure 25(a). The linear relations among curve classes are:

$$\mathcal{C}_3 \simeq 2\mathcal{C}_4 + \mathcal{C}_7, \quad \mathcal{C}_4 \simeq \mathcal{C}_2, \quad \mathcal{C}_6 \simeq \mathcal{C}_1, \quad \mathcal{C}_8 \simeq \mathcal{C}_7. \quad (3.147)$$

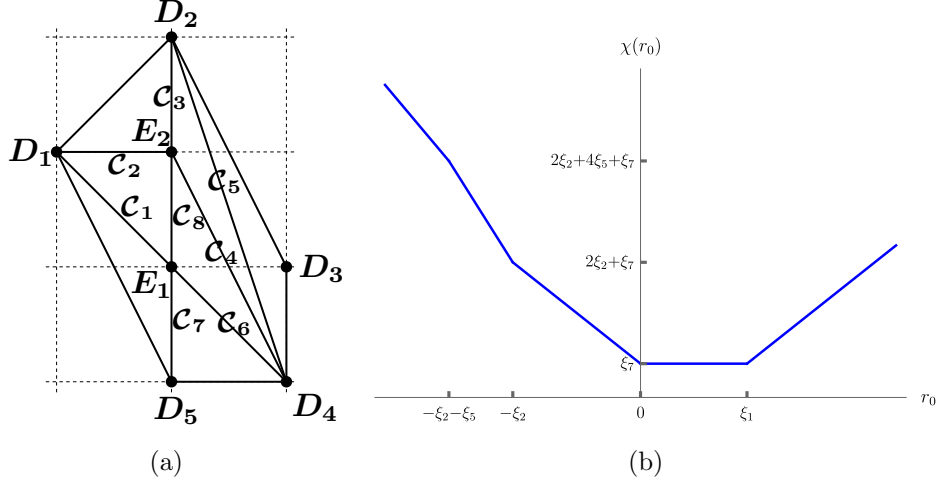


Figure 25. Resolution (d) of the $E_2^{2, \frac{1}{2}}$ singularity and its vertical reduction.

We take $\{\mathcal{C}_1, \mathcal{C}_2, \mathcal{C}_5, \mathcal{C}_7\}$ as generators of the Mori cone. The GLSM charge matrix is:

	D_1	D_2	D_3	D_4	D_5	\mathbf{E}_1	\mathbf{E}_2	$\text{vol}(\mathcal{C})$
\mathcal{C}_1	0	0	0	0	1	-2	1	ξ_1
\mathcal{C}_2	0	1	0	0	0	1	-2	ξ_2
\mathcal{C}_5	0	-1	1	-1	0	0	1	ξ_5
\mathcal{C}_7	1	0	0	1	0	-2	0	ξ_7
$U(1)_M$	0	0	0	0	0	-1	1	r_0

(3.148)

The Kähler cone is parametrized by (3.110). The parameters $(\mu_1, \mu_2, \nu_1, \nu_2)$ are related to the FI parameters by:

$$\xi_1 = -2\nu_1 + \nu_2 \geq 0, \quad \xi_2 = \mu_2 + \nu_1 - 2\nu_2 \geq 0, \quad \xi_5 = -\mu_2 + \nu_2 \geq 0, \quad \xi_7 = \mu_1 - 2\nu_1 \geq 0. \quad (3.149)$$

The relevant triple-intersection numbers are:

$$\begin{aligned} D_1 \mathbf{E}_1 \mathbf{E}_2 &= 1, & D_2 \mathbf{E}_1 \mathbf{E}_2 &= 0, & D_1 D_2 \mathbf{E}_1 &= 0, & D_1 D_2 \mathbf{E}_2 &= 1, \\ D_1 \mathbf{E}_1^2 &= -2, & D_2 \mathbf{E}_1^2 &= 0, & D_1 \mathbf{E}_2^2 &= -2, & D_2 \mathbf{E}_2^2 &= -4, \\ D_1^2 \mathbf{E}_1 &= 0, & D_1^2 \mathbf{E}_2 &= 0, & D_2^2 \mathbf{E}_1 &= 0, & D_2^2 \mathbf{E}_2 &= 2, \\ \mathbf{E}_1^2 \mathbf{E}_2 &= -2, & \mathbf{E}_1 \mathbf{E}_2^2 &= 0, & \mathbf{E}_1^3 &= 8, & \mathbf{E}_2^3 &= 8. \end{aligned} \quad (3.150)$$

Therefore, the compact part of the prepotential is:

$$\mathcal{F}_{(d)}(\nu_1, \nu_2; \mu_1, \mu_2) = -\frac{1}{6} S^3 = -\frac{4}{3} \nu_1^3 - \frac{4}{3} \nu_2^3 + \nu_1^2 \nu_2 + \mu_1 \nu_1^2 + (\mu_1 + 2\mu_2) \nu_2^2$$

$$- \mu_1 \nu_1 \nu_2 - (\mu_1 \mu_2 + \mu_2^2) \nu_2 . \quad (3.151)$$

The IIA profile is:

$$\chi(r_0) = \begin{cases} -3r_0 - 2\xi_2 + \xi_5 + \xi_7, & \text{for } r_0 \leq -\xi_2 - \xi_5 \\ -4r_0 - 2\xi_2 + \xi_7, & \text{for } -\xi_3 - \xi_5 \leq r_0 \leq -\xi_2 \\ -2r_0 + \xi_7, & \text{for } -\xi_2 \leq r_0 \leq 0 \\ \xi_7, & \text{for } 0 \leq r_0 \leq \xi_1 \\ +2r_0 - 2\xi_1 + \xi_7, & \text{for } r_0 \geq \xi_1 . \end{cases} \quad (3.152)$$

This function is sketched in Figure 25(b). At the points $r_0 = -\xi_2$, $r_0 = 0$ and $r_0 = \xi_1$, there are gauge D6-branes wrapping \mathbb{P}^1 's in the resolution of the singularity. There is a flavor D6-brane at $r_0 = -\xi_2 - \xi_5$. The effective Chern-Simons level is still $\frac{1}{2}$. The simple-root W-bosons have masses given by:

$$M(W_1) = \xi_2 = 2\varphi_1 - \varphi_2, \quad M(W_2) = \xi_1 = 2\varphi_2 - \varphi_1 . \quad (3.153)$$

This resolution corresponds to gauge theory chamber 1 (cf. Table 4 and (A.5)), with instanton masses given by:

$$\begin{aligned} M(\mathcal{I}_1) &= \chi(r_0 = -\xi_2) = 2\xi_2 + \xi_7 = h_0 + 4\varphi_1 , \\ M(\mathcal{I}_2) &= \chi(r_0 = 0) = \xi_7 = h_0 + 2\varphi_2 , \\ M(\mathcal{I}_3) &= \chi(r_0 = \xi_1) = \xi_7 = h_0 + 2\varphi_2 . \end{aligned} \quad (3.154)$$

The masses of hypermultiplets are:

$$\begin{aligned} M(\mathcal{H}_1) &= \xi_5 = -\varphi_1 - m , \\ M(\mathcal{H}_2) &= \xi_2 + \xi_5 = \varphi_1 - \varphi_2 - m , \\ M(\mathcal{H}_3) &= \xi_1 + \xi_2 + \xi_5 = \varphi_2 - m . \end{aligned} \quad (3.155)$$

Plugging (3.118) into (3.151), we recover the field theory prepotential,

$$\mathcal{F}_{SU(3)_{3/2}, N_f=1}^{\text{chamber 1}} = \frac{4}{3}\varphi_1^3 + \frac{4}{3}\varphi_2^3 - \varphi_1^2\varphi_2 + h_0(\varphi_1^2 + \varphi_2^2 - \varphi_1\varphi_2) , \quad (3.156)$$

up to φ -independent terms. The monopole string tensions from $\chi(r_0)$ are given by:

$$T_{1,\text{geo}} = \int_{-\xi_2}^0 \chi(r_0) dr_0 = \xi_2(\xi_2 + \xi_7) , \quad T_{2,\text{geo}} = \int_0^{\xi_1} \chi(r_0) dr_0 = \xi_1\xi_7 . \quad (3.157)$$

Using the map $\xi_1 = 2\varphi_2 - \varphi_1$, $\xi_2 = 2\varphi_1 - \varphi_2$, $\xi_5 = -\varphi_1 - m$ and $\xi_7 = h_0 + 2\varphi_2$, one can verify that $T_{i,\text{ft}} = T_{i,\text{geo}}$ for $i = 1, 2$. The loci $\xi_2 = 0$ and $\xi_1 = 0$ are both hard walls, being the boundaries of the Weyl chamber where either W-boson becomes massless. The loci $\{\xi_2 + \xi_7 = 0\} \subset (I)$ and $\{\xi_7 = 0\} \subset (II)$ are both not part of the Kähler chamber of resolution (d) (the curve \mathcal{C}_7 cannot flop). Away from any hard wall, the perturbative hypermultiplet \mathcal{H}_1 can become massless at $\xi_5 = 0$ (signaling a flop of \mathcal{C}_5), leading back to gauge theory resolution (a).

RG flow and decoupling limits. In this resolution, we can decouple divisor D_3 by sending the volume of the curve \mathcal{C}_5 to infinity. As $M(\mathcal{H}_1) = \xi_5 = -\varphi_2 - m$, this is equivalent to taking the limit $m \rightarrow -\infty$, which results in an $SU(3)_1$ pure gauge theory. On the geometry side, this leads to an $SL(2, \mathbb{Z})$ -transformed version of a resolution of the $E_1^{2,1}$ singularity, as shown in Figure 26. For instance, one can apply a $(TS)^2 T^{-1} S^{-1}$ transformation to the figure on the right in Figure 26 to get to resolution (a) of the $E_1^{2,1}$ singularity.

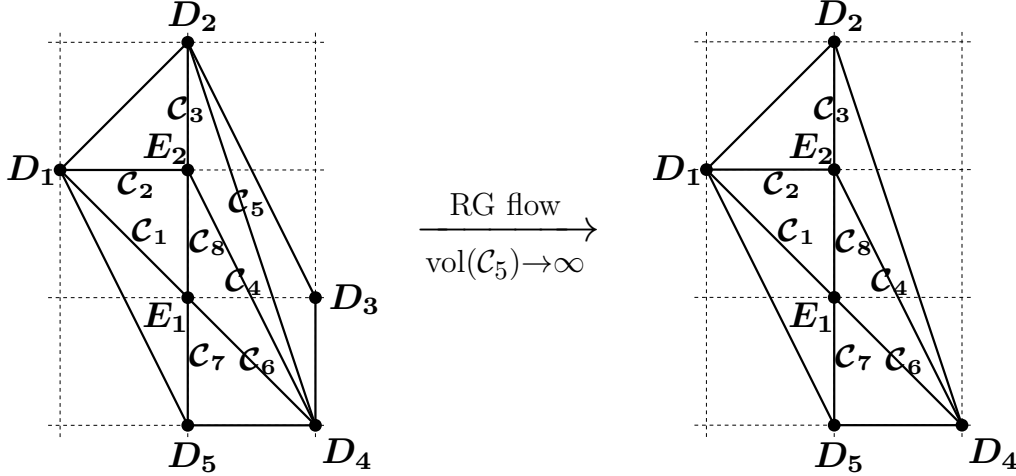


Figure 26. Decoupling the divisor D_3 leads to a crepant resolution of the $E_1^{2,1}$ singularity.

Resolutions (e) and (f). These are non-gauge-theoretic resolutions, related to each other by a flop of a single curve (\mathcal{C}_6). In resolution (f), the divisor D_4 can be decoupled, which leads to an $SL(2, \mathbb{Z})$ -transformed version of resolution (b) of the $E_1^{2,0}$ singularity. For example, one such transformation is $(TS)^2 T^{-1} S^{-1}$, which leads precisely to resolution (b) of the $E_1^{2,0}$ singularity discussed above.

We remark that the resolutions (e) and (f) represent the coupling of a rank-1 E_1 singularity with a rank-1 non-Lagrangian E_0 singularity [1–3]. In the RG flow shown in Figure 27, we end up with a pair of coupled E_0 theories, as is evident from the shape of the final toric diagram.

3.6 The $E_3^{2,1}$ singularity and $SU(3)_1$ $N_f = 2$ gauge theory

The $E_3^{2,1}$ singularity (Figure 3(i)) admits 30 crepant resolutions shown in Figure 28. The first 16 resolutions, Figures 28(a)-28(p), admit vertical reductions to type IIA, which correspond to chambers of the $SU(3)_2$ $N_f = 2$ gauge theory, as we illustrate below.

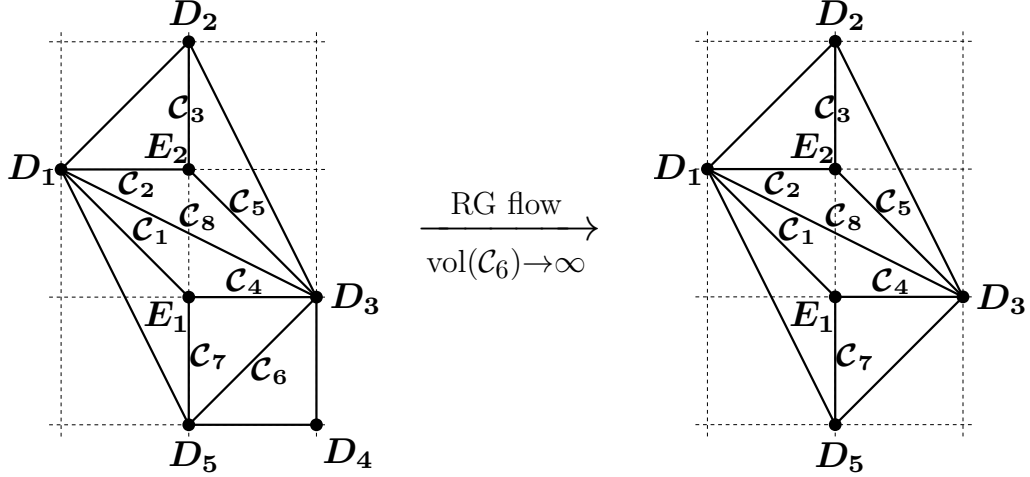


Figure 27. Decoupling the divisor D_4 leads to a crepant resolution of the $E_1^{2,1}$ singularity.

Resolution (a). Consider the crepant resolution of Figure 28(a), with curves and divisors shown in Figure 29(a). There are six non-compact toric divisors D_i ($i = 1, \dots, 6$), and two compact toric divisors \mathbf{E}_1 and \mathbf{E}_2 with the following linear relations:

$$D_5 \simeq D_1 + D_2 - D_4, \quad \mathbf{E}_1 \simeq -3D_1 - 2D_2 + D_3 + D_4 - 2D_6, \quad \mathbf{E}_2 \simeq D_1 - 2D_3 - D_4 + D_6. \quad (3.158)$$

The compact curves \mathcal{C} are given by:

$$\begin{aligned} \mathcal{C}_1 &= \mathbf{E}_1 \cdot D_1, & \mathcal{C}_2 &= \mathbf{E}_1 \cdot D_2, & \mathcal{C}_3 &= \mathbf{E}_2 \cdot D_2, & \mathcal{C}_4 &= \mathbf{E}_2 \cdot D_3, \\ \mathcal{C}_5 &= \mathbf{E}_1 \cdot D_4, & \mathcal{C}_6 &= \mathbf{E}_2 \cdot D_4, & \mathcal{C}_7 &= \mathbf{E}_1 \cdot D_5, & \mathcal{C}_8 &= \mathbf{E}_2 \cdot \mathbf{E}_1. \end{aligned} \quad (3.159)$$

The linear relations among curve classes are:

$$\mathcal{C}_4 \simeq \mathcal{C}_3 + \mathcal{C}_9, \quad \mathcal{C}_6 \simeq \mathcal{C}_3, \quad \mathcal{C}_7 \simeq \mathcal{C}_1 + \mathcal{C}_2 - \mathcal{C}_5, \quad \mathcal{C}_8 \simeq -\mathcal{C}_1 + \mathcal{C}_5 + \mathcal{C}_9. \quad (3.160)$$

We take $\{\mathcal{C}_1, \mathcal{C}_2, \mathcal{C}_3, \mathcal{C}_5, \mathcal{C}_9\}$ as Mori cone generators. The GLSM charge matrix is:

	D_1	D_2	D_3	D_4	D_5	D_6	\mathbf{E}_1	\mathbf{E}_2	$\text{vol}(\mathcal{C})$
\mathcal{C}_1	-1	1	0	0	0	1	-1	0	ξ_1
\mathcal{C}_2	1	-1	0	0	0	0	-1	1	ξ_2
\mathcal{C}_3	0	0	1	0	0	0	1	-2	ξ_3
\mathcal{C}_5	0	0	0	-1	1	0	-1	1	ξ_5
\mathcal{C}_9	0	1	0	1	0	0	-1	-1	ξ_9
$U(1)_M$	0	0	0	0	0	0	-1	1	r_0

(3.161)

where the last line defines the vertical reduction of the 2d GLSM. The nonnegative FI terms $\xi_1 \geq 0$, $\xi_2 \geq 0$, $\xi_3 \geq 0$, $\xi_5 \geq 0$ and $\xi_9 \geq 0$ are, respectively, the volumes of

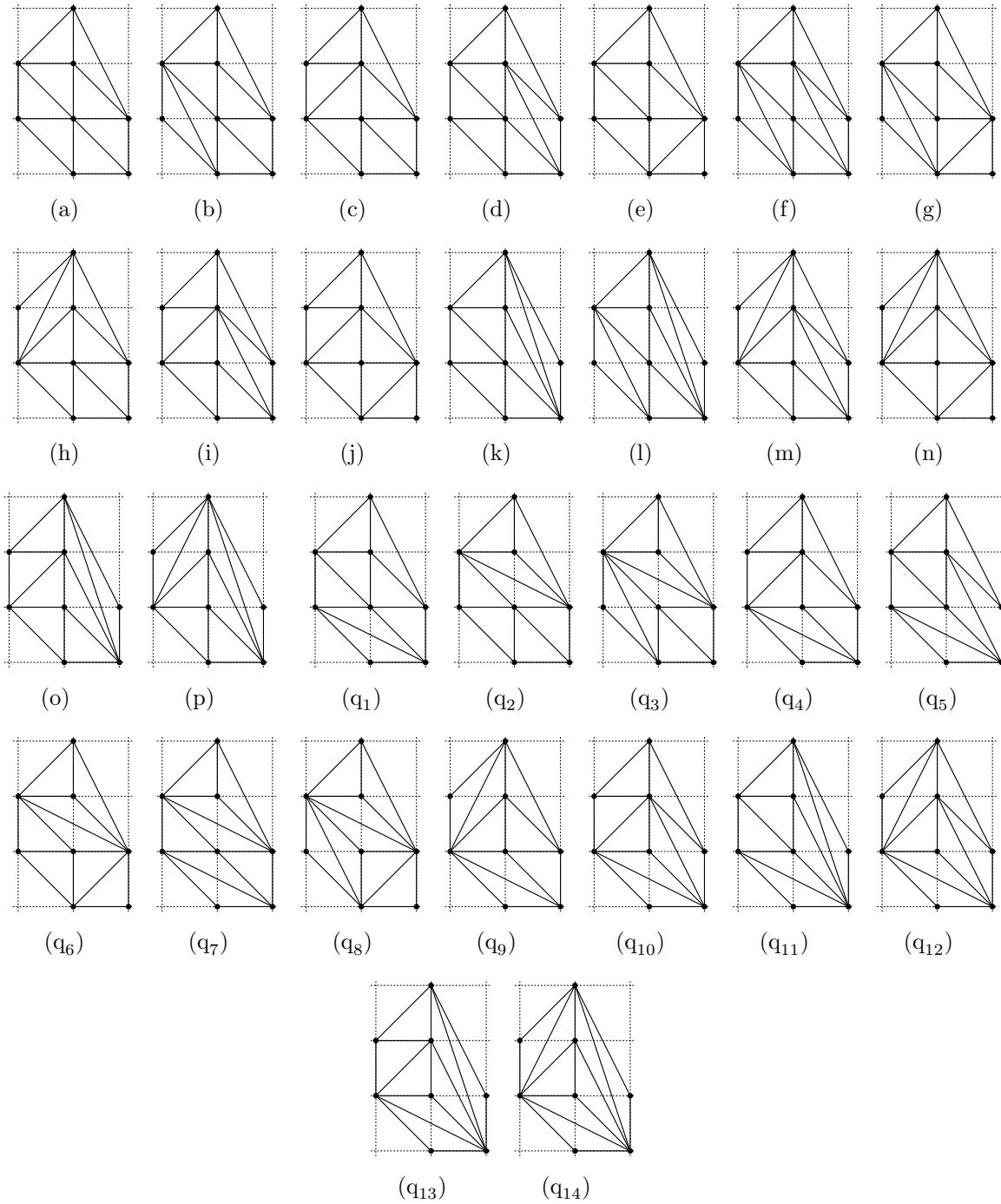


Figure 28. The 30 crepant singularities of the $E_3^{2,1}$ singularity. The first 16, (a)-(p) admit a vertical reduction, corresponding to chambers of the $SU(3)_2$ $N_f = 2$ gauge theory.

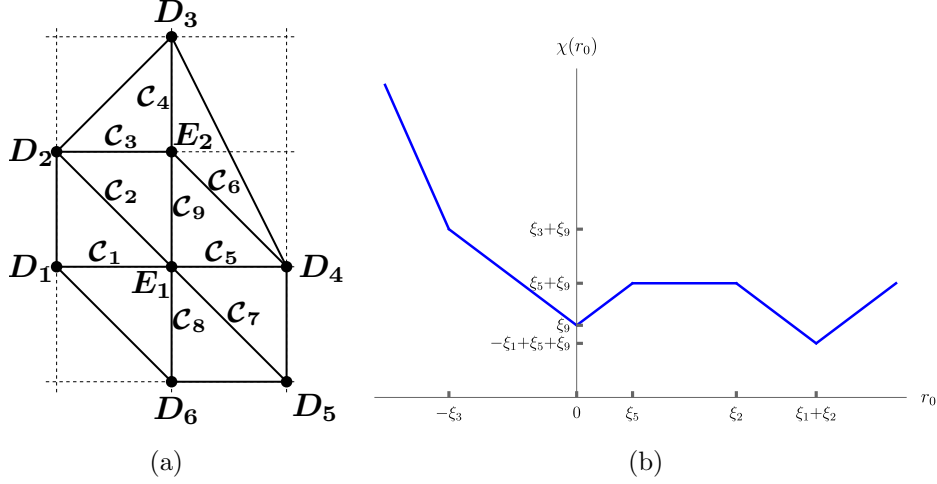


Figure 29. Resolution (a) of the $E_3^{2,1}$ singularity and its vertical reduction.

compact curves $\mathcal{C}_1, \mathcal{C}_2, \mathcal{C}_3, \mathcal{C}_5$ and \mathcal{C}_9 . Note that the requirement that the curves \mathcal{C}_7 and \mathcal{C}_9 have non-negative volume translates to the following conditions on the FI terms in this chamber:

$$\xi_1 + \xi_2 - \xi_5 \geq 0, \quad -\xi_1 + \xi_5 + \xi_9 \geq 0. \quad (3.162)$$

Geometric prepotential. We parametrize the Kähler cone by:

$$S = \mu_1 D_1 + \mu_2 D_2 + \mu_3 D_3 \nu_1 \mathbf{E}_1 + \nu_2 \mathbf{E}_2. \quad (3.163)$$

The parameters $(\mu_1, \mu_2, \mu_3, \nu_1, \nu_2)$ are related to the FI parameters by

$$\begin{aligned} \xi_1 = -\mu_1 + \mu_2 - \nu_1 \geq 0, \quad \xi_2 = \mu_1 - \mu_2 - \nu_1 + \nu_2 \geq 0, \quad \xi_3 = \mu_3 + \nu_1 - 2\nu_2 \geq 0, \\ \xi_5 = -\nu_1 + \nu_2 \geq 0, \quad \xi_9 = \mu_2 - \nu_1 - \nu_2 \geq 0. \end{aligned} \quad (3.164)$$

The relevant triple-intersection numbers are:

$$\begin{aligned} \mathbf{E}_1^3 = 6, \quad \mathbf{E}_2^3 = 8, \quad D_1 \mathbf{E}_1 \mathbf{E}_2 = 0, \quad D_2 \mathbf{E}_1 \mathbf{E}_2 = 1, \quad D_3 \mathbf{E}_1 \mathbf{E}_2 = 0, \\ \mathbf{E}_1^2 \mathbf{E}_2 = -1, \quad \mathbf{E}_1 \mathbf{E}_2^2 = -1, \quad D_1^2 \mathbf{E}_1 = -1, \quad D_1^2 \mathbf{E}_2 = 0, \quad D_1 D_2 \mathbf{E}_1 = 1, \\ D_1 D_2 \mathbf{E}_2 = 0, \quad D_1 D_3 \mathbf{E}_1 = 0, \quad D_1 D_3 \mathbf{E}_2 = 0, \quad D_2^2 \mathbf{E}_1 = -1, \quad D_2^2 \mathbf{E}_2 = 0, \\ D_2 D_3 \mathbf{E}_1 = 0, \quad D_2 D_3 \mathbf{E}_2 = 1, \quad D_3^2 \mathbf{E}_1 = 0, \quad D_3^2 \mathbf{E}_2 = 1, \quad D_1 \mathbf{E}_1^2 = -1, \\ D_1 \mathbf{E}_2^2 = 0, \quad D_2 \mathbf{E}_1^2 = -1, \quad D_2 \mathbf{E}_2^2 = -2, \quad D_3 \mathbf{E}_1^2 = 0, \quad D_3 \mathbf{E}_2^2 = -3. \end{aligned} \quad (3.165)$$

Therefore, the compact part of the prepotential is:

$$\mathcal{F}_{(a)}(\nu_1, \nu_2; \mu_1, \mu_2, \mu_3) = -\nu_1^3 - \frac{4}{3}\nu_2^3 + \frac{1}{2}(\nu_1^2 \nu_2 + \nu_1 \nu_2^2) + \frac{1}{2}(\mu_1 + \mu_2)\nu_1^2 + \left(\mu_2 + \frac{3}{2}\mu_3\right)\nu_2^2$$

$$-\mu_2\nu_1\nu_2 + \frac{1}{2}(\mu_1 - \mu_2)^2\nu_1 - \left(\mu_2\mu_3 + \frac{1}{2}\mu_3^2\right)\nu_2 . \quad (3.166)$$

Type IIA reduction and gauge theory description. The type IIA background is a resolved A_1 singularity fibered over the $x^9 = r_0$ direction. There are three D6-branes wrapping the exceptional \mathbb{P}^1 in the resolved A_1 singularity, resulting in an $SU(3)$ gauge theory. There are two D6-branes wrapping the two noncompact divisors in the resolved ALE space, which give rise to the two fundamental flavors. The volume of the exceptional \mathbb{P}^1 in type IIA is given by the following piecewise linear function,

$$\chi(r_0) = \begin{cases} -3r_0 - 2\xi_3 + \xi_9, & \text{for } r_0 \leq -\xi_3 \\ -r_0 + \xi_9, & \text{for } -\xi_3 \leq r_0 \leq 0 \\ +r_0 + \xi_9, & \text{for } 0 \leq r_0 \leq \xi_5 \\ \xi_5 + \xi_9, & \text{for } \xi_5 \leq r_0 \leq \xi_2 \\ -r_0 + \xi_2 + \xi_5 + \xi_9, & \text{for } \xi_2 \leq r_0 \leq \xi_1 + \xi_2 \\ +r_0 - 2\xi_1 - \xi_2 + \xi_5 + \xi_9, & \text{for } r_0 \geq \xi_1 + \xi_2 . \end{cases} \quad (3.167)$$

This function is sketched in Figure 29(b) (where we have chosen $\xi_3 > \xi_5$ for convenience of plotting). At the points $r_0 = -\xi_3$, $r_0 = 0$ and $r_0 = \xi_1 + \xi_2$, there are gauge D6-branes wrapping \mathbb{P}^1 's in the resolution of the singularity (we denote them by \mathcal{G}_1 , \mathcal{G}_2 and \mathcal{G}_3 respectively). When $\xi_1 = \xi_2 = \xi_3 = 0$, an $SU(3)$ gauge theory is realized (at $r_0 = 0$) with inverse coupling $h_0 = \xi_9$. There are two flavor D6-branes at $r_0 = \xi_5$ and $r_0 = \xi_2$, denoted by \mathcal{F}_1 and \mathcal{F}_2 respectively. In the evaluation of $\chi(r_0)$, we have assumed without loss of generality that $\xi_2 \geq \xi_5$, which is of course consistent with (3.162).

The effective Chern-Simons level is given by:

$$\kappa_{s,\text{eff}} = -\frac{1}{2}(-3 + 1) = 1 . \quad (3.168)$$

which is interpreted as a bare CS level of 2 plus the contribution $-\frac{1}{2} - \frac{1}{2} = -1$ due to the two hypermultiplets (cf. (2.5)). The simple-root W-bosons have masses given by the separation between adjacent gauge D6-branes:

$$M(W_1) = \xi_3 = 2\varphi_1 - \varphi_2, \quad M(W_2) = \xi_1 + \xi_2 = 2\varphi_2 - \varphi_1 . \quad (3.169)$$

From the instanton masses, one can identify that this resolution corresponds to gauge theory chamber 11 (cf. Table 6 and (A.10)):

$$\begin{aligned} M(\mathcal{I}_1) &= \chi(r_0 = -\xi_3) = \xi_3 + \xi_9 = h_0 - m_1 - m_2 + 3\varphi_1 , \\ M(\mathcal{I}_2) &= \chi(r_0 = 0) = \xi_9 = h_0 - m_1 - m_2 + \varphi_1 + \varphi_2 , \\ M(\mathcal{I}_3) &= \chi(r_0 = \xi_1 + \xi_2) = -\xi_1 + \xi_5 + \xi_9 = h_0 + \varphi_2 . \end{aligned} \quad (3.170)$$

The masses of hypermultiplets (due to open strings stretched between gauge and flavor branes) are:

$$\begin{aligned}
M(\mathcal{H}_1) &= M(\mathcal{G}_1\mathcal{F}_1) = \xi_3 + \xi_5 = \varphi_1 + m_1 , \\
M(\mathcal{H}_2) &= M(\mathcal{G}_2\mathcal{F}_1) = \xi_5 = -\varphi_1 + \varphi_2 + m_1 , \\
M(\mathcal{H}_3) &= M(\mathcal{G}_3\mathcal{F}_1) = \xi_1 + \xi_2 - \xi_5 = \varphi_2 - m_1 , \\
M(\mathcal{H}_4) &= M(\mathcal{G}_1\mathcal{F}_2) = \xi_2 + \xi_3 = \varphi_1 + m_2 , \\
M(\mathcal{H}_5) &= M(\mathcal{G}_2\mathcal{F}_2) = \xi_2 = -\varphi_1 + \varphi_2 + m_2 , \\
M(\mathcal{H}_6) &= M(\mathcal{G}_3\mathcal{F}_2) = \xi_1 = \varphi_2 - m_2 .
\end{aligned} \tag{3.171}$$

Note that the choice $\xi_2 \geq \xi_5$ made above while computing $\chi(r_0)$ therefore implies that $m_2 \geq m_1$ in this chamber. From the Kähler volumes (3.164) of the compact curves and masses of W-bosons and instantons, the map between geometry and field theory variables is determined to be:

$$E_3^{2,1} \text{ geometry : } \begin{cases} \mu_1 = h_0 + m_1, \\ \mu_2 = h_0 + 2m_1 - m_2, \\ \mu_3 = 3m_1, \\ \nu_1 = -\varphi_2 + m_1, \\ \nu_2 = -\varphi_1 + 2m_1 . \end{cases} \tag{3.172}$$

Plugging (3.172) into (3.166), we recover the field theory prepotential

$$\begin{aligned}
\mathcal{F}_{SU(3)_2, N_f=2}^{\text{chamber 11}} &= \frac{4}{3}\varphi_1^3 + \varphi_2^3 - \frac{1}{2}(\varphi_1^2\varphi_2 + \varphi_1\varphi_2^2) + (-h_0 + m_1 + m_2)\varphi_1\varphi_2 \\
&+ (h_0 - m_1 - m_2)\varphi_1^2 + \left(h_0 - \frac{m_1 + m_2}{2}\right)\varphi_2^2 - \frac{1}{2}(m_1^2 + m_2^2)\varphi_2 - \frac{1}{3}(m_1^3 + m_2^3) .
\end{aligned} \tag{3.173}$$

up to φ -independent terms. From field theory, the monopole string tensions are given by:

$$\begin{aligned}
T_{1,\text{ft}} &= \frac{\partial \mathcal{F}_{SU(3)_2, N_f=2}^{\text{chamber 11}}}{\partial \varphi_1} = 4\varphi_1^2 - \varphi_1\varphi_2 - \frac{1}{2}\varphi_2^2 + 2(h_0 - m_1 - m_2)\varphi_1 \\
&+ (-h_0 + m_1 + m_2)\varphi_2 ,
\end{aligned} \tag{3.174}$$

$$\begin{aligned}
T_{2,\text{ft}} &= \frac{\partial \mathcal{F}_{SU(3)_2, N_f=2}^{\text{chamber 11}}}{\partial \varphi_2} = -\frac{1}{2}\varphi_1^2 - \varphi_1\varphi_2 + 3\varphi_2^2 + (-h_0 + m_1 + m_2)\varphi_1 \\
&+ (2h_0 - m_1 - m_2)\varphi_2 - \frac{1}{2}(m_1^2 + m_2^2) ,
\end{aligned} \tag{3.175}$$

whereas from geometry, they are given by:

$$T_{1,\text{geo}} = \int_{-\xi_3}^0 \chi(r_0) dr_0 = \frac{\xi_3^2}{2} + \xi_9 \xi_3, \quad (3.176)$$

$$T_{2,\text{geo}} = \int_0^{\xi_1+\xi_2} \chi(r_0) dr_0 = -\frac{\xi_1^2}{2} + \xi_5 \xi_1 + \xi_9 \xi_1 + \xi_2 \xi_5 + \xi_2 \xi_9 - \frac{\xi_5^2}{2}. \quad (3.177)$$

Using the map,

$$\text{Resolution (a) : } \begin{cases} \xi_1 = \varphi_2 - m_2, \\ \xi_2 = -\varphi_1 + \varphi_2 + m_2, \\ \xi_3 = 2\varphi_1 - \varphi_2, \\ \xi_5 = -\varphi_1 + \varphi_2 + m_1, \\ \xi_9 = h_0 + \varphi_1 + \varphi_2 - m_1 - m_2, \end{cases} \quad (3.178)$$

we find that $T_{i,\text{ft}} = T_{i,\text{geo}}$ for $i = 1, 2$.

Magnetic walls. The tensions vanish at loci given by:

$$(I) : \{ \xi_3 = 0 \} \cup \left\{ \frac{1}{2} \xi_3 + \xi_9 = 0 \right\}, \text{ and ,} \quad (3.179)$$

$$(II) : \left\{ \xi_1 \xi_5 - \frac{1}{2} (\xi_1^2 + \xi_5^2) + \xi_1 \xi_9 + \xi_2 \xi_5 + \xi_2 \xi_9 = 0 \right\}.$$

Along the submanifold $\{ \xi_3 = 0 \} \subset (I)$, the W-boson W_1 in this chamber becomes massless. So this submanifold coincides with the hard wall which is the boundary of the Weyl chamber. The submanifold $\{ \frac{1}{2} \xi_3 + \xi_9 \} = 0$ is not part of the Kähler chamber of resolution (1). So the locus (I) contributes no magnetic walls.

The locus defined by (II) is more intricate. The condition (II) has two solutions:

$$\xi_1 \stackrel{(II)}{=} \xi_5 + \xi_9 \pm \sqrt{(\xi_5 + \xi_9)^2 + 2\xi_2(\xi_5 + \xi_9) - \xi_5^2}. \quad (3.180)$$

Since (3.162) requires that $\xi_8 = -\xi_1 + \xi_5 + \xi_9$ in this chamber, only the negative sign in (3.180) is acceptable. However, in this chamber, recall that $\xi_2 \geq \xi_5$. So the quantity $2\xi_2(\xi_5 + \xi_9) - \xi_5^2 = 2\xi_2\xi_9 + \xi_5(2\xi_2 - \xi_5)$ is always non-negative in this chamber. Therefore, the square root in (3.180) is $\geq \xi_5 + \xi_9$, which implies that the right-hand-side of (3.180) is negative, which is unphysical in the Kähler chamber of resolution (a). This implies that there are no magnetic walls in resolution (a) of the $E_3^{2,1}$ singularity.

Away from any hard wall, any one of a number of perturbative hypermultiplets, namely $\mathcal{H}_2, \mathcal{H}_3, \mathcal{H}_5$ and \mathcal{H}_6 , can become massless, respectively at $\xi_5 = 0, \xi_7 = 0, \xi_2 = 0$ and $\xi_1 = 0$, signaling flops of the corresponding compact curves $\mathcal{C}_5, \mathcal{C}_7, \mathcal{C}_2$ and \mathcal{C}_1 . These

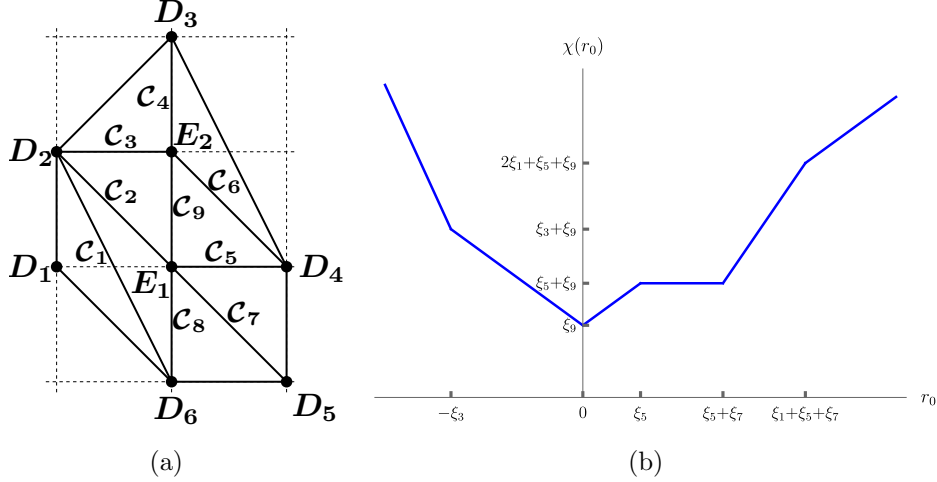


Figure 30. Resolution (b) of the $E_3^{2,1}$ singularity and its vertical reduction.

lead, respectively, to gauge theory phases described by resolutions (d), (e), (c) and (b). Alternatively, away from the hard wall, the BPS instanton particles \mathcal{I}_2 or \mathcal{I}_3 can become massless, respectively, at $\xi_9 = 0$ (signaling a flop of \mathcal{C}_9) or $\xi_8 = -\xi_1 + \xi_5 + \xi_9 = 0$ (signaling a flop of \mathcal{C}_8). These correspond to traversable instantonic wall, which lead, respectively to non-gauge-theoretic resolutions (q₂) or (q₁).

Resolution (b). Consider the crepant resolution of Figure 28(b), with curves and divisors shown in Figure 30(a). This resolution can be obtained by a flop of the curve \mathcal{C}_1 in resolution (a). The linear equivalences among divisors are given by (3.158). The compact curves \mathcal{C} can be read off the toric diagram. The linear relations among curve classes are:

$$\mathcal{C}_2 = \mathcal{C}_5 + \mathcal{C}_7, \quad \mathcal{C}_4 \simeq \mathcal{C}_3 + \mathcal{C}_9, \quad \mathcal{C}_6 \simeq \mathcal{C}_3, \quad \mathcal{C}_8 = \mathcal{C}_5 + \mathcal{C}_9. \quad (3.181)$$

We take $\{\mathcal{C}_1, \mathcal{C}_3, \mathcal{C}_5, \mathcal{C}_7, \mathcal{C}_9\}$ as Mori cone generators. The GLSM charge matrix is:

	D_1	D_2	D_3	D_4	D_5	D_6	\mathbf{E}_1	\mathbf{E}_2	$\text{vol}(\mathcal{C})$
\mathcal{C}_1	1	-1	0	0	0	-1	1	0	ξ_1
\mathcal{C}_3	0	0	1	0	0	0	1	-2	ξ_3
\mathcal{C}_5	0	0	0	-1	1	0	-1	1	ξ_5
\mathcal{C}_7	0	0	0	1	-1	1	-1	0	ξ_7
\mathcal{C}_9	0	1	0	1	0	0	-1	-1	ξ_9
$U(1)_M$	0	0	0	0	0	0	-1	1	r_0

(3.182)

The Kähler cone is parametrized by (3.163). The parameters $(\mu_1, \mu_2, \mu_3, \nu_1, \nu_2)$ are related to the FI parameters by

$$\begin{aligned} \xi_1 = \mu_1 - \mu_2 + \nu_1 \geq 0, \quad \xi_3 = \mu_3 + \nu_1 - 2\nu_2 \geq 0, \quad \xi_5 = -\nu_1 + \nu_2 \geq 0, \\ \xi_7 = -\nu_1 \geq 0, \quad \xi_9 = \mu_2 - \nu_1 - \nu_2 \geq 0. \end{aligned} \quad (3.183)$$

The relevant triple-intersection numbers are:

$$\begin{aligned} \mathbf{E}_1^3 = 7 \quad , \quad \mathbf{E}_2^3 = 8 \quad , \quad D_1 \mathbf{E}_1 \mathbf{E}_2 = 0 \quad D_2 \mathbf{E}_1 \mathbf{E}_2 = 1 \quad , \quad D_3 \mathbf{E}_1 \mathbf{E}_2 = 0 \quad , \\ \mathbf{E}_1^2 \mathbf{E}_2 = -1 \quad , \quad \mathbf{E}_1 \mathbf{E}_2^2 = -1 \quad , \quad D_1^2 \mathbf{E}_1 = 0 \quad D_1^2 \mathbf{E}_2 = 0 \quad , \quad D_1 D_2 \mathbf{E}_1 = 0 \quad , \\ D_1 D_2 \mathbf{E}_2 = 0 \quad , \quad D_1 D_3 \mathbf{E}_1 = 0 \quad , \quad D_1 D_3 \mathbf{E}_2 = 0 \quad D_2^2 \mathbf{E}_1 = 0 \quad , \quad D_2^2 \mathbf{E}_2 = 0 \quad , \\ D_2 D_3 \mathbf{E}_1 = 0 \quad , \quad D_2 D_3 \mathbf{E}_2 = 1 \quad , \quad D_3^2 \mathbf{E}_1 = 0 \quad D_3^2 \mathbf{E}_2 = 1 \quad , \quad D_1 \mathbf{E}_1^2 = 0 \quad , \\ D_1 \mathbf{E}_2^2 = 0 \quad , \quad D_2 \mathbf{E}_1^2 = -2 \quad , \quad D_2 \mathbf{E}_2^2 = -2 \quad D_3 \mathbf{E}_1^2 = 0 \quad , \quad D_3 \mathbf{E}_2^2 = -3 \quad . \end{aligned} \quad (3.184)$$

Therefore, the compact part of the prepotential is:

$$\begin{aligned} \mathcal{F}_{(b)}(\nu_1, \nu_2; \mu_1, \mu_2, \mu_3) = -\frac{7}{6}\nu_1^3 - \frac{4}{3}\nu_2^3 + \frac{1}{2}(\nu_1^2\nu_2 + \nu_1\nu_2^2) + \mu_2^2\nu_1^2 - \mu_2\nu_1\nu_2 + \left(\mu_2 + \frac{3}{2}\mu_3\right)\nu_2^2 \\ - \left(\mu_2\mu_3 + \frac{1}{2}\mu_3^2\right) \end{aligned} \quad (3.185)$$

The IIA profile is:

$$\chi(r_0) = \begin{cases} -3r_0 - 2\xi_3 + \xi_9, & \text{for } r_0 \leq -\xi_3 \\ -r_0 + \xi_9, & \text{for } -\xi_3 \leq r_0 \leq 0 \\ +r_0 + \xi_9, & \text{for } 0 \leq r_0 \leq \xi_5 \\ \xi_5 + \xi_9, & \text{for } \xi_5 \leq r_0 \leq \xi_5 + \xi_7 \\ +2r_0 - \xi_5 - 2\xi_7 + \xi_9, & \text{for } \xi_5 + \xi_7 \leq r_0 \leq \xi_1 + \xi_5 + \xi_7 \\ +r_0 + \xi_1 - \xi_7 + \xi_9, & \text{for } r_0 \geq \xi_1 + \xi_5 + \xi_7. \end{cases} \quad (3.186)$$

This function is sketched in Figure 30(b) (where we have chosen $\xi_3 > \xi_5$ for convenience of plotting). At the points $r_0 = -\xi_3$, $r_0 = 0$ and $r_0 = \xi_5 + \xi_7$, there are gauge D6-branes wrapping \mathbb{P}^1 's in the resolution of the singularity (we denote them by \mathcal{G}_1 , \mathcal{G}_2 and \mathcal{G}_3 respectively). When $\xi_3 = \xi_5 = \xi_7 = 0$, an $SU(3)$ gauge theory is realized (at $r_0 = 0$) with inverse coupling $h_0 = \xi_9$. There are two flavor D6-branes at $r_0 = \xi_5$ and $r_0 = \xi_5 + \xi_7$, denoted by \mathcal{F}_1 and \mathcal{F}_2 respectively.

The effective Chern-Simons level is, of course, still 1. The simple-root W-bosons have masses given by:

$$M(W_1) = \xi_3 = 2\varphi_1 - \varphi_2, \quad M(W_2) = \xi_5 + \xi_7 = 2\varphi_2 - \varphi_1. \quad (3.187)$$

This resolution can be identified with gauge theory chamber 12 (cf. Table 6 and (A.10)), with instanton masses given by:

$$\begin{aligned}
M(\mathcal{I}_1) &= \chi(r_0 = -\xi_3) = \xi_3 + \xi_9 = h_0 - m_1 - m_2 + 3\varphi_1 , \\
M(\mathcal{I}_2) &= \chi(r_0 = 0) = \xi_9 = h_0 - m_1 - m_2 + \varphi_1 + \varphi_2 \\
M(\mathcal{I}_3) &= \chi(r_0 = \xi_5 + \xi_7) = \xi_5 + \xi_9 = h_0 - m_2 + 2\varphi_2 .
\end{aligned} \tag{3.188}$$

The masses of hypermultiplets are:

$$\begin{aligned}
M(\mathcal{H}_1) &= M(\mathcal{G}_1\mathcal{F}_1) = \xi_3 + \xi_5 = \varphi_1 + m_1 , \\
M(\mathcal{H}_2) &= M(\mathcal{G}_2\mathcal{F}_1) = \xi_5 = -\varphi_1 + \varphi_2 + m_1 , \\
M(\mathcal{H}_3) &= M(\mathcal{G}_3\mathcal{F}_1) = \xi_7 = \varphi_2 - m_1 , \\
M(\mathcal{H}_4) &= M(\mathcal{G}_1\mathcal{F}_2) = \xi_1 + \xi_3 + \xi_5 + \xi_7 = \varphi_1 + m_2 , \\
M(\mathcal{H}_5) &= M(\mathcal{G}_2\mathcal{F}_2) = \xi_1 + \xi_5 + \xi_7 = -\varphi_1 + \varphi_2 + m_2 , \\
M(\mathcal{H}_6) &= M(\mathcal{G}_3\mathcal{F}_2) = \xi_1 = -\varphi_2 + m_2 .
\end{aligned} \tag{3.189}$$

It is easy to verify that the map between geometry and field theory variables is the still (3.172), as it must be. Plugging (3.172) into (3.185), we recover the field theory prepotential:

$$\begin{aligned}
\mathcal{F}_{SU(3)_2, N_f=2}^{\text{chamber 12}} &= \frac{4}{3}\varphi_1^3 + \frac{7}{6}\varphi_2^3 + \frac{1}{2}(\varphi_1^2\varphi_2 + \varphi_1\varphi_2^2) + (h_0 - m_1 - m_2)\varphi_1^2 + (-h_0 + m_1 + m_2)\varphi_1\varphi_2 \\
&\quad + \left(h_0 - \frac{1}{2}m_1 - m_2\right)\varphi_2^2 - \frac{1}{2}m_1^2\varphi_2 ,
\end{aligned} \tag{3.190}$$

up to φ -independent terms. The monopole string tensions from the IIA profile are:

$$T_{1,\text{geo}} = \int_{-\xi_3}^0 \chi(r_0) dr_0 = \frac{\xi_3^2}{2} + \xi_3\xi_9 , \tag{3.191}$$

$$T_{2,\text{geo}} = \int_0^{\xi_5+\xi_7} \chi(r_0) dr_0 = \frac{\xi_5^2}{2} + \xi_5\xi_9 + \xi_7(\xi_5 + \xi_9) . \tag{3.192}$$

Using the map,

$$\text{Resolution (b) : } \begin{cases} \xi_1 = -\varphi_2 + m_2 , \\ \xi_3 = 2\varphi_1 - \varphi_2 , \\ \xi_5 = -\varphi_1 + \varphi_2 + m_1 , \\ \xi_7 = -\varphi_2 + m_1 , \\ \xi_9 = h_0 - m_1 - m_2 + \varphi_1 + \varphi_2 , \end{cases} \tag{3.193}$$

we find that $T_{i,\text{ft}} = T_{i,\text{geo}}$ for $i = 1, 2$. The tensions vanish at loci given by:

$$(I) : \{\xi_3 = 0\} \cup \left\{ \frac{1}{2}\xi_3 + \xi_9 = 0 \right\}, \text{ and } (II) : \left\{ \frac{\xi_5^2}{2} + \xi_5\xi_9 + \xi_7(\xi_5 + \xi_9) = 0 \right\}. \quad (3.194)$$

Along the locus $\{\xi_3 = 0\} \subset (I)$, the W-boson W_1 in this chamber becomes massless. So this submanifold coincides with the hard wall which is the boundary of the Weyl chamber. The locus $\{\frac{1}{2}\xi_3 + \xi_9 = 0\} \subset (I)$ is not part of the Kähler chamber of resolution (1). The quadratic condition (II) has two solutions: $\xi_5 = -\xi_7 - \xi_9 \pm \sqrt{\xi_7^2 + \xi_9^2}$. Both sign choices yield a negative value of ξ_5 , which is inconsistent in this Kähler chamber. This implies that there are no magnetic walls in resolution (b) of the $E_3^{2,1}$ singularity.

Away from any hard wall in this chamber, one of the three perturbative hypermultiplets \mathcal{H}_2 , \mathcal{H}_3 or \mathcal{H}_6 can become massless, respectively, at $\xi_5 = 0$, $\xi_7 = 0$ or $\xi_1 = 0$. These are flops of \mathcal{C}_5 , \mathcal{C}_7 or \mathcal{C}_1 , which lead, respectively to gauge-theory resolutions (f), (g) or (a). Alternatively, away from any hard wall, the BPS instanton particle \mathcal{I}_2 can become massless at $\xi_9 = 0$ (signaling a flop of \mathcal{C}_9), indicating a traversible instantonic wall which leads to non-gauge-theoretic resolution (q₃).

RG Flow. In this resolution, one can decouple the divisor D_1 by sending the volume of the curve \mathcal{C}_1 to infinity, which is equivalent to sending the mass m_2 to $+\infty$. It is easy to see that this yields resolution (a) of the $E_2^{2,\frac{1}{2}}$ singularity shown in Figure 12. This is consistent with the fact that the effective Chern-Simons level changes from $k_{\text{eff}} = 1$ to $k_{\text{eff}} = 1 - \frac{1}{2} = \frac{1}{2}$ (recall (2.5)). An inspection of Figure 28 suggests that many such transitions are possible, including those involving non-gauge-theoretic phases.

The geometry \leftrightarrow field theory map. We can repeat the above analysis for the remaining fourteen resolutions that admit vertical reductions, and match each of them to chambers of $SU(3)_2$ $N_f = 2$ field theory (see Table 5). To do so, one may exploit the fact that map (3.172) is constant across all resolutions. The result of this matching is outlined in Table 3.

The triple-intersection numbers of all 30 crepant resolutions (including the 14 which are non-gauge-theoretic phases) are listed in Appendix B, and the expressions for the corresponding M-theory prepotentials are listed in Appendix C.

3.7 The $E_3^{2,0}$ singularity and $SU(3)_0$ $N_f = 2$ gauge theory

The $E_3^{2,0}$ singularity of Figure 3(j) admits 24 crepant resolutions. However, an $SL(2, \mathbb{Z})$ transformation – for example, by $ST^{-1}S^2$ – transforms this singularity to the “beetle singularity” that was extensively analyzed in [10]. An interesting feature of the beetle singularity is that there are both horizontal as well as vertical reductions, and these

Resolution	Chamber	φ_1+m_1	$-\varphi_1+\varphi_2+m_1$	$-\varphi_2+m_1$	φ_1+m_2	$-\varphi_1+\varphi_2+m_2$	$-\varphi_2+m_2$
(a)	11	≥ 0	≥ 0	< 0	≥ 0	≥ 0	< 0
(b)	12	≥ 0	≥ 0	< 0	≥ 0	≥ 0	≥ 0
(c)	10	≥ 0	≥ 0	< 0	≥ 0	< 0	< 0
(d)	7	≥ 0	< 0	< 0	≥ 0	≥ 0	< 0
(e)	15	≥ 0	≥ 0	≥ 0	≥ 0	≥ 0	< 0
(f)	8	≥ 0	< 0	< 0	≥ 0	≥ 0	≥ 0
(g)	16	≥ 0	≥ 0	≥ 0	≥ 0	≥ 0	≥ 0
(h)	9	≥ 0	≥ 0	< 0	< 0	< 0	< 0
(i)	6	≥ 0	< 0	< 0	≥ 0	< 0	< 0
(j)	14	≥ 0	≥ 0	≥ 0	≥ 0	< 0	< 0
(k)	3	< 0	< 0	< 0	≥ 0	≥ 0	< 0
(l)	4	< 0	< 0	< 0	≥ 0	≥ 0	≥ 0
(m)	5	≥ 0	< 0	< 0	< 0	< 0	< 0
(n)	13	≥ 0	≥ 0	≥ 0	< 0	< 0	< 0
(o)	2	< 0	< 0	< 0	≥ 0	< 0	< 0
(p)	1	< 0	< 0	< 0	< 0	< 0	< 0

Table 3. The map between the 16 crepant resolutions of the $E_3^{2,1}$ singularity that admit a vertical reduction, and the 16 chambers of the $SU(3)_2$ $N_f = 2$ field theory, with field theory chamber definitions expressed as inequalities.

describe either the $SU(2) \times SU(2)$ theory, or the $SU(3)_0$ $N_f = 2$ theory. As we have remarked before, this geometry can lead to a number of smaller geometries (see, for instance, Figure 1), including, in particular the $E_2^{\pm\frac{1}{2}}$ geometries, and the $E_1^{2,\ell}$ geometries for $\ell = -1, 0, 1$, but also non-gauge-theoretic geometries. We refer the reader to [10] for details.

Acknowledgements

I would like to especially thank Cyril Closset and Michele Del Zotto for ongoing collaboration on related topics, and for their careful reading of an earlier draft. I thank Andrés Collinucci, Nathan Haouzi, Radu Ionaş, Daniel Lichtblau, Nicolò Piazzalunga, Martin Roček, and Alessandro Tomasiello for interesting discussions and correspondence. This work is supported in part by NSF grant PHY-1620628.

A Field theory prepotentials and instanton masses

In this section, we list the expressions for the field theory prepotential (2.7) evaluated for the models that we have analyzed in this paper, and also the instanton masses in

each chamber. We begin by describing the procedure used to compute the instanton masses in field theory.

For the special case of $\mathbf{G} = \prod_i SU(n_i)$, we follow [10, 83] and consider an auxiliary gauge group $\mathbf{G}' = \prod_i U(n_i)$ obtained by replacing each $SU(n_i)$ gauge group factor with $U(n_i)$. Let us denote the $U(n_i)$ Coulomb branch vevs by $\phi_{i,(1)}, \phi_{i,(2)}, \dots, \phi_{i,(n_i)}$. Then for each such gauge group $U(n_i)$ there are n_i “instanton states” with masses given by the second derivatives of the prepotential:

$$M(\mathcal{I}_{U(n_i)}^{(k)}) = \left. \frac{\partial^2 \mathcal{F}}{\partial \phi_{i,(k)}^2} \right|_{U(n_i) \rightarrow SU(n_i)}, \quad \text{for } k = 1, \dots, n_i. \quad (\text{A.1})$$

Here the notation $U(n_i) \rightarrow SU(n_i)$ refers to the operation of imposing the “traceless condition,” to transform to $SU(n_i)$ variables, *after* computing the second derivative. This entails the following substitution for every $U(n_i)$ factor in \mathbf{G}' :

$$\phi_{i,a} = \varphi_{i,a} - \varphi_{i,a-1}, \quad a = 1, \dots, n_i, \quad \text{with } \varphi_{a,0} = \varphi_{a,n_i} = 0. \quad (\text{A.2})$$

Here we have denoted the Coulomb vevs of $SU(n_i)$ by $\varphi_{i,1}, \dots, \varphi_{i,n_i-1}$. The leading term is $M(\mathcal{I}) = h_0 + \dots$ corresponding to the familiar fact that instanton masses scale as $h_0 = \frac{8\pi^2}{g^2}$.

$U(3)_k$ field theory. The gauge theory prepotential (2.7) for pure 5d $U(3)_k$ gauge theory is:

$$\mathcal{F}_{U(3)_k} = \frac{1}{2} h_0 (\phi_1^2 + \phi_2^2 + \phi_3^2) + \frac{k}{6} (\phi_1^3 + \phi_2^3 + \phi_3^2) + \frac{1}{6} [(\phi_1 - \phi_2)^3 + (\phi_2 - \phi_3)^3 + (\phi_1 - \phi_3)^3]. \quad (\text{A.3})$$

The fundamental Weyl chamber is defined by $\phi_1 \geq \phi_2 \geq \phi_3$.

$SU(3)_{k_{\text{eff}}} + N_f = 1$ field theory. The $U(3)_{k_{\text{eff}}} N_f = 1$ field theory is specified by 3 Coulomb vevs (ϕ_1, ϕ_2, ϕ_3) , one inverse gauge coupling h_0 , and one real mass $m \in \mathbb{R}$. There are 4 chambers inside the fundamental Weyl chamber given by $\phi_1 \geq \phi_2 \geq \phi_3$. These are defined by the allowed ranges of the arguments of the Θ functions in (2.7). The instanton masses in various chambers, computed using (A.1), are listed in Table 4 to facilitate calculations in the main text. Here k denotes the bare CS level, given in terms of the effective CS level k_{eff} for $N_f = 1$ by,

$$k \equiv k_{\text{bare}} = k_{\text{eff}} + \frac{1}{2}, \quad (\text{A.4})$$

in the $U(1)_{-\frac{1}{2}}$ quantization scheme (cf. (2.4)).

#	$\phi_1 + m$ or $\varphi_1 + m$	$\phi_2 + m$ or $-\varphi_1 + \varphi_2 + m$	$\phi_3 + m$ or $-\varphi_2 + m$	$M(\mathcal{I}_1)$	$M(\mathcal{I}_2)$	$M(\mathcal{I}_3)$
1	< 0	< 0	< 0	$h_0 + (k+3)\varphi_1$	$h_0 + (1-k)\varphi_1$ $+ (1+k)\varphi_2$	$h_0 + (3-k)\varphi_2$
2	≥ 0	< 0	< 0	$h_0 - m$ $+ (k+2)\varphi_1$	$h_0 + (1-k)\varphi_1$ $+ (1+k)\varphi_2$	$h_0 + (3-k)\varphi_2$
3	≥ 0	≥ 0	< 0	$h_0 - m$ $+ (k+2)\varphi_1$	$h_0 - m$ $+ (2-k)\varphi_1$ $+ k\varphi_2$	$h_0 + (3-k)\varphi_2$
4	≥ 0	≥ 0	≥ 0	$h_0 - m$ $+ (k+2)\varphi_1$	$h_0 - m$ $+ (2-k)\varphi_1$ $+ k\varphi_2$	$h_0 - m$ $+ (4-k)\varphi_2$

Table 4. Chamber definitions of the $U(3)_{k_{\text{eff}}}$ or $SU(3)_{k_{\text{eff}}}$ gauge theory with $N_f = 1$ and the corresponding instanton masses. The variables (ϕ_1, ϕ_2, ϕ_3) denote $U(3)$ vevs, while the variables (φ_1, φ_2) denote $SU(3)$ vevs.

The $SU(3)_{k_{\text{eff}}}$ $N_f = 1$ theory is specified by 2 Coulomb vevs φ_1, φ_2 , one inverse coupling h_0 and one real mass $m \in \mathbb{R}$. The fundamental Weyl chamber is given by $\{2\varphi_1 - \varphi_2 \geq 0\} \cap \{-\varphi_2 + 2\varphi_2 \geq 0\}$.

Below we list the prepotentials in the four field theory chambers.

$$\mathcal{F}_{SU(3)_{k, N_f=1}}^{\text{chamber 1}} = \frac{4}{3}\varphi_1^3 + \frac{4}{3}\varphi_2^3 + \frac{(k-1)}{2}\varphi_1^2\varphi_2 - \frac{(k+1)}{2}\varphi_1\varphi_2^2 + h_0(\varphi_1^2 + \varphi_2^2 - \varphi_1\varphi_2). \quad (\text{A.5})$$

$$\begin{aligned} \mathcal{F}_{SU(3)_{k, N_f=1}}^{\text{chamber 2}} &= \frac{7}{6}\varphi_1^3 + \frac{4}{3}\varphi_2^3 + \frac{(k-1)}{2}\varphi_1^2\varphi_2 - \frac{(k+1)}{2}\varphi_1\varphi_2^2 + \left(h_0 - \frac{m}{2}\right)\varphi_1^2 + h_0\varphi_2^2 \\ &\quad - h_0\varphi_1\varphi_2 - \frac{m^2}{2}\varphi_1 - \frac{m^3}{6}. \end{aligned} \quad (\text{A.6})$$

$$\begin{aligned} \mathcal{F}_{SU(3)_{k, N_f=1}}^{\text{chamber 3}} &= \frac{4}{3}\varphi_1^3 + \frac{7}{6}\varphi_2^3 + \frac{(k-2)}{2}\varphi_1^2\varphi_2 - \frac{k}{2}\varphi_1\varphi_2^2 + (h_0 - m)\varphi_1^2 + \left(h_0 - \frac{m}{2}\right)\varphi_2^2 \\ &\quad + (m - h_0)\varphi_1\varphi_2 - \frac{m^2}{2}\varphi_2 - \frac{m^3}{3}. \end{aligned} \quad (\text{A.7})$$

$$\begin{aligned} \mathcal{F}_{SU(3)_{k, N_f=1}}^{\text{chamber 4}} &= \frac{4}{3}\varphi_1^3 + \frac{4}{3}\varphi_2^3 + \frac{(k-2)}{2}\varphi_1^2\varphi_2 - \frac{k}{2}\varphi_1\varphi_2^2 + (h_0 - m)\varphi_1^2 + (h_0 - m)\varphi_2^2 \\ &\quad + (m - h_0)\varphi_1\varphi_2 - \frac{m^3}{2}. \end{aligned} \quad (\text{A.8})$$

$SU(3)_{k_{\text{eff}}} + N_f = 2$ field theory. The $SU(3)_{k_{\text{eff}}}$ $N_f = 2$ theory is likewise specified by 2 Coulomb vevs (φ_1, φ_2) , one gauge coupling h_0 and two real masses $m_1, m_2 \in \mathbb{R}$.

Table 5 lists the 16 chambers of the theory, while Table 6 lists the elementary instanton masses in the 16 chambers.

Chamber	$\phi_1 + m_1$ or $\varphi_1 + m_1$	$\phi_2 + m_1$ or $-\varphi_1 + \varphi_2 + m_1$	$\phi_3 + m_1$ or $-\varphi_2 + m_1$	$\phi_1 + m_2$ or $\varphi_1 + m_2$	$\phi_2 + m_2$ or $-\varphi_1 + \varphi_2 + m_2$	$\phi_3 + m_2$ or $-\varphi_2 + m_2$
1	< 0	< 0	< 0	< 0	< 0	< 0
2	< 0	< 0	< 0	≥ 0	< 0	< 0
3	< 0	< 0	< 0	≥ 0	≥ 0	< 0
4	< 0	< 0	< 0	≥ 0	≥ 0	≥ 0
5	≥ 0	< 0	< 0	< 0	< 0	< 0
6	≥ 0	< 0	< 0	≥ 0	< 0	< 0
7	≥ 0	< 0	< 0	≥ 0	≥ 0	< 0
8	≥ 0	< 0	< 0	≥ 0	≥ 0	≥ 0
9	≥ 0	≥ 0	< 0	< 0	< 0	< 0
10	≥ 0	≥ 0	< 0	≥ 0	< 0	< 0
11	≥ 0	≥ 0	< 0	≥ 0	≥ 0	< 0
12	≥ 0	≥ 0	< 0	≥ 0	≥ 0	≥ 0
13	≥ 0	≥ 0	≥ 0	< 0	< 0	< 0
14	≥ 0	≥ 0	≥ 0	≥ 0	< 0	< 0
15	≥ 0	≥ 0	≥ 0	≥ 0	≥ 0	< 0
16	≥ 0	≥ 0	≥ 0	≥ 0	≥ 0	≥ 0

Table 5. Chamber definitions of the $U(3)_{k_{\text{eff}}}$ or $SU(3)_{k_{\text{eff}}}$ gauge theory with $N_f = 2$ flavors. The variables (ϕ_1, ϕ_2, ϕ_3) denote $U(3)$ vevs, while the variables (φ_1, φ_2) denote $SU(3)$ vevs.

Note that in Table 6, the symbol k denotes the bare CS level, which in this case is related to the effective CS level k_{eff} by,

$$k \equiv k_{\text{bare}} = k_{\text{eff}} + 1 \quad (\text{A.9})$$

in the $U(1)_{-\frac{1}{2}}$ quantization scheme (cf. (2.4)).

The prepotential (2.7) of the $SU(3)_{k_{\text{eff}}}$ $N_f = 2$ theory is given by:

$$\begin{aligned} \mathcal{F}_{SU(3)_k, N_f=2} = & h_0(\varphi_1^2 - \varphi_2\varphi_1 + \varphi_2^2) + \frac{4}{3}(\varphi_1^3 + \varphi_2^3) + \frac{1}{2}((k-1)\varphi_1^2\varphi_2 - (k+1)\varphi_1\varphi_2^2) \\ & + \frac{1}{6} \sum_{i=1}^2 [\Theta(\varphi_1 + m_i)(\varphi_1 + m_i)^3 + \Theta(-\varphi_1 + \varphi_2 + m_i)(-\varphi_1 + \varphi_2 + m_i)^3 \\ & + \Theta(\varphi_2 + m_i)(\varphi_2 + m_i)^3] . \end{aligned} \quad (\text{A.10})$$

The arguments of the Θ functions define various chambers, and are listed in Table 5.

#	$M(\mathcal{I}_1)$	$M(\mathcal{I}_2)$	$M(\mathcal{I}_3)$
1	$h_0 + (k+3)\varphi_1$	$h_0 + (1-k)\varphi_1 + (k+1)\varphi_2$	$h_0 + (3-k)\varphi_2$
2	$h_0 + (k+2)\varphi_1 - m_2$	$h_0 + (1-k)\varphi_1 + (k+1)\varphi_2$	$h_0 + (3-k)\varphi_2$
3	$h_0 + (k+2)\varphi_1 - m_2$	$h_0 + (2-k)\varphi_1 + k\varphi_2 - m_2$	$h_0 + (3-k)\varphi_2$
4	$h_0 + (k+2)\varphi_1 - m_2$	$h_0 + (2-k)\varphi_1 + k\varphi_2 - m_2$	$h_0 + (4-k)\varphi_2 - m_2$
5	$h_0 + (k+2)\varphi_1 - m_1$	$h_0 + (1-k)\varphi_1 + (k+1)\varphi_2$	$h_0 + (3-k)\varphi_2$
6	$h_0 + (k+1)\varphi_1 - m_1 - m_2$	$h_0 + (1-k)\varphi_1 + (k+1)\varphi_2$	$h_0 + (3-k)\varphi_2$
7	$h_0 + (k+1)\varphi_1 - m_1 - m_2$	$h_0 + (2-k)\varphi_1 + k\varphi_2 - m_2$	$h_0 + (3-k)\varphi_2$
8	$h_0 + (k+1)\varphi_1 - m_1 - m_2$	$h_0 + (2-k)\varphi_1 + k\varphi_2 - m_2$	$h_0 + (4-k)\varphi_2 - m_2$
9	$h_0 + (k+2)\varphi_1 - m_1$	$h_0 + (2-k)\varphi_1 + k\varphi_2 - m_1$	$h_0 + (3-k)\varphi_2$
10	$h_0 + (k+1)\varphi_1 - m_1 - m_2$	$h_0 + (2-k)\varphi_1 + k\varphi_2 - m_1$	$h_0 + (3-k)\varphi_2$
11	$h_0 + (k+1)\varphi_1 - m_1 - m_2$	$h_0 + (3-k)\varphi_1 + (k-1)\varphi_2 - m_1 - m_2$	$h_0 + (3-k)\varphi_2$
12	$h_0 + (k+1)\varphi_1 - m_1 - m_2$	$h_0 + (3-k)\varphi_1 + (k-1)\varphi_2 - m_1 - m_2$	$h_0 + (4-k)\varphi_2 - m_2$
13	$h_0 + (k+2)\varphi_1 - m_1$	$h_0 + (2-k)\varphi_1 + k\varphi_2 - m_1$	$h_0 + (4-k)\varphi_2 - m_1$
14	$h_0 + (k+1)\varphi_1 - m_1 - m_2$	$h_0 + (2-k)\varphi_1 + k\varphi_2 - m_1$	$h_0 + (4-k)\varphi_2 - m_1$
15	$h_0 + (k+1)\varphi_1 - m_1 - m_2$	$h_0 + (3-k)\varphi_1 + (k-1)\varphi_2 - m_1 - m_2$	$h_0 + (4-k)\varphi_2 - m_1$
16	$h_0 + (k+1)\varphi_1 - m_1 - m_2$	$h_0 + (3-k)\varphi_1 + (k-1)\varphi_2 - m_1 - m_2$	$h_0 + (5-k)\varphi_2 - m_1 - m_2$

Table 6. Instanton masses in the 16 chambers of the $SU(3)_{k_{\text{eff}}}$ $N_f = 2$ field theory.

B Triple-intersection numbers of the $E_3^{2,1}$ geometry

Using the GLSM approach, it is straightforward to compute triple-intersection numbers involving at least one compact divisor, as discussed in the main text. The results are listed below.

Resolutions that have a vertical reduction. Resolutions (a)-(p) (see Figure 28) have an allowed vertical reduction. The relevant triple-intersection numbers are:

$$(a) : \begin{cases} \mathbf{E}_1^3 = 6 & , & \mathbf{E}_2^3 = 8 & , & D_1\mathbf{E}_1\mathbf{E}_2 = 0 & D_2\mathbf{E}_1\mathbf{E}_2 = 1 & , & D_3\mathbf{E}_1\mathbf{E}_2 = 0 & , \\ \mathbf{E}_1^2\mathbf{E}_2 = -1 & , & \mathbf{E}_1\mathbf{E}_2^2 = -1 & , & D_1^2\mathbf{E}_1 = -1 & D_1^2\mathbf{E}_2 = 0 & , & D_1D_2\mathbf{E}_1 = 1 & , \\ D_1D_2\mathbf{E}_2 = 0 & , & D_1D_3\mathbf{E}_1 = 0 & , & D_1D_3\mathbf{E}_2 = 0 & D_2^2\mathbf{E}_1 = -1 & , & D_2^2\mathbf{E}_2 = 0 & , \\ D_2D_3\mathbf{E}_1 = 0 & , & D_2D_3\mathbf{E}_2 = 1 & , & D_3^2\mathbf{E}_1 = 0 & D_3^2\mathbf{E}_2 = 1 & , & D_1\mathbf{E}_1^2 = -1 & , \\ D_1\mathbf{E}_2^2 = 0 & , & D_2\mathbf{E}_1^2 = -1 & , & D_2\mathbf{E}_2^2 = -2 & D_3\mathbf{E}_1^2 = 0 & , & D_3\mathbf{E}_2^2 = -3 & , \end{cases} \quad (B.1)$$

$$(b) : \begin{cases} \mathbf{E}_1^3 = 7 & , & \mathbf{E}_2^3 = 8 & , & D_1\mathbf{E}_1\mathbf{E}_2 = 0 & D_2\mathbf{E}_1\mathbf{E}_2 = 1 & , & D_3\mathbf{E}_1\mathbf{E}_2 = 0 & , \\ \mathbf{E}_1^2\mathbf{E}_2 = -1 & , & \mathbf{E}_1\mathbf{E}_2^2 = -1 & , & D_1^2\mathbf{E}_1 = 0 & D_1^2\mathbf{E}_2 = 0 & , & D_1D_2\mathbf{E}_1 = 0 & , \\ D_1D_2\mathbf{E}_2 = 0 & , & D_1D_3\mathbf{E}_1 = 0 & , & D_1D_3\mathbf{E}_2 = 0 & D_2^2\mathbf{E}_1 = 0 & , & D_2^2\mathbf{E}_2 = 0 & , \\ D_2D_3\mathbf{E}_1 = 0 & , & D_2D_3\mathbf{E}_2 = 1 & , & D_3^2\mathbf{E}_1 = 0 & D_3^2\mathbf{E}_2 = 1 & , & D_1\mathbf{E}_1^2 = 0 & , \\ D_1\mathbf{E}_2^2 = 0 & , & D_2\mathbf{E}_1^2 = -2 & , & D_2\mathbf{E}_2^2 = -2 & D_3\mathbf{E}_1^2 = 0 & , & D_3\mathbf{E}_2^2 = -3 & , \end{cases} \quad (B.2)$$

$$(c) : \begin{cases} \mathbf{E}_1^3 = 7 & , & \mathbf{E}_2^3 = 7 & , & D_1\mathbf{E}_1\mathbf{E}_2 = 1 & D_2\mathbf{E}_1\mathbf{E}_2 = 0 & , & D_3\mathbf{E}_1\mathbf{E}_2 = 0 & , \\ \mathbf{E}_1^2\mathbf{E}_2 = -2 & , & \mathbf{E}_1\mathbf{E}_2^2 = 0 & , & D_1^2\mathbf{E}_1 = 0 & D_1^2\mathbf{E}_2 = -1 & , & D_1D_2\mathbf{E}_1 = 0 & , \\ D_1D_2\mathbf{E}_2 = 1 & , & D_1D_3\mathbf{E}_1 = 0 & , & D_1D_3\mathbf{E}_2 = 0 & D_2^2\mathbf{E}_1 = 0 & , & D_2^2\mathbf{E}_2 = -1 & , \\ D_2D_3\mathbf{E}_1 = 0 & , & D_2D_3\mathbf{E}_2 = 1 & , & D_3^2\mathbf{E}_1 = 0 & D_3^2\mathbf{E}_2 = 1 & , & D_1\mathbf{E}_1^2 = -2 & , \\ D_1\mathbf{E}_2^2 = -1 & , & D_2\mathbf{E}_1^2 = 0 & , & D_2\mathbf{E}_2^2 = -1 & D_3\mathbf{E}_1^2 = 0 & , & D_3\mathbf{E}_2^2 = -3 & , \end{cases} \quad (B.3)$$

Resolutions that have a vertical reduction. (Resolutions (a)-(p) in Figure 28.)

$$\begin{aligned}
\mathcal{F}_a &= \left(\frac{\mu_1^2}{2} - \mu_1\mu_2 + \frac{\mu_2^2}{2} \right) \nu_1 + \left(\frac{\mu_1}{2} + \frac{\mu_2}{2} \right) \nu_1^2 - \nu_1^3 + \left(-\mu_2\mu_3 - \frac{\mu_3^2}{2} \right) \nu_2 - \mu_2\nu_1\nu_2 + \frac{1}{2}\nu_1^2\nu_2 \\
&\quad + \left(\mu_2 + \frac{3\mu_3}{2} \right) \nu_2^2 + \frac{1}{2}\nu_1\nu_2^2 - \frac{4\nu_2^3}{3}, \\
\mathcal{F}_b &= \mu_2\nu_1^2 - \frac{7\nu_1^3}{6} + \left(-\mu_2\mu_3 - \frac{\mu_3^2}{2} \right) \nu_2 - \mu_2\nu_1\nu_2 + \frac{1}{2}\nu_1^2\nu_2 + \left(\mu_2 + \frac{3\mu_3}{2} \right) \nu_2^2 + \frac{1}{2}\nu_1\nu_2^2 - \frac{4\nu_2^3}{3}, \\
\mathcal{F}_c &= \mu_1\nu_1^2 - \frac{7\nu_1^3}{6} + \left(\frac{\mu_1^2}{2} - \mu_1\mu_2 + \frac{\mu_2^2}{2} - \mu_2\mu_3 - \frac{\mu_3^2}{2} \right) \nu_2 - \mu_1\nu_1\nu_2 + \nu_1^2\nu_2 + \left(\frac{\mu_1}{2} + \frac{\mu_2}{2} + \frac{3\mu_3}{2} \right) \nu_2^2 - \frac{7\nu_2^3}{6}, \\
\mathcal{F}_d &= \left(\frac{\mu_1^2}{2} - \mu_1\mu_2 + \frac{\mu_2^2}{2} \right) \nu_1 + \left(\frac{\mu_1}{2} + \frac{\mu_2}{2} \right) \nu_1^2 - \frac{7\nu_1^3}{6} + \left(-\mu_2\mu_3 - \frac{\mu_3^2}{2} \right) \nu_2 - \mu_2\nu_1\nu_2 + \nu_1^2\nu_2 + \left(\mu_2 + \frac{3\mu_3}{2} \right) \nu_2^2 - \frac{7\nu_2^3}{6}, \\
\mathcal{F}_e &= \left(\frac{\mu_1^2}{2} - \mu_1\mu_2 + \frac{\mu_2^2}{2} \right) \nu_1 + \left(\frac{\mu_1}{2} + \frac{\mu_2}{2} \right) \nu_1^2 - \frac{7\nu_1^3}{6} + \left(-\mu_2\mu_3 - \frac{\mu_3^2}{2} \right) \nu_2 - \mu_2\nu_1\nu_2 + \frac{1}{2}\nu_1^2\nu_2 \\
&\quad + \left(\mu_2 + \frac{3\mu_3}{2} \right) \nu_2^2 + \frac{1}{2}\nu_1\nu_2^2 - \frac{4\nu_2^3}{3}, \\
\mathcal{F}_f &= \mu_2\nu_1^2 - \frac{4\nu_1^3}{3} + \left(-\mu_2\mu_3 - \frac{\mu_3^2}{2} \right) \nu_2 - \mu_2\nu_1\nu_2 + \nu_1^2\nu_2 + \left(\mu_2 + \frac{3\mu_3}{2} \right) \nu_2^2 - \frac{7\nu_2^3}{6}, \\
\mathcal{F}_g &= \mu_2\nu_1^2 - \frac{4\nu_1^3}{3} + \left(-\mu_2\mu_3 - \frac{\mu_3^2}{2} \right) \nu_2 - \mu_2\nu_1\nu_2 + \frac{1}{2}\nu_1^2\nu_2 + \left(\mu_2 + \frac{3\mu_3}{2} \right) \nu_2^2 + \frac{1}{2}\nu_1\nu_2^2 - \frac{4\nu_2^3}{3}, \\
\mathcal{F}_h &= \mu_1\nu_1^2 - \frac{7\nu_1^3}{6} + \left(-\mu_1\mu_3 - \mu_3^2 \right) \nu_2 - \mu_1\nu_1\nu_2 + \nu_1^2\nu_2 + \left(\mu_1 + 2\mu_3 \right) \nu_2^2 - \frac{4\nu_2^3}{3}, \\
\mathcal{F}_i &= \mu_1\nu_1^2 - \frac{4\nu_1^3}{3} + \left(\frac{\mu_1^2}{2} - \mu_1\mu_2 + \frac{\mu_2^2}{2} - \mu_2\mu_3 - \frac{\mu_3^2}{2} \right) \nu_2 - \mu_1\nu_1\nu_2 + \frac{3}{2}\nu_1^2\nu_2 + \left(\frac{\mu_1}{2} + \frac{\mu_2}{2} + \frac{3\mu_3}{2} \right) \nu_2^2 - \frac{1}{2}\nu_1\nu_2^2 - \nu_2^3, \\
\mathcal{F}_j &= \mu_1\nu_1^2 - \frac{4\nu_1^3}{3} + \left(\frac{\mu_1^2}{2} - \mu_1\mu_2 + \frac{\mu_2^2}{2} - \mu_2\mu_3 - \frac{\mu_3^2}{2} \right) \nu_2 - \mu_1\nu_1\nu_2 + \nu_1^2\nu_2 + \left(\frac{\mu_1}{2} + \frac{\mu_2}{2} + \frac{3\mu_3}{2} \right) \nu_2^2 - \frac{7\nu_2^3}{6}, \\
\mathcal{F}_k &= \left(\frac{\mu_1^2}{2} - \mu_1\mu_2 + \frac{\mu_2^2}{2} \right) \nu_1 + \left(\frac{\mu_1}{2} + \frac{\mu_2}{2} \right) \nu_1^2 - \frac{7\nu_1^3}{6} + \left(-\mu_2\mu_3 - \mu_3^2 \right) \nu_2 - \mu_2\nu_1\nu_2 + \nu_1^2\nu_2 + \left(\mu_2 + 2\mu_3 \right) \nu_2^2 - \frac{4\nu_2^3}{3}, \\
\mathcal{F}_l &= \mu_2\nu_1^2 - \frac{4\nu_1^3}{3} + \left(-\mu_2\mu_3 - \mu_3^2 \right) \nu_2 - \mu_2\nu_1\nu_2 + \nu_1^2\nu_2 + \left(\mu_2 + 2\mu_3 \right) \nu_2^2 - \frac{4\nu_2^3}{3}, \\
\mathcal{F}_m &= \mu_1\nu_1^2 - \frac{4\nu_1^3}{3} + \left(-\mu_1\mu_3 - \mu_3^2 \right) \nu_2 - \mu_1\nu_1\nu_2 + \frac{3}{2}\nu_1^2\nu_2 + \left(\mu_1 + 2\mu_3 \right) \nu_2^2 - \frac{1}{2}\nu_1\nu_2^2 - \frac{7\nu_2^3}{6}, \\
\mathcal{F}_n &= \mu_1\nu_1^2 - \frac{4\nu_1^3}{3} + \left(-\mu_1\mu_3 - \mu_3^2 \right) \nu_2 - \mu_1\nu_1\nu_2 + \nu_1^2\nu_2 + \left(\mu_1 + 2\mu_3 \right) \nu_2^2 - \frac{4\nu_2^3}{3}, \\
\mathcal{F}_o &= \mu_1\nu_1^2 - \frac{4\nu_1^3}{3} + \left(\frac{\mu_1^2}{2} - \mu_1\mu_2 + \frac{\mu_2^2}{2} - \mu_2\mu_3 - \mu_3^2 \right) \nu_2 - \mu_1\nu_1\nu_2 + \frac{3}{2}\nu_1^2\nu_2 + \left(\frac{\mu_1}{2} + \frac{\mu_2}{2} + 2\mu_3 \right) \nu_2^2 - \frac{1}{2}\nu_1\nu_2^2 - \frac{7\nu_2^3}{6}, \\
\mathcal{F}_p &= \mu_1\nu_1^2 - \frac{4\nu_1^3}{3} + \left(-\mu_1\mu_3 - \frac{3\mu_3^2}{2} \right) \nu_2 - \mu_1\nu_1\nu_2 + \frac{3}{2}\nu_1^2\nu_2 + \left(\mu_1 + \frac{5\mu_3}{2} \right) \nu_2^2 - \frac{1}{2}\nu_1\nu_2^2 - \frac{4\nu_2^3}{3}.
\end{aligned}$$

Resolutions without a gauge theory phase. (Resolutions (q₁)-(q₁₄) in Figure 28.)

$$\begin{aligned}
\mathcal{F}_{q_1} &= \left(-\mu_1\mu_2 + \frac{\mu_2^2}{2}\right)\nu_1 + \left(\mu_1 + \frac{\mu_2}{2}\right)\nu_1^2 - \frac{7\nu_1^3}{6} + \left(-\mu_2\mu_3 - \frac{\mu_3^2}{2}\right)\nu_2 - \mu_2\nu_1\nu_2 + \frac{1}{2}\nu_1^2\nu_2 + \left(\mu_2 + \frac{3\mu_3}{2}\right)\nu_2^2 \\
&\quad + \frac{1}{2}\nu_1\nu_2^2 - \frac{4\nu_2^3}{3}, \\
\mathcal{F}_{q_2} &= \left(\frac{\mu_1^2}{2} - \mu_1\mu_2\right)\nu_1 + \left(\frac{\mu_1}{2} + \mu_2\right)\nu_1^2 - \frac{7\nu_1^3}{6} + \left(-\frac{\mu_2^2}{2} - \mu_2\mu_3 - \frac{\mu_3^2}{2}\right)\nu_2 - \frac{1}{2}\nu_1^2\nu_2 + \left(\frac{3\mu_2}{2} + \frac{3\mu_3}{2}\right)\nu_2^2 - \frac{1}{2}\nu_1\nu_2^2 - \frac{3\nu_2^3}{2}, \\
\mathcal{F}_{q_3} &= -\frac{1}{2}\mu_2^2\nu_1 + \frac{3}{2}\mu_2\nu_1^2 - \frac{4\nu_1^3}{3} + \left(-\frac{\mu_2^2}{2} - \mu_2\mu_3 - \frac{\mu_3^2}{2}\right)\nu_2 - \frac{1}{2}\nu_1^2\nu_2 + \left(\frac{3\mu_2}{2} + \frac{3\mu_3}{2}\right)\nu_2^2 - \frac{1}{2}\nu_1\nu_2^2 - \frac{3\nu_2^3}{2}, \\
\mathcal{F}_{q_4} &= -\frac{1}{2}\mu_1^2\nu_1 + \frac{3}{2}\mu_1\nu_1^2 - \frac{4\nu_1^3}{3} + \left(\frac{\mu_1^2}{2} - \mu_1\mu_2 + \frac{\mu_2^2}{2} - \mu_2\mu_3 - \frac{\mu_3^2}{2}\right)\nu_2 - \mu_1\nu_1\nu_2 + \nu_1^2\nu_2 + \left(\frac{\mu_1}{2} + \frac{\mu_2}{2} + \frac{3\mu_3}{2}\right)\nu_2^2 - \frac{7\nu_2^3}{6}, \\
\mathcal{F}_{q_5} &= \left(-\mu_1\mu_2 + \frac{\mu_2^2}{2}\right)\nu_1 + \left(\mu_1 + \frac{\mu_2}{2}\right)\nu_1^2 - \frac{4\nu_1^3}{3} + \left(-\mu_2\mu_3 - \frac{\mu_3^2}{2}\right)\nu_2 - \mu_2\nu_1\nu_2 + \nu_1^2\nu_2 + \left(\mu_2 + \frac{3\mu_3}{2}\right)\nu_2^2 - \frac{7\nu_2^3}{6}, \\
\mathcal{F}_{q_6} &= \left(\frac{\mu_1^2}{2} - \mu_1\mu_2\right)\nu_1 + \left(\frac{\mu_1}{2} + \mu_2\right)\nu_1^2 - \frac{4\nu_1^3}{3} + \left(-\frac{\mu_2^2}{2} - \mu_2\mu_3 - \frac{\mu_3^2}{2}\right)\nu_2 - \frac{1}{2}\nu_1^2\nu_2 + \left(\frac{3\mu_2}{2} + \frac{3\mu_3}{2}\right)\nu_2^2 - \frac{1}{2}\nu_1\nu_2^2 - \frac{3\nu_2^3}{2}, \\
\mathcal{F}_{q_7} &= -\mu_1\mu_2\nu_1 + (\mu_1 + \mu_2)\nu_1^2 - \frac{4\nu_1^3}{3} + \left(-\frac{\mu_2^2}{2} - \mu_2\mu_3 - \frac{\mu_3^2}{2}\right)\nu_2 - \frac{1}{2}\nu_1^2\nu_2 + \left(\frac{3\mu_2}{2} + \frac{3\mu_3}{2}\right)\nu_2^2 - \frac{1}{2}\nu_1\nu_2^2 - \frac{3\nu_2^3}{2}, \\
\mathcal{F}_{q_8} &= -\frac{1}{2}\mu_2^2\nu_1 + \frac{3}{2}\mu_2\nu_1^2 - \frac{3\nu_1^3}{2} + \left(-\frac{\mu_2^2}{2} - \mu_2\mu_3 - \frac{\mu_3^2}{2}\right)\nu_2 - \frac{1}{2}\nu_1^2\nu_2 + \left(\frac{3\mu_2}{2} + \frac{3\mu_3}{2}\right)\nu_2^2 - \frac{1}{2}\nu_1\nu_2^2 - \frac{3\nu_2^3}{2}, \\
\mathcal{F}_{q_9} &= -\frac{1}{2}\mu_1^2\nu_1 + \frac{3}{2}\mu_1\nu_1^2 - \frac{4\nu_1^3}{3} + (-\mu_1\mu_3 - \mu_3^2)\nu_2 - \mu_1\nu_1\nu_2 + \nu_1^2\nu_2 + (\mu_1 + 2\mu_3)\nu_2^2 - \frac{4\nu_2^3}{3}, \\
\mathcal{F}_{q_{10}} &= -\frac{1}{2}\mu_1^2\nu_1 + \frac{3}{2}\mu_1\nu_1^2 - \frac{3\nu_1^3}{2} + \left(\frac{\mu_1^2}{2} - \mu_1\mu_2 + \frac{\mu_2^2}{2} - \mu_2\mu_3 - \frac{\mu_3^2}{2}\right)\nu_2 - \mu_1\nu_1\nu_2 + \frac{3}{2}\nu_1^2\nu_2 + \left(\frac{\mu_1}{2} + \frac{\mu_2}{2} + \frac{3\mu_3}{2}\right)\nu_2^2 \\
&\quad - \frac{1}{2}\nu_1\nu_2^2 - \nu_2^3, \\
\mathcal{F}_{q_{11}} &= \left(-\mu_1\mu_2 + \frac{\mu_2^2}{2}\right)\nu_1 + \left(\mu_1 + \frac{\mu_2}{2}\right)\nu_1^2 - \frac{4\nu_1^3}{3} + (-\mu_2\mu_3 - \mu_3^2)\nu_2 - \mu_2\nu_1\nu_2 + \nu_1^2\nu_2 + (\mu_2 + 2\mu_3)\nu_2^2 - \frac{4\nu_2^3}{3}, \\
\mathcal{F}_{q_{12}} &= -\frac{1}{2}\mu_1^2\nu_1 + \frac{3}{2}\mu_1\nu_1^2 - \frac{3\nu_1^3}{2} + (-\mu_1\mu_3 - \mu_3^2)\nu_2 - \mu_1\nu_1\nu_2 + \frac{3}{2}\nu_1^2\nu_2 + (\mu_1 + 2\mu_3)\nu_2^2 - \frac{1}{2}\nu_1\nu_2^2 - \frac{7\nu_2^3}{6}, \\
\mathcal{F}_{q_{13}} &= -\frac{1}{2}\mu_1^2\nu_1 + \frac{3}{2}\mu_1\nu_1^2 - \frac{3\nu_1^3}{2} + \left(\frac{\mu_1^2}{2} - \mu_1\mu_2 + \frac{\mu_2^2}{2} - \mu_2\mu_3 - \mu_3^2\right)\nu_2 - \mu_1\nu_1\nu_2 + \frac{3}{2}\nu_1^2\nu_2 + \left(\frac{\mu_1}{2} + \frac{\mu_2}{2} + 2\mu_3\right)\nu_2^2 \\
&\quad - \frac{1}{2}\nu_1\nu_2^2 - \frac{7\nu_2^3}{6}, \\
\mathcal{F}_{q_{14}} &= -\frac{1}{2}\mu_1^2\nu_1 + \frac{3}{2}\mu_1\nu_1^2 - \frac{3\nu_1^3}{2} + \left(-\mu_1\mu_3 - \frac{3\mu_3^2}{2}\right)\nu_2 - \mu_1\nu_1\nu_2 + \frac{3}{2}\nu_1^2\nu_2 + \left(\mu_1 + \frac{5\mu_3}{2}\right)\nu_2^2 - \frac{1}{2}\nu_1\nu_2^2 - \frac{4\nu_2^3}{3}.
\end{aligned}$$

References

- [1] N. Seiberg, “Five-dimensional SUSY field theories, nontrivial fixed points and string dynamics,” *Phys. Lett.* **B388** (1996) 753–760, [arXiv:hep-th/9608111](#) [[hep-th](#)].

- [2] O. Aharony and A. Hanany, “Branes, superpotentials and superconformal fixed points,” *Nucl. Phys.* **B504** (1997) 239–271, [arXiv:hep-th/9704170 \[hep-th\]](#).
- [3] O. Aharony, A. Hanany, and B. Kol, “Webs of (p,q) five-branes, five-dimensional field theories and grid diagrams,” *JHEP* **01** (1998) 002, [arXiv:hep-th/9710116 \[hep-th\]](#).
- [4] D. R. Morrison and N. Seiberg, “Extremal transitions and five-dimensional supersymmetric field theories,” *Nucl. Phys.* **B483** (1997) 229–247, [arXiv:hep-th/9609070 \[hep-th\]](#).
- [5] M. R. Douglas, S. H. Katz, and C. Vafa, “Small Instantons, Del Pezzo Surfaces and Type I’ Theory,” *Nucl. Phys.* **B497** (1997) 155–172, [arXiv:hep-th/9609071](#).
- [6] K. A. Intriligator, D. R. Morrison, and N. Seiberg, “Five-dimensional supersymmetric gauge theories and degenerations of Calabi-Yau spaces,” *Nucl. Phys.* **B497** (1997) 56–100, [arXiv:hep-th/9702198 \[hep-th\]](#).
- [7] E. Witten, “Phase transitions in M theory and F theory,” *Nucl. Phys.* **B471** (1996) 195–216, [arXiv:hep-th/9603150 \[hep-th\]](#).
- [8] S. H. Katz, A. Klemm, and C. Vafa, “Geometric engineering of quantum field theories,” *Nucl. Phys.* **B497** (1997) 173–195, [arXiv:hep-th/9609239 \[hep-th\]](#).
- [9] S. Katz, P. Mayr, and C. Vafa, “Mirror symmetry and exact solution of 4-D N=2 gauge theories: 1.,” *Adv.Theor.Math.Phys.* **1** (1998) 53–114, [arXiv:hep-th/9706110 \[hep-th\]](#).
- [10] C. Closset, M. Del Zotto, and V. Saxena, “Five-dimensional SCFTs and gauge theory phases: an M-theory/type IIA perspective,” *SciPost Phys.* **6** no. 5, (2019) 052, [arXiv:1812.10451 \[hep-th\]](#).
- [11] S. A. Cherkis, “Phases of Five-dimensional Theories, Monopole Walls, and Melting Crystals,” *JHEP* **06** (2014) 027, [arXiv:1402.7117 \[hep-th\]](#).
- [12] M. Del Zotto, J. J. Heckman, and D. R. Morrison, “6D SCFTs and Phases of 5D Theories,” *JHEP* **09** (2017) 147, [arXiv:1703.02981 \[hep-th\]](#).
- [13] D. Xie and S.-T. Yau, “Three dimensional canonical singularity and five dimensional $\mathcal{N} = 1$ SCFT,” *JHEP* **06** (2017) 134, [arXiv:1704.00799 \[hep-th\]](#).
- [14] P. Jefferson, H.-C. Kim, C. Vafa, and G. Zafrir, “Towards Classification of 5d SCFTs: Single Gauge Node,” [arXiv:1705.05836 \[hep-th\]](#).
- [15] S. Alexandrov, S. Banerjee, and P. Longhi, “Rigid limit for hypermultiplets and five-dimensional gauge theories,” *JHEP* **01** (2018) 156, [arXiv:1710.10665 \[hep-th\]](#).
- [16] P. Jefferson, S. Katz, H.-C. Kim, and C. Vafa, “On Geometric Classification of 5d SCFTs,” *JHEP* **04** (2018) 103, [arXiv:1801.04036 \[hep-th\]](#).

- [17] L. Bhardwaj and P. Jefferson, “Classifying 5d SCFTs via 6d SCFTs: Rank one,” [arXiv:1809.01650 \[hep-th\]](#).
- [18] L. Bhardwaj and P. Jefferson, “Classifying 5d SCFTs via 6d SCFTs: Arbitrary rank,” [arXiv:1811.10616 \[hep-th\]](#).
- [19] F. Apruzzi, L. Lin, and C. Mayrhofer, “Phases of 5d SCFTs from M-/F-theory on Non-Flat Fibrations,” [arXiv:1811.12400 \[hep-th\]](#).
- [20] Apruzzi, Fabio and Lawrie, Craig and Lin, Ling and Schäfer-Nameki, Sakura and Wang, Yi-Nan, “5d Superconformal Field Theories and Graphs,” [arXiv:1906.11820 \[hep-th\]](#).
- [21] Apruzzi, Fabio and Lawrie, Craig and Lin, Ling and Schäfer-Nameki, Sakura and Wang, Yi-Nan, “Fibers add Flavor, Part I: Classification of 5d SCFTs, Flavor Symmetries and BPS States,” [arXiv:1907.05404 \[hep-th\]](#).
- [22] Apruzzi, Fabio and Lawrie, Craig and Lin, Ling and Schäfer-Nameki, Sakura and Wang, Yi-Nan, “Fibers add Flavor, Part II: 5d SCFTs, Gauge Theories, and Dualities,” [arXiv:1909.09128 \[hep-th\]](#).
- [23] L. Bhardwaj, P. Jefferson, H.-C. Kim, H.-C. Tarazi, and C. Vafa, “Twisted Circle Compactifications of 6d SCFTs,” [arXiv:1909.11666 \[hep-th\]](#).
- [24] O. Bergman, D. Rodríguez-Gómez, and G. Zafrir, “5-Brane Webs, Symmetry Enhancement, and Duality in 5d Supersymmetric Gauge Theory,” *JHEP* **03** (2014) 112, [arXiv:1311.4199 \[hep-th\]](#).
- [25] G. Zafrir, “Duality and enhancement of symmetry in 5d gauge theories,” *JHEP* **12** (2014) 116, [arXiv:1408.4040 \[hep-th\]](#).
- [26] O. DeWolfe, A. Hanany, A. Iqbal, and E. Katz, “Five-branes, seven-branes and five-dimensional E(n) field theories,” *JHEP* **03** (1999) 006, [arXiv:hep-th/9902179 \[hep-th\]](#).
- [27] F. Benini, S. Benvenuti, and Y. Tachikawa, “Webs of five-branes and N=2 superconformal field theories,” *JHEP* **09** (2009) 052, [arXiv:0906.0359 \[hep-th\]](#).
- [28] H. Hayashi, Y. Tachikawa, and K. Yonekura, “Mass-deformed T_N as a linear quiver,” *JHEP* **02** (2015) 089, [arXiv:1410.6868 \[hep-th\]](#).
- [29] A. Brandhuber and Y. Oz, “The D-4 - D-8 brane system and five-dimensional fixed points,” *Phys. Lett.* **B460** (1999) 307–312, [arXiv:hep-th/9905148 \[hep-th\]](#).
- [30] O. Bergman and D. Rodriguez-Gomez, “5d quivers and their AdS(6) duals,” *JHEP* **07** (2012) 171, [arXiv:1206.3503 \[hep-th\]](#).
- [31] A. Passias, “A note on supersymmetric AdS₆ solutions of massive type IIA supergravity,” *JHEP* **01** (2013) 113, [arXiv:1209.3267 \[hep-th\]](#).

- [32] Lozano, Yolanda and Ó Colgáin, Eoin and Rodríguez-Gómez, Diego and Sfetsos, Konstadinos, “Supersymmetric AdS_6 via T Duality,” *Phys. Rev. Lett.* **110** no. 23, (2013) 231601, [arXiv:1212.1043 \[hep-th\]](#).
- [33] O. Bergman, D. Rodríguez-Gómez, and G. Zafrir, “5d superconformal indices at large N and holography,” *JHEP* **08** (2013) 081, [arXiv:1305.6870 \[hep-th\]](#).
- [34] F. Apruzzi, M. Fazzi, A. Passias, D. Rosa, and A. Tomasiello, “ AdS_6 solutions of type II supergravity,” *JHEP* **11** (2014) 099, [arXiv:1406.0852 \[hep-th\]](#). [Erratum: JHEP05,012(2015)].
- [35] O. Bergman and G. Zafrir, “5d fixed points from brane webs and O7-planes,” *JHEP* **12** (2015) 163, [arXiv:1507.03860 \[hep-th\]](#).
- [36] H. Kim, N. Kim, and M. Suh, “Supersymmetric AdS_6 Solutions of Type IIB Supergravity,” *Eur. Phys. J.* **C75** no. 10, (2015) 484, [arXiv:1506.05480 \[hep-th\]](#).
- [37] E. D’Hoker, M. Gutperle, A. Karch, and C. F. Uhlemann, “Warped $AdS_6 \times S^2$ in Type IIB Supergravity I: Local Solutions,” *JHEP* **08** (2016) 046, [arXiv:1606.01254 \[hep-th\]](#).
- [38] M. Gutperle, A. Trivella, and C. F. Uhlemann, “Type IIB 7-branes in warped AdS_6 : partition functions, brane webs and probe limit,” *JHEP* **04** (2018) 135, [arXiv:1802.07274 \[hep-th\]](#).
- [39] O. Bergman, D. Rodríguez-Gomez, and C. F. Uhlemann, “Testing AdS_6/CFT_5 in Type IIB with stringy operators,” *JHEP* **08** (2018) 127, [arXiv:1806.07898 \[hep-th\]](#).
- [40] C.-M. Chang, “5d and 6d SCFTs Have No Weak Coupling Limit,” [arXiv:1810.04169 \[hep-th\]](#).
- [41] C. Cordova, T. T. Dumitrescu, and K. Intriligator, “Deformations of Superconformal Theories,” *JHEP* **11** (2016) 135, [arXiv:1602.01217 \[hep-th\]](#).
- [42] C. Cordova, T. T. Dumitrescu, and K. Intriligator, “Multiplets of Superconformal Symmetry in Diverse Dimensions,” [arXiv:1612.00809 \[hep-th\]](#).
- [43] K. Hori, S. Katz, A. Klemm, R. Pandharipande, R. Thomas, C. Vafa, R. Vakil, and E. Zaslow, *Mirror symmetry*, vol. 1 of *Clay mathematics monographs*. AMS, Providence, USA, 2003. <http://www.claymath.org/library/monographs/cmim01.pdf>.
- [44] D. Cox, J. Little, and H. Schenck, *Toric Varieties*. American Mathematical Society, July, 2011. <https://doi.org/10.1090/gsm/124>.
- [45] X. Wei and R. Ding, “Lattice polygons with two interior lattice points,” *Mathematical Notes* **91** no. 5, (May, 2012) 868–877. <https://doi.org/10.1134/S0001434612050343>.

- [46] A. C. Cadavid, A. Ceresole, R. D’Auria, and S. Ferrara, “Eleven-Dimensional Supergravity Compactified on Calabi-Yau Threefolds,” *Phys. Lett.* **B357** (1995) 76–80, [arXiv:hep-th/9506144](#).
- [47] S. Ferrara, R. R. Khuri, and R. Minasian, “M-theory on a Calabi-Yau Manifold,” *Phys. Lett.* **B375** (1996) 81–88, [arXiv:hep-th/9602102](#).
- [48] M. Aganagic, “A Stringy Origin of M2 Brane Chern-Simons Theories,” *Nucl. Phys.* **B835** (2010) 1–28, [arXiv:0905.3415 \[hep-th\]](#).
- [49] F. Benini, C. Closset, and S. Cremonesi, “Chiral flavors and M2-branes at toric CY4 singularities,” *JHEP* **02** (2010) 036, [arXiv:0911.4127 \[hep-th\]](#).
- [50] D. L. Jafferis, “Quantum corrections to $\mathcal{N} = 2$ Chern-Simons theories with flavor and their AdS₄ duals,” *JHEP* **08** (2013) 046, [arXiv:0911.4324 \[hep-th\]](#).
- [51] F. Benini, C. Closset, and S. Cremonesi, “Quantum moduli space of Chern-Simons quivers, wrapped D6-branes and AdS₄/CFT₃,” *JHEP* **09** (2011) 005, [arXiv:1105.2299 \[hep-th\]](#).
- [52] M. R. Douglas and G. W. Moore, “D-branes, quivers, and ALE instantons,” [arXiv:hep-th/9603167](#).
- [53] E. Witten, “Phases of N=2 theories in two-dimensions,” *Nucl. Phys.* **B403** (1993) 159–222, [arXiv:hep-th/9301042 \[hep-th\]](#). [AMS/IP Stud. Adv. Math.1,143(1996)].
- [54] N. Seiberg and E. Witten, “Gapped Boundary Phases of Topological Insulators via Weak Coupling,” *PTEP* **2016** no. 12, (2016) 12C101, [arXiv:1602.04251 \[cond-mat.str-el\]](#).
- [55] E. Witten, “The “Parity” Anomaly On An Unorientable Manifold,” *Phys. Rev.* **B94** no. 19, (2016) 195150, [arXiv:1605.02391 \[hep-th\]](#).
- [56] L. Alvarez-Gaume and P. H. Ginsparg, “The Structure of Gauge and Gravitational Anomalies,” *Annals Phys.* **161** (1985) 423. [Erratum: *Annals Phys.*171,233(1986)].
- [57] C. Closset, T. T. Dumitrescu, G. Festuccia, Z. Komargodski, and N. Seiberg, “Comments on Chern-Simons Contact Terms in Three Dimensions,” *JHEP* **09** (2012) 091, [arXiv:1206.5218 \[hep-th\]](#).
- [58] C. Closset, H. Kim, and B. Willett, “Seifert fibering operators in 3d $\mathcal{N} = 2$ theories,” [arXiv:1807.02328 \[hep-th\]](#).
- [59] C. Closset and H. Kim, “Three-dimensional $\mathcal{N} = 2$ supersymmetric gauge theories and partition functions on Seifert manifolds: A review,” *Int. J. Mod. Phys.* **A34** no. 23, (2019) 1930011, [arXiv:1908.08875 \[hep-th\]](#).
- [60] S. Cremonesi and A. Tomasiello, “6d holographic anomaly match as a continuum limit,” [arXiv:1512.02225 \[hep-th\]](#).

- [61] G. Ferlito, A. Hanany, N. Mekareeya, and G. Zafrir, “3d Coulomb branch and 5d Higgs branch at infinite coupling,” *JHEP* **07** (2018) 061, [arXiv:1712.06604 \[hep-th\]](#).
- [62] S. Cabrera, A. Hanany, and F. Yagi, “Tropical Geometry and Five Dimensional Higgs Branches at Infinite Coupling,” [arXiv:1810.01379 \[hep-th\]](#).
- [63] E. Cremmer, “Supergravities in 5 Dimensions,” in *In *Salam, A. (ed.), Sezgin, E. (ed.): Supergravities in diverse dimensions, vol. 1* 422-437. (In *Cambridge 1980, Proceedings, Superspace and supergravity* 267-282) and Paris Ec. Norm. Sup. - LPTENS 80-17 (80,rec.Sep.) 17 p. (see Book Index). 1980.*
- [64] S. Ferrara and M. Porrati, “AdS(5) superalgebras with brane charges,” *Phys. Lett.* **B458** (1999) 43–52, [arXiv:hep-th/9903241 \[hep-th\]](#).
- [65] L. Alvarez-Gaume, S. Della Pietra, and G. W. Moore, “Anomalies and Odd Dimensions,” *Annals Phys.* **163** (1985) 288.
- [66] F. Bonetti, T. W. Grimm, and S. Hohenegger, “One-loop Chern-Simons terms in five dimensions,” *JHEP* **07** (2013) 043, [arXiv:1302.2918 \[hep-th\]](#).
- [67] R. Hartshorne, *Algebraic Geometry*. Springer New York, 1977. <https://doi.org/10.1007/978-1-4757-3849-0>.
- [68] P. Griffiths and J. Harris, *Principles of Algebraic Geometry*. John Wiley & Sons, Inc., Aug., 1994. <https://doi.org/10.1002/9781118032527>.
- [69] C. Closset, “Toric geometry and local Calabi-Yau varieties: An Introduction to toric geometry (for physicists),” [arXiv:0901.3695 \[hep-th\]](#).
- [70] S. Ishii, *Introduction to Singularities*. Springer Japan, 2014. <https://doi.org/10.1007/978-4-431-55081-5>.
- [71] D. A. Cox, “Recent developments in toric geometry,” 1996.
- [72] A. Hatcher, C. U. Press, and C. U. D. of Mathematics, *Algebraic Topology*. Algebraic Topology. Cambridge University Press, 2002. <https://books.google.com/books?id=BjKs86kosqC>.
- [73] J. Hofscheier, *Introduction to toric geometry with a view towards lattice polytopes*, pp. 1–37. https://www.worldscientific.com/doi/abs/10.1142/9789811200489_0001.
- [74] W. Fulton, *Introduction to Toric Varieties. (AM-131)*. Princeton University Press, Dec., 1993. <https://doi.org/10.1515/9781400882526>.
- [75] N. C. Leung and C. Vafa, “Branes and Toric Geometry,” *Adv. Theor. Math. Phys.* **2** (1998) 91–118, [arXiv:hep-th/9711013](#).
- [76] V. Bouchard, “Lectures on complex geometry, Calabi-Yau manifolds and toric geometry,” [arXiv:hep-th/0702063 \[HEP-TH\]](#).

- [77] C. Closset and S. Cremonesi, “Toric Fano varieties and Chern-Simons quivers,” *JHEP* **05** (2012) 060, [arXiv:1201.2431 \[hep-th\]](#).
- [78] C. Closset, “Seiberg duality for Chern-Simons quivers and D-brane mutations,” *JHEP* **03** (2012) 056, [arXiv:1201.2432 \[hep-th\]](#).
- [79] R. E. Tarjan, *Data Structures and Network Algorithms*. Society for Industrial and Applied Mathematics, Philadelphia, PA, USA, 1983.
- [80] F. R. K. Chung, *Spectral Graph Theory*, vol. 92 of *CBMS Regional Conference Series in Mathematics*. American Mathematical Society, 1997.
<http://www.ams.org/bookstore-getitem/item=cbms-92><http://www.math.ucsd.edu/~fan/research/revised.html>.
- [81] B. Bollobás, *Modern Graph Theory*. Graduate Texts in Mathematics 184. Springer-Verlag New York, 1 ed., 1998.
- [82] Harary, Frank, and Manvel, Bennet, “On the number of cycles in a graph,” *Matematický časopis* **21** no. 1, (1971) 55–63. <http://eudml.org/doc/29956>.
- [83] B. Assel and A. Sciarappa, “Wilson loops in 5d $\mathcal{N} = 1$ theories and S-duality,” [arXiv:1806.09636 \[hep-th\]](#).